Master's thesis

NTNU
Norwegian University of Science and Technology
Faculty of Medicine and Health Sciences
Department of Clinical and Molecular Medicine

Kirusika Elamurugan

Regulation of bacteria phagocytosis by anti-inflammatory SLAMF1-derived peptides

Master's thesis in Molecular Medicine
Supervisor: Mariya Yurchenko
September 2022

NTNU
Norwegian University of
Science and Technology

Kirusika Elamurugan

Regulation of bacteria phagocytosis by anti-inflammatory SLAMF1- derived peptides

Master's thesis in Molecular Medicine
Supervisor: Mariya Yurchenko
September 2022

Norwegian University of Science and Technology
Faculty of Medicine and Health Sciences
Department of Clinical and Molecular Medicine

NTNU
Norwegian University of
Science and Technology

Acknowledgement

This master project was performed during 2021-2022 at the Centre of Molecular Inflammation Research (CEMIR), the Institute for Clinical and Molecular Medicine (IKOM) at the Faculty of Medicine and Health Sciences, Norwegian University of Science and Technology (NTNU).

I want to give thanks to my supervisor, Mariya Yurchenko for trusting me and taking me in as a master student at short notice. Thank you for the excellent lab training and for challenging me. I have learned so much from you. I appreciate that you have been available for always answering questions and for the constructive feedback during lab and writing. Your support has been essential for allowing me to write this master thesis.

I also want to acknowledge the PhD students Kaja Elisabeth Nilsen, Ingvild Mestvedt and Caroline Gravastrand for lab training and offering to help and answer my questions at the lab. A special thanks to PhD student Ingvild Mestvedt for helping me at the lab and answering countless questions, but also making me feel comfortable and safe at the lab.

Thank you to the lab engineers for providing with cells but also with technical assistance. Also, thanks to the people at CEMIR for making me feel welcomed and making it a wonderful workplace.

Lastly, thanks to my friends and family for continuous support and encouragement throughout my masters.

Kirusika Elamurugan,

Trondheim, September 2022

Abstract

Signaling lymphocytic activation molecule family 1 (SLAMF1) are type I transmembrane receptors which is required for the induction *IFN-β* expression and the killing of Gram-negative bacteria through TLR4 signalling pathway. Researchers at CEMIR developed anti-inflammatory peptides derived from the cytoplasmic tail of SLAMF1, such as P7-pen and its variants P7G10-pen and P7N4-pen. Preliminary data of LC-MS obtained from the Trafficking group at CEMIR found that P7-pen interacted with proteins involved in the regulation of phagocytosis. Additionally, P7-pen showed decreased uptake of *E. coli* bioparticles in primary human monocytes. In this study we explore the effect of P7-pen on bacterial uptake and the mechanism of uptake inhibition.

We showed by flow cytometry and live bacteria uptake that P7-pen efficiently inhibits the uptake of Gram-negative and Gram-positive bacteria. The proinflammatory and *IFN-β* expression was also decreased by P7-pen. The P7 variant, P7N4-pen showed decreased inhibitory activity of *E. coli* bioparticle at longer time periods, while it was efficiently inhibiting uptake of live *E. coli* at shorter time. P7G10-pen did not inhibit uptake of *E. coli* bioparticle or live bacteria. We showed by flow cytometry that P7-pen did not inhibit complement mediated phagocytosis, but treatment of heat inactivated serum and compstatin restored the inhibitory activity of P7-pen. We showed that P7-pen or P7G10-pen co-precipitated with target proteins from MS hits, where only RhoG and Rab14 are target proteins.

SLAMF1 protein showed co-precipitation with Rab14 and RhoG and could be further explored in studies with measles virus. SLAMF1 and SLAMF1 mutant (deletion of IgV-like domain) showed no effect of uptake of bacterial bioparticles, while SLAMF1 and the mutant showed uptake of live bacteria. These results are difficult to explain and should be investigated further.

Sammendrag

Signaling lymphocytic activation molecule family 1 (SLAMF1) er type I transmembran reseptor som er nødvendig for uttrykkelse av *IFN-β* og drepe av Gram-negative bakterier via TLR4 signalleringsvei. Forskere ved CEMIR har utviklet anti-inflammatoriske peptider fra den cytoplasmiske halen til SLAMF1. Noen av peptidene som er blitt utviklet er P7-pen og variantene P7G10-pen og P7N4-pen. Trafficking group ved CEMIR har gjort et innledende funn, der P7-pen dannet interaksjoner med protein som er involvert i regulering av fagocytose. I tillegg, har gruppen vist gjennom konfokal at P7-pen hemmer opptaket av *E. coli* biopartikler i monocytter. I denne tesen utforsker vi effekten av opptak av bakterie av P7-pen og mekanismene ved opptaksinhibering.

Flow cytometri og opptak av levende bakterier viste at P7-pen inhiberer opptaket av Gram-negative og Gram-positive bakterier. Uttrykket av proinflammatoriske cytokiner og *IFN- β* var hemmet av P7-pen. Flow cytometri resultatet for P7 varianten, P7N4-pen viste svekket inhiberende effekt av *E. coli* biopartikler over lengre tidsperioder, men peptidet inhiberte levende bakterier effektivt. P7G10-pen hemmet ikke opptak av biopartikler av bakterier eller levende bakterier. Flow cytometri data viste at P7-pen ikke inhiberer komplement mediert fagocytose. Behandling av compstatin og inaktivert serum ved varme gjenopprettet funksjonen til P7-pen. Av proteinene som hadde slått ut som bindingspartnere av peptidene, var det bare RhoG og Rab14 som co-presipiterte med P7-pen eller P7G10-pen.

SLAMF1 co-presipiterte med Rab14 og RhoG og kan bli testet videre i studier som omhandler meslinger. SLAMF1 og dets mutant (fjernet IgV-lik domene) viste ingen effekt i opptak av biopartikler av bakterier, men de viste opptak av levende bakterier. Disse resultatene er vanskelige å tolke og bør forskes på videre.

Table of contents

Abbreviations

AF488	Alexa fluor 488
Cdc42	Cell division control protein 42
CFU	Colony-forming units
CLR	C-type Lectin receptor
CPP	Cell penetrating peptide
CR	Complement receptor
CRISPR/Cas9	Clustered regularly interspaced short palindromic repeats/CRISPR associated protein 9
CytoD	Cytochalasin D
DC	Dendritic cells
DTT	Dithiothreitol
E. coli	*Escherichia coli*
EDTA	Ethylenediamine tetraacetic acid
EHD4	EH Domain containing 4
ERC	Endocytic recycling compartment
FACS	Fluorescence-activated cell sorting
FCS	Fetal bovine calf serum
FcγR	Fcγ-receptor
FIP2	Family interacting protein 2
FSC	Forward Scatter
GDP	Guanosine 5'-diphosphate
GTP	Guanosine 5'-phosphate
IFN-β	Type I interferon beta
Ig	Immunoglobulin
IL-1β	Interleukin-1 β
IL-6	Interleukin-6
IP	Immunoprecipitate
IRAK1/4	Interleukin-1 receptor-associated kinase 1/4
IRF3	Interferon regulatory factor-3
ITAM	Immunoreceptor tyrosine-based activation motif
ITSM	Immunoreceptor tyrosine-based switch motifs
LB	Lysogeny broth

LC-MS	Liquid chromatography-mass spectrometry
LDS	Lithium Dodecyl Sulfate
LPS	Lipopolysaccharides
LRR	Leucine-rich repeats
Mal	MyD88 adaptor-like
M-CSF	Macrophage colony-stimulating factor
MDM	Monocyte derived macrophage
MD-2	Myeloid differentiation factor 2
MyD88	Myeloid differentiation primary response 88
NF-kB	nuclear factor- kB
NK	Natural killer cells
NLR	NOD-like receptor
OmpC/F	Outer membrane protein C/F
PAMP	Pathogen-associated molecular pattern
PBMC	Peripheral blood mononuclear cell
PBS	Phosphate buffered saline
PCR	Polymerase chain reaction
PMA	Phorbol 12-myristate 13-acetate
PRR	Pattern recognition receptor
P/S	Penicillin/streptomycin
Rab14	Ras-related protein Rab14
Rac1/2	Ras-related C3 botulinum toxin substrate 1/2
Rac-GEF	Ras-related C3 botulinum toxin substrate (Rac)- Guanine Nucleotide Exchange factor
Rho G	Rho-related GTP-binding protein Rho G
RIPA	Radioimmunoprecipitation assay buffer
RLR	RIG-I-like receptor
RT-qPCR	Reverse transcription quantitative real-time PCR
S. aureus	*Staphylococcus aureus*
SLAMF1	Signaling lymphocytic activator of transcription 1
SR	Scavenger receptor
SSC	Side Scatter
Syk	Spleen tyrosine kinase

TAK1	Transforming growth factor-β (TGF- β)- activated kinase
TBP	TATA- Box binding protein
TBST	Tris buffered saline-tween
TIR	Intracellular toll-interleukin 1 (IL-1) receptor
TIRAP	TIR-associated protein
TLR	Toll-like receptor
TNF-α	Tumor necrosis factor alpha
TRAF	Tumor necrosis factor receptor-associated factor
TRAM	TRIF-related adaptor molecule
TRIF	TIR domain-containing adaptor-inducing Interferon-β

1. Introduction

1.1.1 Immune response induced by bacteria

The immune system is divided into two main parts: innate and adaptive immunity [1]. They are determined by speed and the specificity of the reaction. Innate immune system includes the physical, chemical, and microbiological barriers as well as the cellular innate responses [2, 3]. The innate immune system provides the first line of defence against pathogens, including bacteria [4]. Whereas adaptive immune system consists of the recognition of antigens through T and B lymphocytes [2, 5]. The highly conserved innate immune response is rapid, but lack specificity, while adaptive immune response is precise but takes days to week to develop [2].

The constituent cells of the innate immune system include phagocytes such as macrophages and neutrophils, dendritic cells (DC), mast cells, basophils, eosinophils, natural killer (NK) and innate lymphoid cells [1]. It is established that the innate immune system recognises pathogens, but also discriminates between self and non self [4]. This is possible through interaction with pathogen associated molecular patterns (PAMPs) and pattern recognition receptors (PRRs). Bacteria have well conserved cell-wall molecules, PAMPs which are recognised by specific PRRs on the host cell [6, 7]. PAMPs can be found in both Gram- negative and Gram-positive bacteria, some examples are lipopeptides, peptidoglycans and flagellin. Other PAMPs are more specific to the respective bacterial strains, lipopolysaccharides (LPS) are specific for Gram-negative bacteria whilst lipoteichoic acid is specific to Gram-positive bacteria [7]. When the pathogen is detected, the innate immune responses are activated through the complement system, phagocytosis, and inflammatory response [8, 9].

The adaptive immune response is activated by signals produced by the innate immune system [10]. The targeted response is mediated by B and T cells, through high affinity recognition of the rearranged receptors [2, 11]. The rearranged receptors recognise variety of receptors which recognise the component of pathogens. Additionally, the adaptive immunity results in the generation of immunologic memory from B and T cells generated in pathogen encounters. In subsequent encounters of the pathogen, the cells are activated quicker and generate more rapid response [12]. Bacterial stimulus results in the presentation of bacterial antigen to naïve T cells. Subsequently, the T cells differentiate to four classes with respective immune responses such as secretion of pro inflammatory cytokines to promote phagocytosis and attracting innate immune cells for priming of phagocytosis [6].

1.1.2 Pattern recognition receptors

There are many classes of PRRs, which includes the transmembrane proteins Toll-like receptors (TLRs), C-type lectin receptors (CLRs), the cytoplasmic proteins Retinoic acid-inducible gene (RIG)-I-like receptors (RLRs) and NOD- like receptors (NLRs). These receptors are expressed by macrophages and DCs, but also by many other cell types [13]. RLRs induces antiviral responses via type I IFN after the recognition of RNA species which are released in the cytoplasm. The intracellular NLR induces inflammatory responses to various PAMPs and CLRs which triggers inflammatory responses by recognition of fungal and bacterial PAMPs [14]. Dectin-1, a CLR which is coupled on the immunoreceptor tyrosine-based activation motif (ITAM) and recognises β-glucans from fungi [13].

TLRs are the best characterized PRRs, and 10 functional classes of TLRs have been found in humans which ranges from TLR1-TLR10 [15]. TLRs are type I transmembrane proteins

with ectodomains compromising of leucine-rich repeats (LRR) and intracellular Toll-interleukin 1 (IL-1) receptor (TIR) domain. The extracellular LRR sequences at the plasma membrane or in endosomal compartments detects PAMPs and transmits signals through TIR domains oligomerisation, inducing downstream signalling [16, 17]. TLR receptors are located either on the cell surface or intracellularly. TLR1,2, 4, 5 and 6 are expressed on the cell surface and recognises membrane components of microbes, while TLR 3,7,8 and 9 are mostly present in intracellular compartments and recognises viral nucleic acids [16].

The activation of TLR by ligand recognition triggers adaptor proteins of the myeloid differentiation factor 88 (MyD88) dependent or the TIR-domain-containing adaptor protein-inducing IFN-β (TRIF) dependent signalling pathway which leads to the production of proinflammatory cytokines and type I interferons [13, 18-20]. The primary events of the TLR mediated signalling are initiated by the interactions between the TIR domain and the TIR-domain- containing cytosolic adapters such as MyD88, TIR-associated protein (TIRAP)/MyD88-adaptor-like (Mal), TRIF and TRIF-related adapter molecule (TRAM) [21]. The responses mediated by the TLRs is partly due to the selective use of the adaptor molecules [19].

All TLRs except for TLR3 are dependent on MyD88. When ligand binds to the ectodomain of LRR a conformation change is induced. The cytoplasmic TIR domain elicits a signal, recruiting the adaptor molecules [22]. Subsequently, MyD88 recruits a complex of IRAKs, TRAF6 and TAK1 which leads to early activation of NF-kB and MAP kinases [14]. Only TLR3 and TLR4 utilises the TRIF-dependent pathway [23].

TLR4 responds to lipopolysaccharide (LPS), an endotoxin on the outer membrane of gram-negative bacteria The response is initiated by the association of LPS and TLR4/myeloid differentiation factor 2 (MD-2) complex and the coreceptor CD14 [18, 24, 25]. TLR4 activates both MyD88 dependent and TRIF-dependent pathway [15]. The MyD88 dependent pathway is induced by the recruitment of MyD88 and TIRAP/Mal adapter proteins which leads to early activation of NF-kB and pro inflammatory cytokines. TRIF-dependent pathway recruits TRIF and TRAM for late NF-KB activation and dimerization of interferon regulatory factor-3 (IRF3), which leads to production of interferon- β (*IFN-β*) [24]. TLR2 receptors forms a heterodimer with either TLR1 or TLR6 in the recognition of gram- positive bacteria [13]. TLR2 recognises lipopeptides, peptidoglycan and lipoteichoic acid from gram-positive bacteria and initiate the MyD88-dependent signalling pathway and the subsequent cytokine production [14, 26].

TLRs are important defence against pathogens but excessive response of TLRs can lead to septic shock syndrome. It is crucial that the TLR activation is eradicating pathogen without causing damage to the host [13].

1.1.3 Phagocytosis of bacteria

Phagocytosis defines the internalising process of particles larger than 0.5 μm [27]. Phagocytes such as macrophages, neutrophils, monocytes, DC, and osteoclasts recognises microbial pathogens utilising surface receptors, engulf and kill them [27, 28]. Surface receptors which are involved in phagocytosis are scavenger receptors (SR), Fcγ receptors (FcγR), complement receptors (CR), dectin-1 (CLR) and TLRs [29].

These receptors recognise the pathogen in two ways, either directly recognising the particle (non-opsonic receptors) or recognising targets which are coated with opsonic molecules (opsonic receptors) [27, 30]. Phagocytes ingest microbial pathogens but also apoptotic cells. The cells contribute to eliminating pathogens, but also apoptotic cells making it essential for tissue homeostasis [27].

First and foremost, the surface receptor binds the particle which induces the actin polymerisation under the membrane. The membrane extends around the particle and pulls it to the center of the cell. The phagosome matures to phagolysosome where the particle subsequently is killed and digested due to the acidic and hydrolytic properties in the phagolysosome. The digested particle is later prepared for antigen presentation [31].

TLRs binds to the respective ligands and responds accordingly, but the receptors do not ingest microbes. TLRs are not directly functioning as phagocytic receptors. However, the receptors activate molecules which are essential in phagocytosis, such as Rac1 and Rho GTPase family and may affect the phagosome formation efficiency. They can also activate transcription of the gene that participate in actin cytoskeletal dynamics and membrane trafficking amongst others [32].

SR have a range of subclasses and can bind to ligands such as LPS or lipoteichoic acid. It is not clear if the involvement of SR is enough to initiate phagocytosis. The receptors might function as co-receptor, with TLRs to activate another phagocytic receptor or it could act with integrins [27, 33].

FcγR binds to the Fc region of IgG- opsonised particles. It triggers the internalisation of the particle and subsequently the production of reactive oxygen species [32, 33]. The FcγR promotes microbicidal activity of the phagocytes. Through phosphorylation of ITAM domains by SRC family kinases the syk kinase is activated which in turn stimulates the intracellular signalling [32, 34]. The intracellular signalling leads to the activation of targets such as RAC-guanine nucleotide exchange factors (RAC-GEFs) which ultimately leads to the activation of cell division cycle 42 (Cdc42). The actin cytoskeleton is rearranged and results in phagocytosis [34]. F-actin promotes the pseudopod formation, and the Cdc42 activity is decreased for the closure of phagocytic cup [35].

Dectin-1 binds to the ligands in the C-type lectin part of the receptor and initiate signalling through ITAM-like motif [36]. Dectin-1 activates the tyrosine kinase, Syk and the plasma membrane wraps around the pathogen of F-actin structures by protrusion and requires Rho GTPase activity. The further downstream signalling are similar as FcR, as they share signalling motifs [35].

CR binds to complement molecules on the microorganism or cells. The most efficient phagocytic receptor of the CRs is C3 which binds to the component iC3b [37]. The receptor is not constitutively active and requires pre-activation [38]. When activated, the F-actin of the plasma membrane forms *bona fide* phagocytic cup, where the plasma membrane surrounds the particle from one side and fuses into the cell and engulfs it. CR3 phagocytosis requires rapid activation and inactivation of Rho GTPases for engulfing the particle [35].

1.1.4 Phagocytosis regulation

Phagocytosis is regulated by the orchestrated activity of multiple proteins, where GTPases play a very important role, with different combination and players for different types of phagocytosis. Rac1, Cdc42 and Rac2 have different roles in regulating the FcR dependent anti-pathogenic phagocytosis. Blocking the activity of Cdc42 or Rac1 in FcR mediated anti-pathogenic phagocytosis prevents the filopodia formation or membrane ruffles. This results in the cells inability to take up the ligand because the phagocytic cup cannot close. Also, the recruitment of F-actin to the phagocytic cup is abolished when RhoG is depleted. The inactivation and activation of Cdc42 is important for the formation of the phagocytic cup. If it is constitutively active the phagocytosis decreases [35].

Complement mediated phagocytosis is shown to require the RhoA activity as well as possibly RhoG activity, but not Rac1 or Cdc42. Inhibition of RhoA induced by C3

transferase results in decreased F-actin recruitment under the particle and decreased uptake of particles [35].

1.1.5 SLAMF1: regulation of TLR4 mediated signalling

Signaling lymphocytic activation molecule family 1 (SLAMF1), also called CD150 is a member of the SLAM family receptor. The SLAM family receptors are type I transmembrane receptors and a subfamily of CD2 immunoglobulin (Ig)-like receptors' superfamily [39, 40]. They are expressed by immune cells and characterized by an extracellular domain with two Ig-like domains, variable (V)-like domain and constant 2 (C2)- like domain [40]. SLAMF1 has two intracellular signalling domains, immunoreceptor tyrosine-based switch motifs (ITSM) in the receptor's cytoplasmic tail, which binds kinases, phosphatases, and adaptor proteins in phosphorylation-dependent manner [41, 42].

A study done by Yurchenko et al. showed that SLAMF1 is required for induction of *IFN-β* and killing Gram-negative bacteria through TLR4 mediated signalling pathway [43]. The majority of SLAMF1 in human resting macrophages was in endocytic recycling compartment (ERC). Endogenous SLAMF1 is already prebound to TRAM via C-terminal part of SLAMF1 protein, and upon addition of LPS or/*E. coli,* the interaction is enhanced, and the complex is recruited to the LPS/*E. coli* phagosome in Rab-11-dependent manner. Thus, SLAMF1 is an important regulator of TLR4-mediated TRAM-TRIF signalling axis by the regulating of TRAM trafficking.

TLR4 signalling results in the activation of Rab11 from GDP bound to GTP bound active state. After the GDP/GTP ratio shift, the activated Rab11 signals the recruitment of SLAMF1 and TRAM via the Rab11 effector protein Rab11 FIP2/FIP2. FIP2 connects the Rab11 vesicles and the protein cargo which enhances the delivery of the SLAMF1 and TRAM complex via FIP2 from ERC to phagosomes. At the phagosome, FIP2 may link SLAMF1-TRAM complex to Rab11. SLAMF1-regulated transport of TRAM to the phagosome further amplifies the *IFN-β* secretion, thus targeting SLAMF1-TRAM interaction can be used to regulate the TLR4 mediated cytokine production [43].

1.1.6 SLAMF1-derived peptides

Researchers at CEMIR have constructed anti-inflammatory peptides which are derived from the C-terminal ITSM of SLAMF1 protein. The peptides are conjugated with cell-penetrating peptides (CPPs), and the complex interacts with key regulators of TLRs. CPPs are short cationic peptide sequences which provide delivery of biologically active compounds, such as proteins without disrupting the plasma membrane [44, 45]. SLAMF1 derived peptides co-precipitates with TRAM and in addition with TIRAP, TRAF6, TAK1, IRAK1 and IRAK4 proteins, which are crucial for the TLR4 and TLR9 cytokine expression (unpublished, Trafficking group).

P7 peptide with penetratin CPP (P7-pen) is the active peptide which consists of ten amino acids linked with penetrating peptide (**table 1.1**). Several variants of P7-pen have been synthesised which give the respective peptides different structural characteristics and functionality. The variants are P7N4-penetratin peptide (P7N4-pen) and P7G10-penetratin peptide (P7G10-pen). In P7N4-pen, tyrosine (Y) is substituted to asparagine (N) at position 4. Threonine is substituted to glycine (G) at position 10 in P7G10-pen (**table 1.1**). C3-penetratin peptide (C3-pen) has several amino acid (aa) substitutions and used as negative control. The size and aa of C3-pen is similar to P7-pen, but it does not have the same anti-inflammatory effect as P7-pen.

Table 1.1: **Peptide sequence of SLAMF1 derived peptides.** The amino acid sequence of the peptides is shown for the SLAMF1 peptides. The red letter shows the amino acid substitution in the peptides

Peptides	Peptide sequence
C3-pen	I don't have the sequence
P7-pen	ITVYASVTLT G RQIKIWFQNRRMKWKK
P7G10-pen	ITVYASVTLG G RQIKIWFQNRRMKWKK
P7N4-pen	ITVNASVTLT G RQIKIWFQNRRMKWKK

The peptides were tested in different model systems, primary human monocytes and macrophages and *ex vivo*- whole blood model. P7-pen peptide inhibits TLR4-mediated signalling through inhibition of MyD88 complex formation, which results in inhibition of pro-inflammatory cytokine production such as *TNF-α*, *IL-1β*, *IL-6* and type I IFNs (*IFN-β*) expression and secretion (**Figure 1.1**). P7N4-pen is not very efficient in inhibiting TLR4-mediated pro-inflammatory signalling. P7G10-pen on the other hand could inhibit *IFN-β* expression and secretion but has less effect on pro-inflammatory cytokine expression and no effect on phagocytosis (unpublished data, Trafficking group, CEMIR).

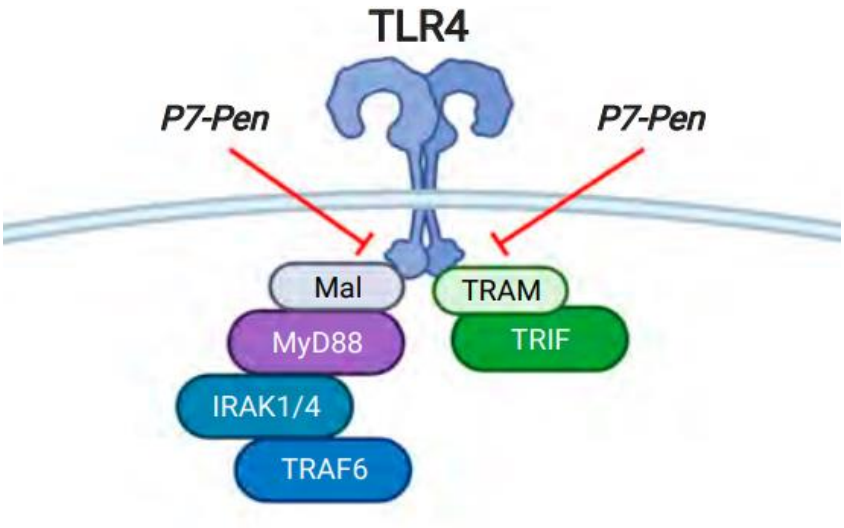

Figure 1.1: **P7-pen inhibits TLR4-signalling pathway.** The SLAMF1 derived peptide targets both MyD88 dependent and TRAM-TRIF signalling which results in the inhibition of proinflammatory cytokines and *IFN* type I expression

The mechanism of P7-pen was further investigated at protein level. Liquid chromatography mass spectrometry (LC-MS) was performed to identify the potential binding partners of P7-pen. The samples were prepared by researcher Mariya Yurchenko and PhD Ingvild Bergdal Mestvedt and Dr. Sneha Pinto performed the LC-MS analysis. The data with protein score and functionality are shown in **table 1.2**.

The data base of LC-MS machine has a computer algorithm which identifies amino acid sequences from the sample with the matching sequences in the data base. A score is then calculated for each amino acid sequence, and the highest score indicates the best match [46, 47]. The table shows that Cell division control protein 42 homolog (Cdc42), proto- oncogene vav (Vav), Ras-related protein Rab 14 (Rab14), Rho-related GTP-binding protein RhoG (RhoG) and EH domain containing protein 4 (EHD4) are binding partners to P7-pen. P7-pen interacts with proteins which are involved in phagocytosis, membrane invagination, endocytosis, and vesicle trafficking respectively.

Table 1.2: **Hits for P7-pen from MS analysis of co-precipitated lysates from THP-1 cells**

Protein IDs	Gene symbol	Function	Unique sequence coverage (%)	Molecular weight (kDa)	Score
CDC42_HUMAN Cell division control protein 42 homolog	CDC42	Phagocytosis, membrane invagination, endocytosis	53.9	21.258	98.255
VAV_HUMAN Proto-oncogene vav	VAV1	Vesicle trafficking	35.7	98.313	131.37
RAB14_HUMAN Ras-related protein Rab-14	RAB14	Phagocytosis	231.09	23.897	231.09
RHOG_HUMAN Rho-related GTP-binding protein RhoG	RHOG	Membrane invagination, endocytosis	258.8	21.308	258.8
EHD4_HUMAN EH domain-containing protein 4	EHD4	Endocytosis	262.76	61.174	262.76

Trafficking group at CEMIR further investigated the function of P7-pen peptides on cells. Live bacteria uptake was performed in pre-treated primary human monocytes with 15μM pen or P7-pen and 3μM cytochalasin D (CytoD) and stimulated with fluorescent bioparticles for 15-, 30- and 45-minute timepoints (**Figure 1.2)**. CytoD is a compound which inhibits the polymerisation and depolymerisation of the actin cytoskeleton [48, 49]. The fluorescence, which indicates uptake of the bioparticles were measured in confocal microscopy and subsequently counted.

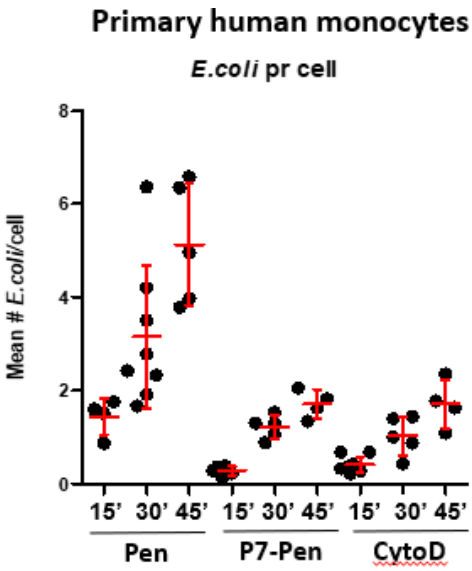

Figure 1.2: **P7-pen peptide inhibits uptake of *E. coli* by primary human monocytes.** Cells were pre-incubated with 15 µM pen, P7-pen peptide or 3 µM cytochalasin (CytoD) followed by addition of Alexa Fluor 488-labelled *E. coli* bioparticles for the timepoints indicated on the figure (15, 30 or 45 min). Fluorescent *E. coli* was counted by spot-detection in Bitplane Imaris imaging software and used to calculate the average number of *E. coli* particles per cell. Data from Trafficking group/CEMIR, unpublished, confidential.

The mean number of *E. coli* per cell was reduced in monocytes pre-treated with P7-pen and CytoD which suggests that P7-pen inhibits the uptake of *E. coli* bioparticles in human monocytes.

1.1.7 Aim of the study

Since SLAMF1 derived peptides could inhibit excessive inflammation and thus have the potential to be used as a novel drug against sepsis, it was interesting to target TLRs-mediated signalling induced by live bacteria and follow the uptake of live bacteria in primary human monocytes, macrophages, and macrophage-like cell lines. Thus, the aim of this thesis is to address the effect of the SLAMF1-derived peptides on bacterial uptake and signalling initiated by live bacteria with focus on mechanism of action of uptake inhibition.

We aim to:

- Evaluate the effect of P7-pen or P7-variants (P7N4-pen and P7G10-pen) treatment on uptake of *E. coli, S. aureus* and Zymosan bioparticles by monocytes and macrophages using flow cytometry approach and fluorescent particles (pHRodo, AF488)
- Examine if opsonisation of bacterial particles affects inhibitory activity of P7-pen- both in relation to phagocytosis and to TLR4-mediated cytokines' expression
- Evaluate the effect of peptide on the uptake of live bacteria of Gram- negative and Gram-positive bacteria by THP-1 cells using phagocytic assay
- Address the effect of treatment by P7-pen peptide on *TNF* and *IFN-β* mRNA expression mediated by live bacteria
- Evaluate the effect of SLAMF1 overexpression on uptake of live bacteria-, bacterial bioparticles and bacteria-mediated cytokines expression in THP-1 cells
- Follow up the interaction of SLAMF1 receptor and peptides' variants (P7-pen and P7G10-pen) with mass spectrometry hits- RhoG and Rab14 using co-precipitation assays from primary monocytes and HEK293T cell

2. Methodology

2.1 Cell culture and differentiation

Peripheral blood mononuclear cells

Usage of buffycoats from blood donors were approved by Regional Etisk Komite (REK). Peripheral blood mononuclear cells (PBMC) was isolated from buffycoats obtained from blood donors (Blodbanken, St. Olav's Hospital) and maintained in RPMI-1640 (Sigma-Aldrich, #R8758) supplemented with L-glutamine (L-glut, 1:100, 200 mM, Sigma-Aldrich, #G7513), Penicillin/Streptomycin (P/S, 1:100, 100 nM, Sigma-Aldrich, #P0781) as well as 30% human serum (A+, The Blood bank, St. Olav's Hospital, Trondheim Norway) for monocytes and macrophage differentiation.

PBMCs were isolated the following day of blood donation. The whole blood was diluted in 80 mL Dulbecco's Phosphate Buffered Saline (PBS, Sigma-Aldrich, #D8537) and subsequently 30 mL of the diluted blood was applied on top of the density gradient medium, Lymphoprep (15 mL, Axis-Shield Poc AS™, #11508545). The buffy coat was spun down (680 x *g*, 25 min, no deceleration, 22ºC) to separate the different constituents by density. Next, the white layer of PBMC in the interphase of the plasma and granulocyte layers was carefully transferred to a conical tube (50 mL) and spun down (840 x *g*, 10 min, full deceleration, 22ºC) to collect the pellet and remove leftovers of lymphoprep. The supernatant was discarded, and cell pellet was resuspended in 15 mL HANKS' Balanced Salt Solution (HANKS, Sigma-Aldrich, #H9269) and washed three times. The first two washes with the same setting (200 x *g*, 8 min, 22ºC) and the last with a lower setting (170 x *g*, 8 min, 22ºC) to clear away smaller cells, such as platelets. The cells were counted in 10 mL isotone solution with 2 drops of ZAP-OGLOBIN II (Beckman Coulter, #7546138) which lyse erythrocytes on Z2 Coulter Particle Count Analyzer (Beckman Coulter) on program B. The calculated volume of the cell suspension was centrifugated (800 x *g*, 7 min, 22ºC) and the pellet was resuspended in RPMI-1640 (Sigma) supplemented with 5% human serum. PBMCs were seeded at a concentration of 10 x 10^6 cells per well in 6-well plate (1 mL per well) and incubated for one hour to allow surface adherence to the well (5% CO_2, 37 ºC). After one hour of incubation, the cells were carefully washed three times with 1.5-2 mL HANKS (Sigma) to remove non-adherent cells. RPMI-1640 (Sigma) media supplemented with P/S (100 nM, Sigma) and 10% human serum was added and plates were incubated overnight (5% CO_2, 37 ºC). For monocyte- derived macrophages (MDMs), the cells were incubated with RPMI-1640 (Sigma) supplemented with 10% human serum, Macrophage colony-stimulating factor (M-CSF, 25 ng/mL, R&D systems, #216-MC) and 100 nM P/S (Sigma) for macrophage differentiation over four days.

THP-1 cells

THP-1, human leukaemia monocytic cell line was obtained from ATCC (TIB 202) and is referred as THP-1 wildtype (wt). They were maintained in RPMI-1640 (Sigma) complemented by β-mercaptoethanol (2-Mercaptoethanol, 50 µM, Sigma-Aldrich, #MG250), L-glut (200 mM), 10% fetal bovine calf serum (FCS, Gibco, #10270), HEPES (450 g/L, Gibco, #15630056), sodium-pyruvate (100mM, Sigma-Aldrich, #S8636), D (+) Glucose (1M, Sigma-Aldrich, #G8769), and P/S (100 nM, Sigma). Sublines of THP-1 cell line was also used in the study, made by Mariya Yurchenko and PhD student Kaja Nilssen (CEMIR, NTNU) using CRISPR/Cas9 SLAMF1 knock out cells transduced by lentiviral particles containing either pLVX-IRES-ZsGreen empty vector, or coding for SLAMF1 gene,

either wildtype or deletion mutant without IgV-like domain. Sublines are referred later as SLAMF1 KO with pLVX empty, SLAMF1 and ΔIgV. THP-1 and the sublines were incubated at 37 ºC in 5% CO_2 and split at 1:3 ratio every third day.

Both THP-1 and the sublines were spun down (400 x *g*, 5 min, 22ºC) and resuspended in THP-1 media RPMI-1640 (Sigma) supplemented with β-mercaptoethanol (50 µM, Sigma), L-glut (200 mM), 10% FCS, HEPES (450 g/L), sodium-pyruvate (100 mM), glucose (1M), and P/S (100 nM) prior to cell counting. The cells were counted using Coulter Counter (Beckman Coulter) on program C. Calculated cell suspension was centrifugated (400 x *g*, 5 min, 22ºC) and resuspended in growth medium, RPMI-1640 (Sigma) containing phorbol 12-myristate 13-acetate (PMA, 60 ng/ml) for cell differentiation. The cells were seeded at 0,2 x 10^6 and 0,5 x 10^6 in 24-well and 6- well plate respectively for 24 hours. Fresh media without PMA was added the following day and incubated for 48 hours prior to experiment.

HEK293T cells

HEK293T cells (human epithelial cells), were obtained from ATCC and maintained in Dulbecco's modified Eagle's medium (DMEM, BioWhittaker, #12-604F) supplemented with 10% FCS, P/S (100 nM) and L-glut (200 mM). The cells were incubated at 37 ºC, 8% CO_2 and split at 1:40 ratio every fourth day.

HEK293T were washed with 10 mL PBS and detached by adding 3 mL of pre-heated trypsin-EDTA solution (170 µ/l Trypsin 1:250, 0.2 g/L EDTA, BioWhittaker, #BE17-161E) for five minutes (8% CO_2, 37 ºC). A total of 15 mL of DMEM media (BioWhittaker) with 10% FCS was added to stop trypsinisation. FCS was added to stop trypsinisation. The cell suspension was resuspended where 14.5 mL was transferred to a 50 mL tube while 0.5 mL was remaining in the flask. The cells were split (1:40), while the cell suspension was diluted at approximately 1:4. Furthermore, the cells were counted on the cell counter (Beckman Coulter) in isotone solution on program B and seeded at 350 000 cells/well in 6-well plate and incubated overnight (8% CO_2, 37 ºC) prior to transfection by DNA constructs.

2.2.1 Flow cytometry of peptide pre-treated peripheral blood mononuclear cells

Flow cytometry can analyse single cells or particles through single or multiple lasers as the fluid stream pass the light source. The optical and fluorescence characteristics of the cells or particles are measured [50, 51]. The light scatter is measured in the forward direction, also called Forward Scatter (FSC) at 90º. The forward scatter shows the relative size of the cell, while Side Scatter (SSC) shows the complexity and granularity of the cell [51].

Flow cytometry was performed to assess the phagocytic effect of SLAMF1 and SLAMF1-derived peptides (P7-pen, P7G10-pen, and P7N4-pen) by monocytes, stimulated by fluorescent dye-conjugated bioparticles. The phagocytic activity was measured in respect to the uptake of the fluorescent bioparticles. When the bioparticle had been phagocytosed, it emitted fluorescence at a particular wavelength which was measured in the flow cytometry [52]. Additionally, the function of dectin-1 and complement mediated phagocytosis was also investigated as well as the effect of serum IgG in FCS by using low-IgG FCS.

Table 2.1: **Bioparticles and antibodies used in flow cytometry experiments**

Bioparticle/antibodies	Manufacturer; catalogue number
PHrodo™ E. coli Bioparticles™ conjugate for phagocytosis	Invitrogen by Thermo Fisher Scientific: P35361
PHrodo™ Red S. aureus Bioparticles™ conjugate for phagocytosis	Invitrogen by Thermo Fisher Scientific: A10010
Escherichia coli Bioparticles™ Alexa Fluor™ 488 conjugate	Invitrogen by Thermo Fisher Scientific: E13231
Zymosan A Bioparticles™ Alexa Fluor™ 488 conjugate	Invitrogen by Thermo Fisher Scientific: Z23373
PE rat IgG1, κ Isotype Ctrl Antibody	Biolegend: 400213
PE anti- mouse CD369 (Dectin-1/CLEC7A) antibody	Biolegend: 355404

2.2.2 Flow cytometry of SLAMF1 receptor

THP-1 cells were seeded and differentiated in THP-1 media RPMI-1640 (Sigma) with PMA (60 ng/mL) for 24 hours, and later incubated in PMA free media for 48 hours. The bioparticles were vortexed (10-15 sec) and sonicated (2 min, 23ºC, 5) and vortexed again (10-15 sec). The cells were stimulated with pHrodo-conjugated *E. coli* bioparticles (see **table 2.1**) for 60 min (5% CO_2, 37 ºC), and later placed on ice to stop the phagocytosis. The cells were washed with 1 mL cold PBS (Sigma) and detached by 700 µL Accutase treatment (Sigma-Aldrich, #A6964) for five minutes in room temperature (RT). The Accutase treated cells were gently scraped using cell scraper and transferred to Fluorescence-activated Cell Sorting (FACS) tubes, followed by centrifugation (1500 rpm, 5 min, 4 ºC). Next, the THP-1 cells were washed with 1 mL flow buffer (2% FBS in PBS) and resuspended in 1 mL flow buffer. The fluorescence intensity was measured with BD LSRII flow cytometer and FACS Diva software (BD Biosciences) and the data was analysed and interpreted with FlowJo (v.10).

2.2.3 Flow cytometry of SLAMF1 derived peptides without prior opsonisation of bioparticles

The monocytes seeded the previous day were incubated with 900 µl of the respective peptides (C3-pen (15 µM), P7-pen (15 µM), P7G10-pen (15 µM) or P7N4-pen (15 µM), 990 µM cytochalasin D (CytoD) and water (solvent control) in RPMI- 1640 (Sigma) supplemented with 10% human serum (A+) or 10% FCS for 30 minutes (5% CO_2, 37 ºC). Subsequently, the bioparticles were vortexed (10-15 seconds) and sonicated (2 min, 23ºC, 5) and vortexed again (10-15 sec). The cells were stimulated with pHrodo-conjugated *E. coli* (25 µl) and *S. aureus* (20 µl), Alexa Fluor 488 (AF488, 7 µl) and pHrodo conjugated *E. coli* (25 µl) and AF488- conjugated Zymosan (20 µl) and *E. coli* Bioparticles (see **table 2.1**) for 30- and 60- minute timepoints and later placed on ice to stop the phagocytosis. The cells were washed with 1 mL cold PBS (Sigma) and detached by 700 µL Accutase treatment (Sigma) for five minutes in room temperature (RT). The Accutase treated cells were gently scraped using cell scraper and transferred to FACS tubes, followed by centrifugation (1500 rpm, 5 min, 4 ºC). Next, the monocytes were washed with 1 mL flow buffer (2% FBS in PBS) and resuspended in 1 mL flow buffer. The fluorescence intensity was measured with BD LSRII flow cytometer and FACS Diva software (BD Biosciences) and the data was analysed and interpreted with FlowJo (v.10).

2.2.4 Flow cytometry of SLAMF1 derived peptides with opsonised bioparticles

The monocytes which were seeded the previous day and the monocyte derived macrophages (MDMs) with M-CSF (25 µg/mL) incubated for four days were incubated with 900 µl of 15 µM C3-pen (positive control) or P7-pen and water (solvent control) in RPMI-1640 (Sigma) supplemented with 10% FCS for 30 minutes (5% CO_2, 37 ^{0}C). Meanwhile, AF488 conjugated *E. coli* or Zymosan (see **table 2.1**) were vortexed and sonicated. 7 µl/per well of AF488 *E. coli* and 10 µl/per well of AF488 Zymosan A were opsonised in RPMI-1640 (Sigma) media supplemented with 30% human serum (A+) in 1.5 mL Eppendorf tubes. The bioparticles were shortly vortexed and incubated on water bath (37 ^{0}C) for approximately 25-30 min. 100 µL of AF488 conjugated *E. coli* or Zymosan bioparticles were added to the monocytes or macrophages and incubated (5% CO_2, 37 ^{0}C) for 30- and 60-minute time points. The remaining procedure follows as described above (2.2.3).

2.2.5 Flow cytometry of SLAMF1 derived peptides with opsonisation in compstatin-treated bioparticles

The cells were carefully washed with 2 mL of RPMI 1640 (Sigma) twice. Subsequently, the cells were incubated with RPMI-1640 (Sigma) media supplemented with 10% FCS and 15 µM P7-Pen peptide and water (solvent control) (5% CO_2, 37 ^{0}C) for 35 min. During incubation of cells, the respective treatments were prepared in respective Eppendorf tubes. This included untreated sample with media, supplemented with 10% FCS and AF488 conjugated *E. coli* bioparticles (see **table 2.1**). The other treatments were as following; opsonisation with normal human A+ serum, opsonisation with 2% heat inactivated A+ serum, opsonisation normal A+ serum with compstatin and lastly with only 10% FCS. Apart from the sample treated with compstatin, *E. coli* bioparticle (14/28 µL) was added to the Eppendorf tubes and opsonised in warm bath (37 ^{0}C). *E. coli* bioparticle (14/28 µL) was only added to the Eppendorf tube ten minutes before incubation period was done in compstatin treatment. 100 µl of the bioparticles were added to the cells and incubated for one hour (5% CO_2, 37 ^{0}C). The remaining procedure follows as described in (2.2.3).

2.2.6 Flow cytometry of FCS and human serum treated monocytes

The method follows the one described in 2.2.5, but with modifications in peptide and treatments. 15 µM of P7-pen or C3-pen were incubated in media with 10% FCS, 1% FCS, normal A+ serum and heat inactivated A+ serum respectively for 30 minutes (5% CO_2, 37 ^{0}C). Meanwhile, AF488 conjugated *E. coli* bioparticles (7 µl/per well) (see **table 2.1**) were prepared in normal A+ human serum and heat inactivated A+ serum and incubated at water bath for 30 minutes (37 ^{0}C). 100 µl of bioparticle was added dropwise to respective well and incubated for 60 minutes (5% CO_2, 37 ^{0}C). The remaining procedure follows as described in (2.2.3).

2.2.7 Flow cytometry of SLAMF1 derived peptides with 10% FCS of normal and low IgG treated bioparticles

The cells were carefully washed with 2 mL of RPMI-1640 (Sigma) twice. 15µM P7-pen or C3-pen in RPMI-1640 (Sigma) media supplemented with 10% FCS for 30 minutes (5% CO_2, 37 ^{0}C). AF488 conjugated *E. coli* bioparticles (approximately 7,4 µl/per well) (see **table 2.1**) was incubated with 10% FCS with normal or low IgG levels in RPMI-1640 (Sigma) media. 100 µl of the bioparticles were added to the cell for 30- and 60-minute timepoints. The remaining procedure follows as described in (2.2.3).

2.2.8 Flow cytometry of THP-1 cells, monocytes and macrophages stimulated with monocytes and macrophages

For dectin-1 stimulated flow cytometry, the cells were primarily washed with 1 mL cold PBS on ice and treated with 700 µl Accutase (Sigma) for five minutes (5% CO_2, 37 ^{0}C). The Accutase treated cells were scraped with a cell scraper and the suspension was transferred to FACS tubes and spun down (1500 RPM, 5 min, 4 ^{0}C). The suspension was discarded and washed with flow buffer (2% FBS in PBS) and pelleted once more (1500 RPM, 5 min, 4 ^{0}C) and the supernatant discarded. 2 µl of IgG and α-dectin-1 (see **table 2.1**) was added and incubated on ice for 30 minutes avoiding direct sunlight. Thereafter, the cells were diluted with 1 mL flow buffer and spun down twice (1500 RPM, 5 min, 4 ^{0}C). The pellet was diluted in 400 µl cold PBS and vortexed before measuring the fluorescence with BD LSRII flow cytometer and FACS Diva Software (BD Biosciences). The data was analysed and interpreted with FlowJo Software (v.10).

2.3 Phagocytic assay of live bacteria

Phagocytic assay was performed to investigate the phagocytic efficiency of C3-pen, P7-pen, or P7G10-pen in THP1-wt infected cells by Gram- negative *E. coli* (DH5α) and Gram-positive *S. aureus* (wood strain, protein- A deficient). DH5α is RecA and Endonuclease 1 deficient, which employs the strain with genetic stability and reduced endogenous nuclease activity [53]. The wood strain is protein A deficient and has reduced virulence [54]. The role of overexpressed SLAMF1 in phagocytosis of *E. coli* was investigated using THP-1 sublines SLAMF1 KO with overexpressed empty vector or Crispr/Cas9-resistant construct of SLAMF1 or SLAMF1 ΔIgV.

To investigate the phagocytic efficiency of the peptides, media with the peptide solvent (sterile H_2O) were used as negative control, 15 µM of C3-pen (positive control), P7-pen, P7G10-pen, and P7N4-pen were utilised.

Table 2.2: **Peptides used in live bacteria uptake experiments**

Peptides	Stock concentration (µM)	Volume (µl)
C3-pen	1000	Volume that gives 15 µM
P7-pen	500	Volume that gives 15 µM
P7G10-pen	1000	Volume that gives 15 µM
P7N4-pen	1000	Volume that gives 15 µM

2.3.1 Live bacteria uptake of *E. coli* and *S. aureus* in THP-1 cells pre-treated with SLAMF1-derived peptides

One colony of *E. coli* (DH5α) or *S. aureus* (wood strain) was incubated in 3 mL Lysogeny broth (LB) media a day prior to the experiment (250 RPM, 37^{0}C). 400 µl of bacteria was diluted in 25 mL LB media and incubated (250 RPM, 37^{0}C) until cultures reached an optical density of 0.35-0.42 (*E. coli*) and 0.30-0.34 (*S. aureus*). The peptides (C3-pen,

P7-pen, and P7G10-pen) were thawed and spun shortly (max velocity, 22 ºC) to retrieve as much peptide as possible.

10 mL of bacteria culture was spun down (max velocity, 15 min, 4 ºC), and 500 µl of warm RPMI-1640 (Sigma) media supplemented with (200 mM L-glut, 10% FCS, water/peptide) was added to 24-well plate and incubated for 30 min (5% CO_2, 37 ºC). After centrifugation of bacteria, the pellet was transferred to an Eppendorf tube (1.5 mL) and washed with 1 mL of cold PBS three times (max velocity, 1 min, 22 ºC). Bacteria pellet was diluted in 500 µl (*E. coli*) and 900 µl (*S. aureus*) PBS and shortly vortexed before it was placed on ice. Next, the 24-well plate was put on ice and 500 µl of cold RPMI-1640 (Sigma) media supplemented with (200 mM L-glut and water/peptide) was added, and subsequently 25 µl of bacteria stock to the respective wells. The bacteria were spun down (1900 RPM, 7 min, 4 ºC) onto the cell layer and later put on warm bath (37ºC) for 15 minutes to facilitate phagocytosis.

1 mL of warm RPMI-1640 (Sigma) media supplemented with (200mM L-glut, 10% FCS and water/peptide) was added to the 6-well plate for 30 min (5% CO_2, 37 ºC). Followingly the 24-well plate was put on ice and washed with approximately 1 mL cold PBS (three times) to remove extracellular bacteria. 1 mL of warm RPMI-1640 (Sigma) media supplemented with (1:400, 40 mg/mL Gentamicin (Sanofi-Aventis, #453130) and 10% FCS) was added and the plate incubated for 30 min (5% CO_2, 37 ºC). Gentamicin was supplemented in the media to remove remaining bacteria in the well by antibiotics treatment. After 30 min incubation, 50 µl of bacteria was added to the 6-well plate and incubated for one hour (5% CO_2, 37 ºC).

Subsequently, the 24-well plate was put on ice and the cells were washed with approximately 1 mL cold PBS (three times). The cells were washed to essentially make sure there were no antibiotics when the cells were lysated. 1 mL distilled water was added to the wells for 20 min which lysate the cells and release phagocytosed bacteria. Additionally, 100µl of 1X Radioimmunoprecipitation assay buffer (RIPA) was added to the last two rows for total protein quantification by BCA assay (see 2.4). The plate was shaken regularly during incubation time. The 1X RIPA lysates were transferred to Eppendorf tubes and stored in - 20ºC. The remaining lysates were vortexed, and serial diluted in PBS (D1, 1:20, D2, 1:10) and the bacteria stock were diluted 5x (D1, 1:40, D2, 1:20, D3, 1:20, D4, 1:10, D5, 1:4). 10 µl of D4 and D5 of bacteria stock were seeded on LB agar plates. 10 µl of D1 and D2 of the *E. coli* lysates, or undiluted, D1 and D2 of the *S. aureus* lysates were seeded on LB agar plates. The plates were incubated overnight (5% CO_2, 37 ºC) and counted in colony-forming units (CFU).

The 6-well plate was placed on ice and washed with approximately 2 mL cold PBS (three times) to remove the bacteria, since it was not treated with gentamicin. The cells were lysated with 500 µl QIAzol lysis reagent (QIAzol, QIAGEN sciences, #79306) for five minutes in RT and transferred to 1.5 mL RNAse free Eppendorf tubes. The sample were stored in -80ºC and total mRNA levels were analysed (see 2.5)

2.4 BCA assay

BCA assay was performed on the cell lysates with RIPA buffer treatment from the phagocytic assay experiment. The colorimetric assay, following microplate procedure in Pierce™ BCA Protein Assay Kit determined the total protein concentration in the cell lysates. The data presented was used to normalise data from the phagocytic assay.

The cell lysates were thawed and centrifugated (max velocity, 15 min, 4 ºC). Subsequently, the supernatant was collected in new Eppendorf tubes and 25 µl of BCA standards and sample was added to flat bottom 96-well plates. 200 µl of working reagent

(1:20) was added and mixed well on a plate shaker for 30 seconds. The plate was subsequently incubated (5% CO_2, 37 ^{0}C) for 30 minutes and the absorbance was measured near 562 nm on a plate reader (Bio-Plex, Bio-Rad Laboratories Inc.).

2.5 RNA isolation and counting, cDNA synthesis and qPCR

Real-time polymerase chain reaction (qPCR) was performed to investigate the cytokine production/expression of the infected THP-1 cells and compstatin treated monocytes.

Total RNA isolation of the cells was performed using QIAzol lysis reagent (Qiagen). RNA was extracted following the manufacturers protocol. The cells were extracted with chloroform, followed by purification and DNase digestion using RNeasy Mini Kit (Qiagen, #74104). RNA concentration and purity of the isolated RNA was quantified using NanoDrop ND-1000 spectrophotometer (Saveen Werner).

cDNA was synthesised by converting RNA to cDNA following the manufacturer's protocol for RNA High-Capacity RNA-to-Cdna™ kit (Applied Biosystems, Vilnius, Lithuania). RT-qPCR was carried out using PerfeCTa qPCR FastMix (Quanta Biosciences, #733-1394). To explore the production of pro-inflammatory cytokines and *IFN-β* in the samples, *IFN-β* (Hs01077958), *TNFa* (Hs000174128) and the endogenous control TATA-Box Binding Protein (*TBP*, Hs00427629) from TaqMan Gene expression Assay (Applied Biosystems, Bleiswijk, Netherlands) were used. RT-qPCR was run on replicates with StepOnePlus real-time PCR cycler (Applied Biosystems), and gene expression was calculated as fold change normalised against TBP.

2.6 Transfection and immunoprecipitation from HEK293T and endogenous precipitation of monocytes

Transfection is the process of introducing nucleic acid, either DNA or RNA into cells and change the property of the cell. This allows the study of protein expression [55]. In this study, HEK293T cells were used as transfected cells. Transfection can be divided into transient and stable transfection. In transient transfection, the nucleic acid is not integrated into the genome and only exists for a limited time. Stable transfection introduces DNA into the cellular genome or through an episomal plasmid [56]. This study utilises transient transfection. HEK293T cells were transfected the next day with respective plasmids once the cells had reached a confluence of 30-40%.

2.6.1 Endogenous precipitation of monocytes

80 µl of NeutrAvidin™ Agarose Resin beads (Thermo Fisher Scientific;29201) were transferred to three Eppendorf tubes and 160 µl of beads to the last tube for pre-clearance and washed with 1 mL PBS twice (2000xg, 1 min, 4 ^{0}C). Next, 400 µl of PBS and 20 µl of pen, P7-pen, or P7G10-pen to the three tubes, and 600 µl of PBS and 40 µl of pen was added to the pre-clearance tube and rotated in RT for 60 min (16 RPM). The pre-clearance tube was washed with 1 mL 1X RIPA buffer twice (2000xg, 1 min, 4 ^{0}C) and transferred to a 15 mL tube, centrifugated (2000xg, 1 min, 4 ^{0}C) and kept on ice.

Monocytes from donor were seeded with 30% human A+ serum in RPMI-1640 media (Sigma). The cells had a concentration of 50 mill PBMC/10 cm^2 dish. The monocytes were washed with 1 mL PBS and lysated with 1 mL 1X RIPA buffer with inhibitor (see **table 2.3**). The dish was places on shaker (600 RPM) to cover the whole cell layer for 15 min at 4 ^{0}C. 1X RIPA with inhibitors is a chemical reagent which lyse the monocytes and gives access to the proteins expressed in the cells. After 15 min incubation, the lysates were collected in pre-cooled Eppendorf tubes and spun down (20 000xg, 15 min, 4 ^{0}C).

The lysates were transferred to the pre-clearance tube (15 mL) with beads and rotated for 30 min in 4 ºC. Subsequently, the pre-clearance tube and peptides with beads were centrifugated (200xg, 1 min, 4 ºC) and the total volume were measured. 120µl of lysate were aliquoted for loading control for gel and NaCl was added to the pre-clearance tubes to a final concentration of 300 mM (additional 150 mM) and distributed between the three tubes with peptides on beads.

The peptide/beads tube were precipitated for 45 min on rotation in 4 ºC and subsequently washed 3 times with 1X RIPA (300 mM NaCl) and 2 washes with buffer A and buffer B from the kit (Pierce™ MS-Compatible Magnetic IP Kits, Thermo Fisher Scientific, #90408) (0.5 mL each). The pen/beads tubes were centrifugated (200xg, 1 min, 4 ºC) and all leftover of washing buffer was removed.

60 µl of elution buffer was added per tube and vortexed every 1 min (5 min in total) in RT. The Eppendorf tubes were centrifugated and the eluates were collected to new tubes. 60 µl of elution buffer was added once more and vortexed again. The eluates were collected to the same tubes. The Eppendorf tubes were centrifugated once more from residual beads, and 40 µl of 4 NuPAGE® LDS sample buffer (4X) (Thermo Fisher Scientific: NP0007) and 100 mM dithiothreitol (DTT, Thermo Fisher Scientific: R0862) was added and the samples were heated for 7 min at 80 ºC. Thereafter, the cooled tubes were centrifugated (2000xg, 30 sec, 4 ºC) and supernatant transferred to fresh tubes. The samples were ready to be run on electrophoresis.

2.6.2 Transfection of HEK293T cells

50 µl-100 µl OptiMEM (Gibco Life Technologies;11058021) and 1.5-4 µl Genejuice (Novagen;70967) per well were mixed, vortexed for 2 sec and incubated in Eppendorf tubes at RT for five minutes. HEK293T cells were transfected with concentration ranging from 200-1600 ng Rab14 or 200-800 ng RhoG, 100 ng empty flag and Rab11 and subsequently transferred to the respective tubes. The transfection mix was transferred to the Eppendorf tubes with plasmids and incubated at RT for 15 minutes. 100 µl of the mixture was added dropwise to the respective wells and incubated (8% CO_2, 37 ºC) for 24 hours. The cells were rested in fresh optiMEM (Gibco) media (1 mL) for 48 additional hours (8% CO_2, 37 ºC).

2.6.3 Immunoprecipitation by biotinylated peptides

Immunoprecipitation (IP) is a technique commonly used to purify antigens using an immobilised antibody to a solid support, such as magnetic particles or agarose resin. It is widely used for protein isolation from i.e., cell lysates for further detection by western blot.

In this study the peptide is immobilised onto the insoluble support, the agarose resin against the target protein in the cell lysates. Gentle agitation during the incubation period allows binding of the target protein and the immobilised peptide which is then eluated from the agarose resin and analysed [57]. The peptides (pen, P7-pen, or P7G10-pen) were immobilised by a biotin tag through the binding of neutravidin beads.

80 µl of NeutrAvidin™ Agarose Resin beads (Thermo Fisher Scientific) were transferred to the selective Eppendorf tubes and washed with 1 mL PBS twice (2000xg, 1 min, 4 ºC). Next, 600 µl of PBS and 45 µl of pen and P7-pen and 22 µl of P7G10-pen was added to the respective Eppendorf tubes and rotated in RT for 45 min (16 RPM).

The cells were washed with PBS (1-1,5 mL). The plate was put on ice and 200 µl of 1X RIPA (with inhibitors) were added to each well. The content of 1X RIPA with inhibitors are presented in **table 2.3**. The 6-well plate were placed on shaker (600 RPM) to cover the

whole cell layer for 15 min at 4 ºC. After 15 min incubation, the lysates were collected in pre-cooled Eppendorf tubes and spun down (20 000xg, 15 min, 4 ºC). 60 µl of the lysate were transferred to Eppendorf tubes which were used as lysate control. 20 µl of NuPAGE® LDS sample buffer (4X) (Thermo Fisher Scientific) and 100 mM DTT (Thermo Fisher Scientific) was added, while the remaining lysates were transferred to another set of Eppendorf tubes.

Next step was pre-clearance which remove potential reactive components prior to the immunoprecipitation [57]. The tube with pen/bead/PBS was shortly spun (2000xg, 1min, 4 ºC) and the supernatant was discarded. The beads were washed with 1 mL 1X RIPA twice (2000xg, 30 sec, 4 ºC). After the last wash 1 mL of 1X RIPA resuspended and transferred to a 15 mL tube. 2 mL of 1X RIPA was added and evenly distributed to the Eppendorf tubes. The tubes were spun down again (2000xg, 30 sec, 4 ºC) and supernatant was discarded. The remaining lysates were added to the Eppendorf tubes and subsequently rotated for 30 min (16 RPM) at 4 ºC. Similarly, the pen/bead, P7-pen/bead and P7G10-pen/bead were washed.

The pre-clearance tube (pen/bead/lysate) were spun shortly (2000xg, 30 sec, 4 ºC) and the lysates were transferred to new pre-cooled Eppendorf tubes. The volume of the lysates was checked and the respective volume of NaCl (5 mM, 1:33) was added. NaCl was added to prevent protein aggregation [58]. The volume of lysate and NaCl was distributed between the peptide/bead tubes for precipitation by P7-pen or P7G10-pen (16 RPM, 45 min, 4 ºC, rotation). NaCl was added to increase the specific binding between the target protein and peptide. Beads were spun (2000xg, 30 sec, 4 ºC) and the supernatant with unbound molecules discarded with vacuum aspirator (INTEGRA Vacusafe). The immunoprecipitants were washed five times with 1 mL 1X RIPA (with 400 mM NaCl) to remove remaining unbound molecules. After the last wash, the precipitates were spun once more to remove as much supernatant as possible.

Target proteins were eluated from the beads by adding 90 µl of 1X LDS (Thermo Fisher Scientific) with 100 mM DTT (Thermo Fisher Scientific), input control and eluates were heated for 7-8 min (80 ºC). Then the tubes were cooled down and centrifugated (2000xg, 30 sec, 4 ºC). The supernatant was transferred to fresh Eppendorf tubes. The samples were ready to be run on electrophoresis and further identification by Western Blot (WB).

Table 2.3: **Recipe for 1X RIPA buffer with inhibitors**

Reagent	Amount	Manufacturer, Catalogue number
Pierce™ Protease inhibitor tablets, EDTA-free	1 tablet	Thermo Fisher Scientific; A32965
Phosphatase inhibitors (PhosSTOP EASYpack)	1 tablet	Roche;04906837001
NaF	0.5 mL (50 mM)	Sigma Aldrich;201154
Na_3VO_4	0.1 mL (2 mM)	Sigma Aldrich; S6508
2X RIPA buffer Tris/HCl pH 7.5 (100 mM) NaCl (300 mM) EDTA pH 8.0 (10 mM) Triton X-100 (2%)	5 mL 1X RIPA: Tris/HCl (50 mM) NaCl (150 mM) EDTA (5 mM) Triton X-100 (1%)	 Sigma Aldrich; 648317 Gibco; 24740011 Sigma Aldrich; 324506 Sigma Aldrich; I8896
MilliQ water	To 10 mL	Merck Millipore

2.6.4 Transfection of SLAMF1 receptor

The interaction of Rab14 and RhoG with SLAMF1 was investigated through co-immunoprecipitation. Instead of Neutravidin beads, Sigma Agarose beads (Sigma-Aldrich, #M8823 were utilised. HEK293T cells were transfected with 100 ng empty flag, SLAMF1/CD150 pcDNA3.1 wt and SLAMF1 with deleted C-terminal (CD150 Δct) with Rab14 and RhoG in DYKDDDDK-N terminal vector (Takara Bio).

Transfection of the HEK293T follows the procedure described in 2.6.2.

Immunoprecipitation of SLAMF1

HEK293T cells were washed and lysated as described (see 2.6.2). 40 µl of Sigma-M2 agarose beads (Sigma-Aldrich) were transferred to the selective tubes and pelleted (2000 x *g*, 30 sec). The beads were washed with 1 mL 1X RIPA twice (2000 x *g*, 30 sec). The beads were transferred to 15 mL tube and diluted in 6.2 mL 1X RIPA buffer. 1 mL of the solution were aliquoted between six Eppendorf tubes and spun (2000 x *g*, 30 sec). The supernatant was discarded.

HEK293T lysates were transferred to cold Eppendorf tubes and centrifugated (20 000 x *g*, 15 min, 4 ºC). The lysates were transferred to new Eppendorf tubes, where 45 µl was used as lysate control. 15 µl of 4x LDS (Thermo Fisher Scientific) with 100 mM DTT (Thermo Fisher Scientific) was added to the control. The remaining lysates was added to the agarose beads and precipitated for three hours (16 rpm, 4 ºC, rotation). Lysate control was heated (80 ºC, 7 minutes) and stored at (4 ºC).

After three hours rotation, the beads (lysate/target protein) were pelleted (2000 x *g*, 30 sec) and supernatant discarded. The IPs were washed with 1X RIPA five times (2000 x *g*, 30 sec). After the last wash, the tubes were spun down and the remaining supernatant discarded. 50 µl of 1X LDS (Thermo Fisher Scientific) was added to the samples and heated (80 ºC, 7 minutes) to elute the immunocomplexes. After the samples had cooled down, they were centrifugated shortly (max velocity) and the lysates were transferred to clean tubes. 1,5 µl 1M DTT (Thermo Fisher Scientific) was added and heated again (80 ºC, 7 minutes) prior to loading on the gel.

2.7 Gel electrophoresis and western blot analysis of immunoprecipitates and Simple Blue staining

Western Blot was performed to visualise co- precipitations of RhoG and Rab14 with the respective peptides, but also with SLAMF1.

The lysates and immunoprecipitations were separated by 4-12% NuPAGE Bis-Tris gels (Invitrogen; 10-well, #NB0321BOX, 20- well, #WB1402BOX). 5µl of SeeBlue™ PreStained protein standard (Invitrogen; LC5925) and 1 µl Magic Mark™ Western Protein Standard (Invitrogen; LC5603) were used as ladder and the gel(s) were run in 1X MES buffer for 25 min at 90V and 1.35 h at 190 V.

The proteins in the gel were transferred to a nitrocellulose membrane, using iBlot regular transfer stacks (Invitrogen regular, #IB23001) and the iBlot™ Gel transfer device (Invitrogen, #IB21001) instrument on the P0 template program for seven min. The nitrocellulose membrane was washed with 1X Tris-Buffered Saline, 0.1% Tween (TBST) and blocked with blocking buffer (5% milk) for minimum of 40 minutes and up to one hour. After blocking, the membrane was rinsed with TBST until there was no remaining blocking buffer left. The blot was incubated with primary antibody overnight (diluted following the manufacturer' datasheet) (50 rpm, 4 ºC) and washed with TBST three times

(4 min) the next day. Secondary antibody was incubated for one hour followed by washing with TBST three times (4 min). Table with primary and secondary antibody is listed in **table 2.4**. The blots were developed using Super Signal West Femto Maximum Sensitivity Substrate (Thermo Fisher Scientific, #34095) and visualised in LI-COR Odyssey imager.

Table 2.4: **Primary and secondary antibodies used for western blot**

Gene	Primary antibody (manufacturer, origin, dilution, diluent)	Secondary antibody (manufacturer, origin, dilution, diluent)
IRAK1	Monoclonal anti-IRAK1 antibody Cell signalling Technology (#4504), rabbit, 1:500, 5% BSA in TBS-T	Polyclonal Swine Anti-Rabbit Immunoglobulins/HRP DAKO (P0399), 1:4000, 1% BSA in TBS-T
IRAK4	Polyclonal anti- IRAK4 antibody MRC PPU (#5522C), goat, 1:1000, 5% BSA in TBS-T	Polyclonal Rabbit Anti-Goat Immunoglobulins/HRP DAKO (P0449), 1:2000, 1% BSA in TBS-T
TIRAP	Polyclonal anti-TIRAP antibody Invitrogen (#PA 588657), goat, 1:1000, 5% BSA in TBS-T	Polyclonal Rabbit Anti-Goat Immunoglobulins/HRP DAKO (P0449), 1:2000, 1% BSA in TBS-T
TRAM	Gentex (#GTX 112785), rabbit, 1:1000, 5% BSA in TBS-T	Polyclonal Swine Anti-Rabbit Immunoglobulins/HRP DAKO (P0399), 1:4000, 1% BSA in TBS-T
RhoG	Monoclonal anti-RhoG antibody Cell Signalling Technology (#60370), rabbit, 1:1000, 5% BSA in TBS-T	Polyclonal Swine Anti-Rabbit Immunoglobulins/HRP DAKO (P0399), 1:4000, 1% BSA in TBS-T
Cdc42	Polyclonal anti-Cdc42 antibody SCBT (#sc-87), rabbit, 1:1000, 5% BSA in TBS-T	Polyclonal Swine Anti-Rabbit Immunoglobulins/HRP DAKO (P0399), 1:4000, 1% BSA in TBS-T
B- tubulin	Polyclonal anti-β-tubulin-loading control Abcam (ab6046), rabbit, 1:10000, 5% BSA in TBS-T	Polyclonal Swine Anti-Rabbit Immunoglobulins/HRP DAKO (P0399), 1:4000, 1% BSA in TBS-T
Vav1	Monoclonal anti-Vav1 antibody Cell Signalling Technology (#4657), rabbit, 1:1000, 5% BSA in TBS-T	Polyclonal Swine Anti-Rabbit Immunoglobulins/HRP DAKO (P0399), 1:4000, 1% BSA in TBS-T
EHD4	Polyclonal anti-EHD4 antibody NOVUS (#NBP1-54873), rabbit, 1:1000, 5% BSA in TBS-T	Polyclonal Swine Anti-Rabbit Immunoglobulins/HRP DAKO (P0399), 1:4000, 1% BSA in TBS-T

SLAMF1	SinoBiological (#10837-R008, rabbit, 1:500, 5% BSA in TBS-T	Polyclonal Swine Anti-Rabbit Immunoglobulins/HRP DAKO (P0399), 1:4000, 1% BSA in TBS-T
Flag	Monoclonal anti-flag M2 antibody Sigma-Aldrich (F1804), mouse, 1:3000, 5% BSA in TBS-T	Polyclonal Goat Anti-Mouse Immunoglobulins/HRP DAKO (P0447), 1:5000, 1% BSA in TBS-T
Flag	DYKDDDDK Tag antibody Cell Signalling Technology (#14793), rabbit (anti DYKDDDDK tag), 1:3000, 5% BSA in TBS-T	Polyclonal Swine Anti-Rabbit Immunoglobulins/HRP DAKO (P0399), 1:4000, 1% BSA in TBS-T

Staining of Simple Blue staining

When the lower band from the gel electrophoresis had reached the buffer entrance, the gel electrophoresis was stopped. The gel was cut between the two bands and transferred to box with distilled water. The gel was heated in microwave for 1.30 minutes three times. SimplyBlue ™ safe stain (Invitrogen, #LC6060) was added to the gel and heated until it started to bubble. The gels were incubated on shaker for five minutes (50 RPM) and later changed with distilled water. Proteins in biotinylated peptides were quantified by Image Studio Software the following day.

3. Results

3.1 Analysis of bacterial particles uptake by flow cytometry

Phagocytosis assay can be evaluated by the measurement of engulfed fluorescent bacterial particles or Zymosan particles by flow cytometry [59].This approach was used in phagocytic assays presented below to evaluate the effect of SLAMF1 overexpression, or effect of treatment by SLAMF1-derived peptides on phagocytosis by THP-1 cells, human monocytes, or macrophages. THP-1 cells were differentiated to macrophage like cells using PMA as described in methods. Human monocytes were isolated from buffycoats obtained from blood bank St. Olavs Hospital one day prior to the experiment. Macrophages were obtained by differentiation of human monocytes in media containing 10% human serum and M-CSF (25 ng/ml) for four days. After stimulation of cells with bioparticles the cells were extensively washed by PBS and detached from the plate by Accutase treatment. Fluorescent intensity that correlated with number of phagocytosed particles was measured using flow cytometer.

3.1.1 SLAMF1 overexpression does not affect uptake of *E. coli* bioparticles by THP-1 cells

In murine macrophages SLAMF1 acts as a bacterial sensor and is involved in the clearance of Gram-negative bacteria by recognition of porins and contributing to phagocytosis [60, 61]. Interaction of murine SLAMF1 with bacterial porins is mediated by the N-terminal IgV-like domain of murine SLAMF1 [61]. Human SLAMF1, however, is not expressed on monocyte and macrophage surface without activation of the cells. Moreover, IgV-like domain of human SLAMF1 differ from such domain of murine receptor as only human SLAMF1 serve as receptor for measles virus [62]. Human SLAMF1 was not tested for interactions with bacterial porins and may not function as a bacterial sensor. A previous study showed that SLAMF1 silencing in human macrophages did not affect the uptake of *E. coli* particles, which could be linked to the intracellular localisation of SLAMF1 in inactive human macrophages [43]. It is not known if surface SLAMF1 will affect phagocytosis. SLAMF1 is highly upregulated on the cell surface of monocytes and macrophages after stimulation by PRR ligands. We have used overexpression system in THP-1 cells to mimic surface SLAMF1 expression on activated monocytes/macrophages and address the possible contribution of surface SLAMF1 to phagocytosis of *E. coli* bacterial particles.

THP-1 sublines were generated in Trafficking group, CEMIR. We have used pHrodo conjugated *E. coli* bioparticles in the assays. These bioparticles have high fluorescence intensity when they get to the compartment with low pH (phagosomes). Analysed sublines included: THP-1 wild type (WT) cells, THP-1 SLAMF1 knock out cells (SLAMF1 KO) with re-introduced full size SLAMF1, or mutant SLAMF1 ΔIgV (IgV-like domain), or empty vector. Vector in addition is coding for ZsGreen protein, which allows to compare the level of its expression between sublines (**figure 3.1A**). Uptake of bacterial *E. coli* bioparticles (not opsonised by serum proteins) was addressed in 60 min of incubation of PMA differentiated cells (**figure 3.1B**).

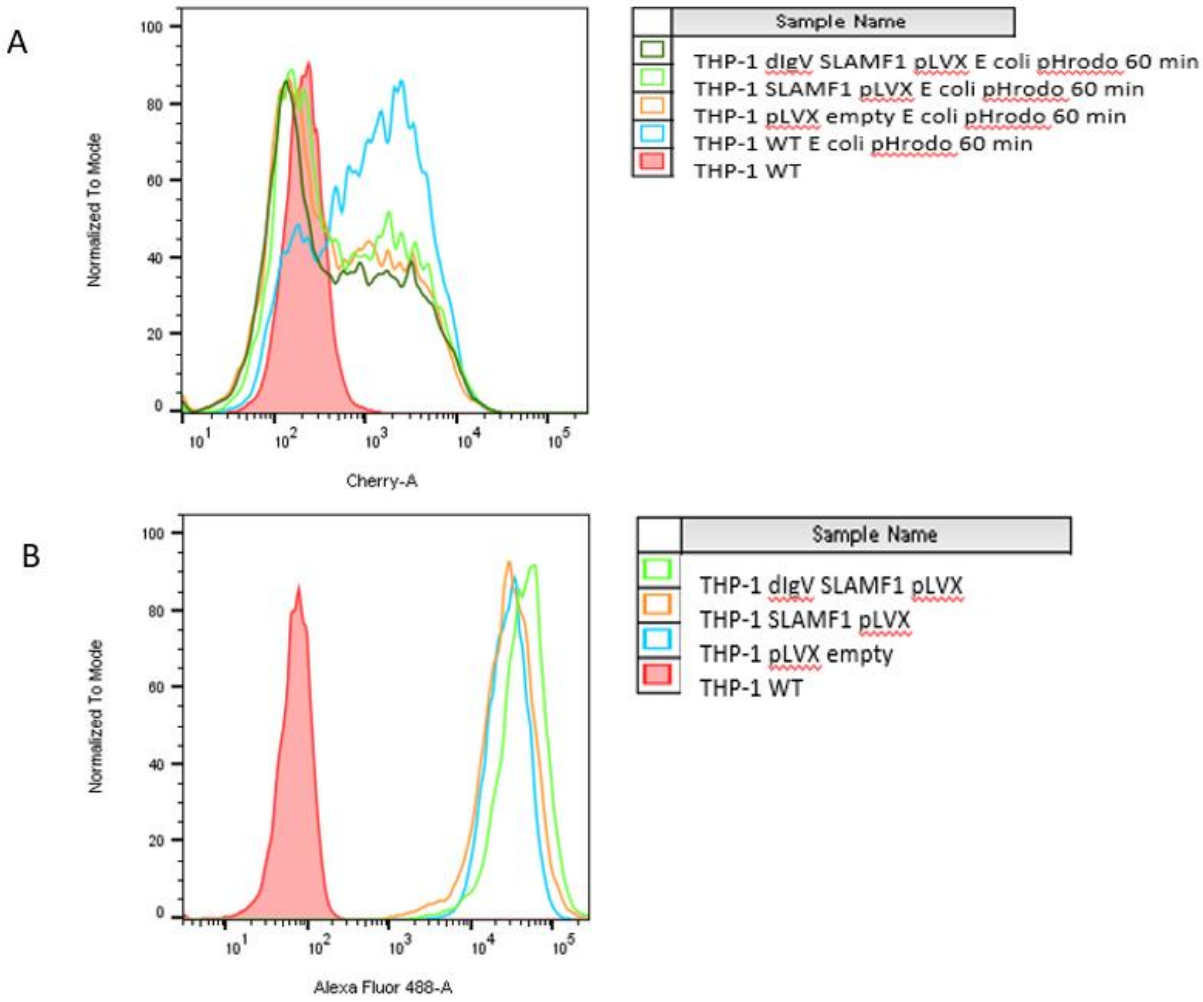

Figure 3.1: **SLAMF1 overexpression in THP-1 cells does not affect phagocytosis of *E. coli* bioparticles.** Differentiated THP-1 cells (sublines indicated by different line colour as presented in the table on the right) were incubated with pHrodo conjugated *E. coli* bioparticles for 60 min, detached by Accutase and analysed using flow cytometry approach. (A) Graph for the red channel to address pHrodo particles uptake, normalised to mode in FlowJo software with untreated THP-1 WT cells for negative control. (B) ZsGreen expression analysis in THP-1 sublines. One independent experiment.

The graph shows an overall decrease in fluorescence intensity for all THP-1 SLAMF1 KO sublines compared to THP-1 WT cells, which could be induced by viral transduction that was applied for the generation of KO cells and further overexpression of different constructs. THP-1 pLVX empty (empty vector), SLAMF1 pLVX (SLAMF1 WT) and SLAMF1 ΔIgV pLVX (mutant SLAMF1) cells have demonstrated similar levels of bacterial particles uptake in 60 min of co-incubation with particles (**figure 3.1A**). pLVX vector was expressed at the same level in all three THP-1 sublines (**figure 3.1B**). Thus, SLAMF1 overexpression or deletion of its IgV-like domain had no effect on *E. coli* bioparticles uptake.

3.1.2 P7-pen peptide inhibits uptake of bacteria particles by primary human monocytes

A preliminary experiment testing the regulation of bacteria particles uptake with P7-pen peptide (see **figure 1.2**) with the help from confocal microscopy showed reduced uptake of *E. coli* bioparticles by primary human monocytes. Here we have tested the possibility to inhibit phagocytosis by SLAMF1 derived peptides using flow cytometry approach. Several variants of the P7-pen peptide (P7N4 and P7G10, see **table 1.1**) were previously shown to have different efficacy in inhibiting TLR4-mediated signalling (data not shown),

and we included these peptides to some of the experiments to explore their effect on phagocytosis.

Monocytes were isolated from buffy coats of healthy blood donors one day prior to the experiment. The monocytes were pre-treated with 15 μM P7-pen or C3-pen and 3 or 10μM of CytoD. C3-pen which is similar to P7-pen in amino acid composition, but lacks anti-inflammatory effect, was used as a negative control (control peptide) (see **table 1.1**). CytoD is an inhibitor of actin polymerisation, reducing the number of internalised bacteria [63] and was used as a positive control of phagocytosis inhibition. In some experiments water was added instead of peptide as a solvent control, instead of control peptide. Subsequently, the monocytes were stimulated with pHrodo-conjugated *E. coli* and *S. aureus* bioparticles (not opsonised by serum proteins) for 30- and 60- min to evaluate the kinetics of the bacterial uptake. By using both *E. coli* and *S. aureus* bioparticles, we aimed to explore if P7-pen peptide is a specific inhibitor of Gram-negative bacteria uptake or if it also could affect the uptake of Gram-positive bacteria.

The experiment was performed twice with the cells from overall three donors. Flow cytometry data for one of the donors is shown on **figure 3.2,** with graphs and quantification for other two donors shown in supplementary (**supplementary figure 7.1**).

Overall, **figure 3.2** (and **supplementary figure 7.1, S1** and **S2**) show a substantial decrease in percentage of positive cells and mean fluorescence intensity (MFI) for *E. coli* and *S. aureus* particles in monocytes pre-treated by P7-pen peptide or CytoD phagocytosis inhibitor when compared to cells pre-treated with control peptide C3-pen. Thus, P7-pen was inhibiting phagocytosis of both *E. coli* and *S. aureus* particles by human primary monocytes.

P7N4-pen is a P7-pen variant with a tyrosine (Y) and asparagine (N) substitution at position 4 (see **table 1.1**), which was shown to bind different set of proteins than P7-pen in mass spectrometry assays performed by CEMIR researchers and was not able to inhibit TLR4-mediated cytokine expression (data not shown). One set of preliminary experiments was performed to explore and compare the phagocytic effect by P7N4-pen with P7-pen peptide. Monocytes isolated from the buffy coats were pre-treated with water (solvent control), 15 μM P7N4-pen or P7-pen and later stimulated with pHrodo conjugated *E. coli* and *S. aureus* bioparticles (not opsonised by serum proteins) for 30- or 60- min. The results are presented in supplementary (**supplementary 7.1, S3**). Both *E. coli* and *S. aureus* bioparticles induced strong MFI increase and high percentage of positive cells for monocytes pre-treated with P7N4-pen at 60 min. On the other hand, P7-pen had considerably low percentage of positive cells for both types of particles for both 30- and 60- min. This indicates that P7N4-pen has decreased inhibitory activity towards bacterial phagocytosis when compared to P7-pen, which correlates with the different interactome for these peptides in mass spectrometry assays.

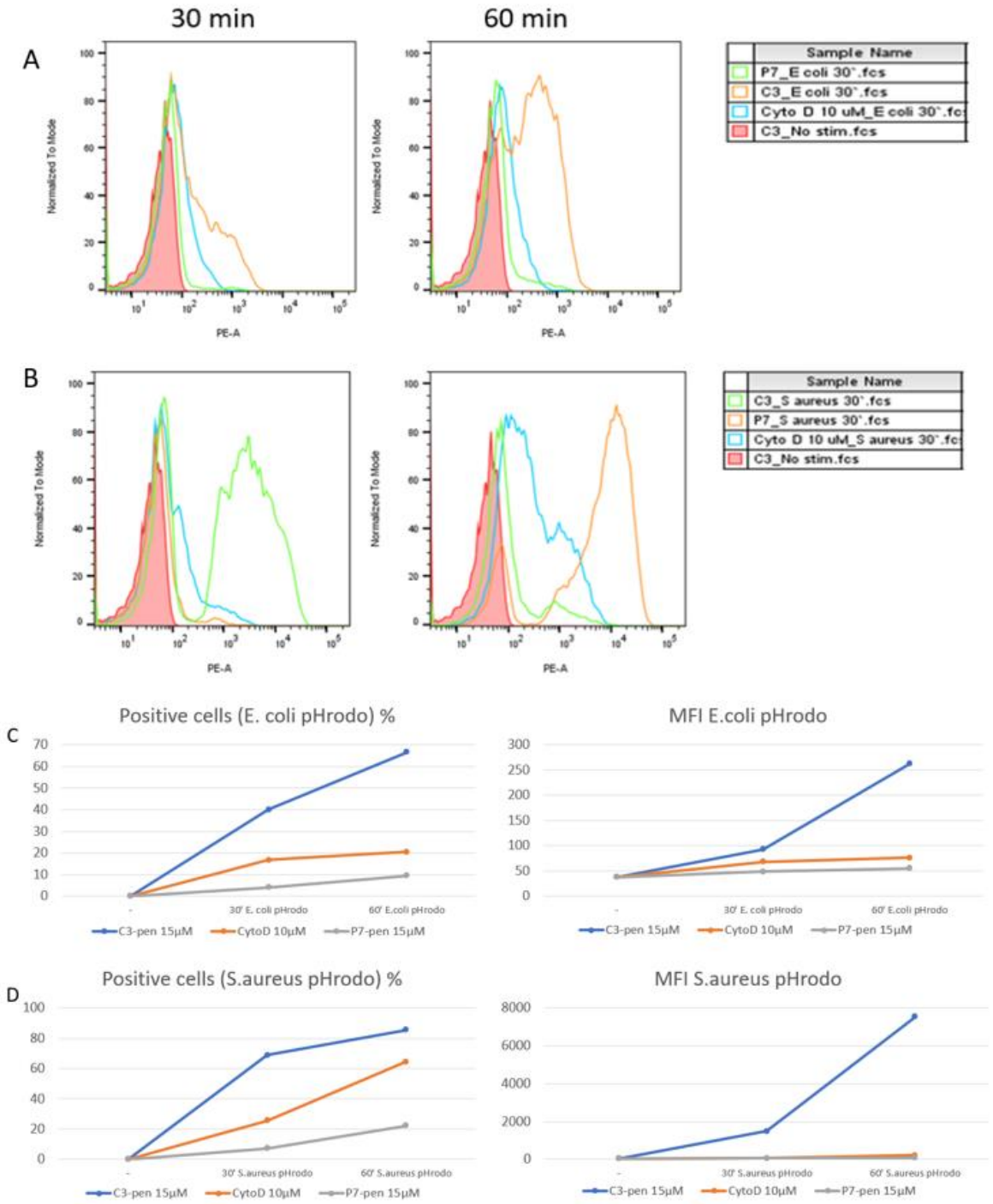

Figure 3.2: **P7-pen peptide inhibits phagocytosis of *E. coli* and *S. aureus* pHrodo bioparticles**. Human monocytes were pre-treated with 15 µM P7-pen or C3-pen, or 10 µM CytoD followed by incubation with pHrodo *E. coli* (A, C) or *S. aureus* (B, D) bioparticles for 30- and 60- min. (A, B) Data presented as normalised to mode graphs from FlowJo software. (C, D) Graphs showing percentage of positive cells and mean fluorescent intensity (MFI) for *E. coli* (C) or *S. aureus* (D) particles uptake. Results of one independent experiment.

P7G10-pen is another P7-pen variant with substitution of the amino acids threonine (T) to glycine (G) in the 10th position (see **table 1.1**). Position 10 in P7 amino acids sequence was previously shown to be sensitive to modifications, and from previous screens P7G10-pen was suggested to have decreased effect on phagocytosis (data from CEMIR, not shown). Here we aimed to explore how this peptide variant affects phagocytosis by primary human monocytes compared to P7-pen peptide.

In addition, we have also tested if we can use Alexa Fluor (AF488) conjugated bioparticles instead of pHrodo bioparticles, considering that some of the bioparticles we wanted to compare to bacteria are only produced as AF488 conjugates (like Zymosan). pHrodo bioparticles are pH sensitive and emits high fluorescence signal after acidification in the lysosome but has low fluorescence intensity at neutral pH [64]. Thus, pHrodo particles will not give considerable signal when bound to the cell surface and are not taken up by the cell. AF488- conjugated particles have good photostability and acquire pH-independent fluorescence, thus they will emit similar signal when bound to the cell surface as if they were taken up. We were treating cells with Accutase and washed them by PBS prior to flow cytometry analysis, which could significantly reduce the amount of surface bound particles. Thus, we wanted to test if we will get comparable results for pHrodo and AF488 conjugates after phagocytosis inhibition by P7-pen to determine if we indeed have the issue with surface bound particles using our protocol for phagocytic assays.

Monocytes were pre-treated with water (solvent control) and 15μM of P7-pen or P7G10-pen, followed by incubation with pHrodo or AF488 conjugated *E. coli* bioparticles (not opsonised by serum proteins) for 30- and 60- min. The results are presented in supplementary (**supplementary figure 7.1**).

The graphs showed that pre-treatment of cells by P7G10-pen had no effect on percentage of positive cells and MFI for monocytes incubated with both pHrodo and AF488 particles, when compared to solvent (water) control (**supplementary 7.1, S4 C, D**). Therefore, P7G10-pen was not inhibiting *E. coli* phagocytosis. At the same time, pre-treatment of cells by P7-pen significantly decreased the number of positive cells and MFI for cells incubated with both pHrodo and AF488 particles, with comparable values for the inhibitory effect (**supplementary 7.1, S4**). Thus, the results show that AF488 particle can be used in future experiments.

3.1.3 P7-pen does not affect uptake of Zymosan particles

Zymosan is a β-1,3- glucan polysaccharide from *Saccharomyces cerevisiae*, one of the main components of yeast cells are β-glucan. It is recognised by dectin-1 and complement receptor 3 (CR3) by phagocytes such as monocytes and macrophages, and dectin-1 and CR3 regulate the internalisation of Zymosan coated particles [65, 66]. The recognition of Zymosan by dectin-1 receptor trigger phagocytosis, and the receptor is essential in the antimicrobial responses of macrophages [67]. The inflammatory response of Zymosan is dependent on the heterodimerisation of TLR2 and TLR6 receptors [65]. Thus, uptake of Zymosan coated particles is regulated by different set of receptors and intracellular molecules like small Rho family GTPases [35]. To elucidate if P7-pen could interfere with different mechanism of phagocytosis, Zymosan particles uptake was tested.

Prior to selection of the cellular model for Zymosan particles uptake studies, we have established which cells express dectin-1 receptor. Primary human monocytes, macrophages, or THP-1 cells were incubated with PE conjugated control IgG or anti-Dectin-1 antibodies for 30 min. The primary cells had high background signal with control IgG, but it is still visible that they are positive for dectin-1, while THP-1 cells did not express dectin-1 (**figure 3.3**). Thus, Zymosan particles uptake regulation by P7-pen was not addressed in THP-1 cells.

Here we examined if pre-treatment by P7-pen could alter Zymosan AF488 bioparticles uptake and compared it to P7-pen effect on *E. coli* AF488 particles uptake. Monocytes were pre-treated with 15 μM P7-pen or C3-pen control peptide, or water, (solvent control) and incubated with either AF488- conjugated *E. coli* or Zymosan bioparticles (not opsonised by serum proteins) for 30- and 60- min (**figures 3.4, 3.5**).

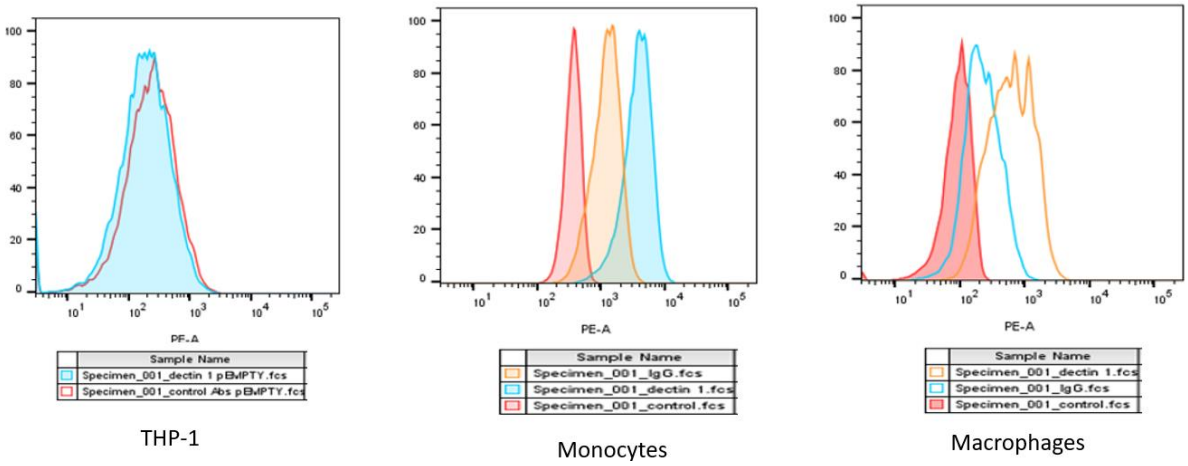

Figure 3.3: **Monocytes and macrophages, but not THP-1 cells expressed Dectin-1 receptor.** THP-1 cells, primary human monocytes and macrophages were either untreated or incubated with PE conjugated control IgG or a-Dectin-1 incubated with IgG and α-Dectin-1 for 30 min. Graphs show dectin-1 expression in monocytes and macrophages, but not in THP-1 cells. Data presented as normalised to mode graphs from FlowJo software. Results of three independent experiments.

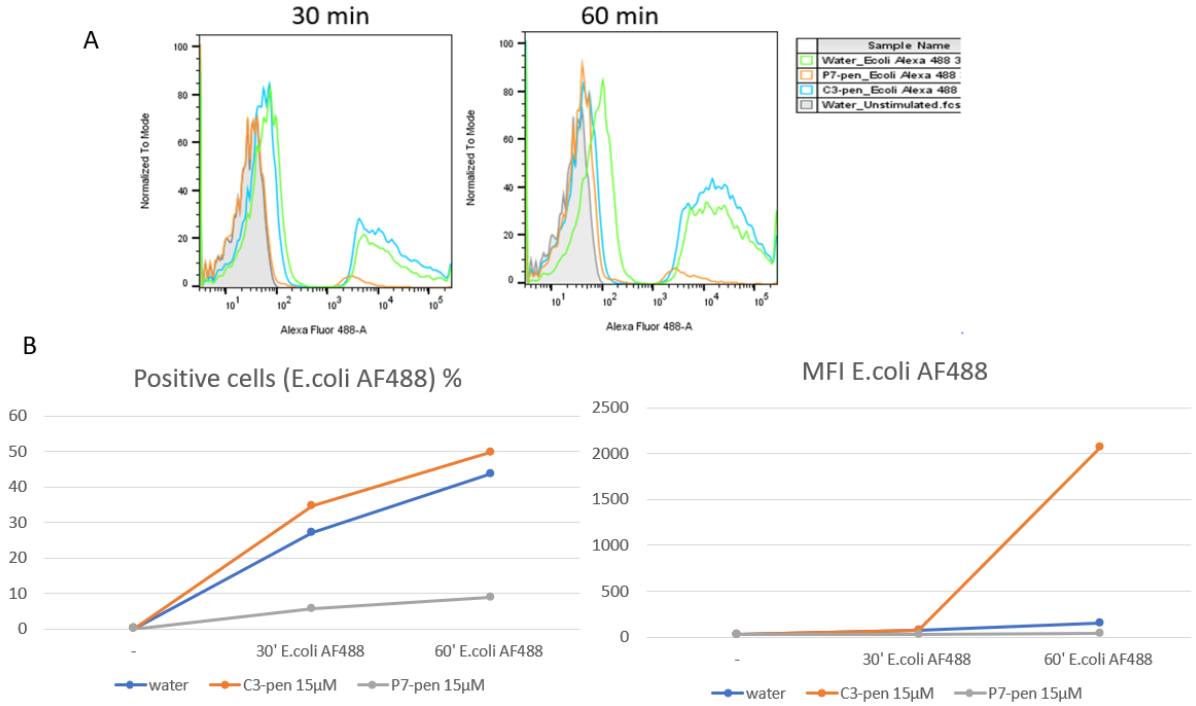

Figure 3.4: **P7-pen peptide inhibits phagocytosis of *E. coli* AF488 bioparticles**. Human monocytes were pre-treated with 15µM P7-pen or C3-pen, or water (solvent control) followed by incubation with AF488 *E. coli* (A) bioparticles for 30- and 60 min. (A) Data presented as normalised to mode graphs from FlowJo software. (B) Graphs for percentage of positive cells and (MFI) for *E. coli* particle uptake in monocytes. Results for one independent experiment.

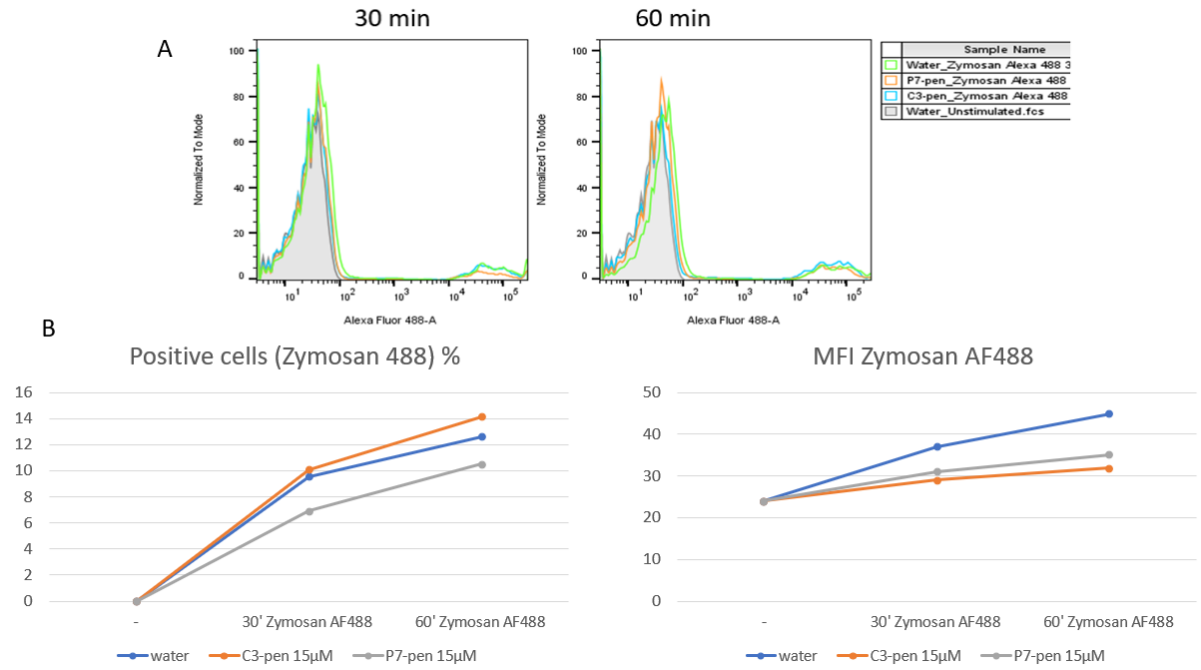

Figure 3.5: **P7-pen does not inhibit phagocytosis of Zymosan AF488 bioparticles**. Human monocytes were pre-treated with 15µM P7-pen or C3-pen, and water (solvent control) followed by incubation with AF488 Zymosan (A) bioparticles for 30- and 60- min. (A) Data presented as normalised to mode graphs from FlowJo software. (B) Graphs for percentage of positive cells and (MFI) for Zymosan particle uptake in monocytes.

As we expected based on our previous experiments (see **supplementary 7.1, S4**), P7-pen strongly inhibited the uptake of AF488 conjugated *E. coli* bioparticles (**figure 3.4**). However, pre-treatment by P7-pen had not much effect on the uptake of Zymosan particles by monocytes (**figure 3.5**), which is true both for the percentage of positive cells or MFI, with MFI very close to the ones for control peptide (C3-pen) pre-treatment. Thus, P7-pen does not impair phagocytosis of Zymosan particles.

3.1.4 Evaluation of P7-pen effect on phagocytosis of serum opsonised bioparticles by human monocytes and macrophages

Opsonisation is the process when a particle or foreign organism is covered by opsonin proteins. An opsonin is usually an extracellular molecule and when it is bound to its target, it makes it visible for the phagocytic cells. Common opsonin include immunoglobulins and parts of complement such as C3, C4 and C5, which stimulated phagocytosis by conserved mechanisms (complement-mediated phagocytosis, Fcγ-receptor mediated phagocytosis [68, 69].

In our previous assays we have used 10% of human serum while pre-treating cells with peptides, and bioparticles were added directly to the wells without preliminary opsonisation by serum proteins. Opsonisation facilitates the uptake and initiates additional mechanisms to drive the uptake (via complement receptor, Fcγ). Thus, in the next round of assays we have evaluated if P7-pen could alter the uptake of opsonised bacterial (*E. coli*) and Zymosan bioparticles. We also compared the regulation of *E. coli* uptake by P7-pen for monocytes and macrophages from the same donor. Additionally, we have explored different opsonisation conditions and included complement inhibitor for further insight to P7-pen inhibitory mechanism of action.

Opsonisation of particles by 30% human serum

First, monocytes and monocytes derived macrophages (MDMs) were treated with media containing 15µM C3-pen or P7-pen, or water (solvent control), followed by stimulation with AF488 conjugated *E. coli* or Zymosan bioparticles for 30- and 60- min (**figures 3.6,**

3.7). Bioparticles were opsonised in 30% human A+ serum prior to addition to the cells for 30 min on 37 ºC water bath.

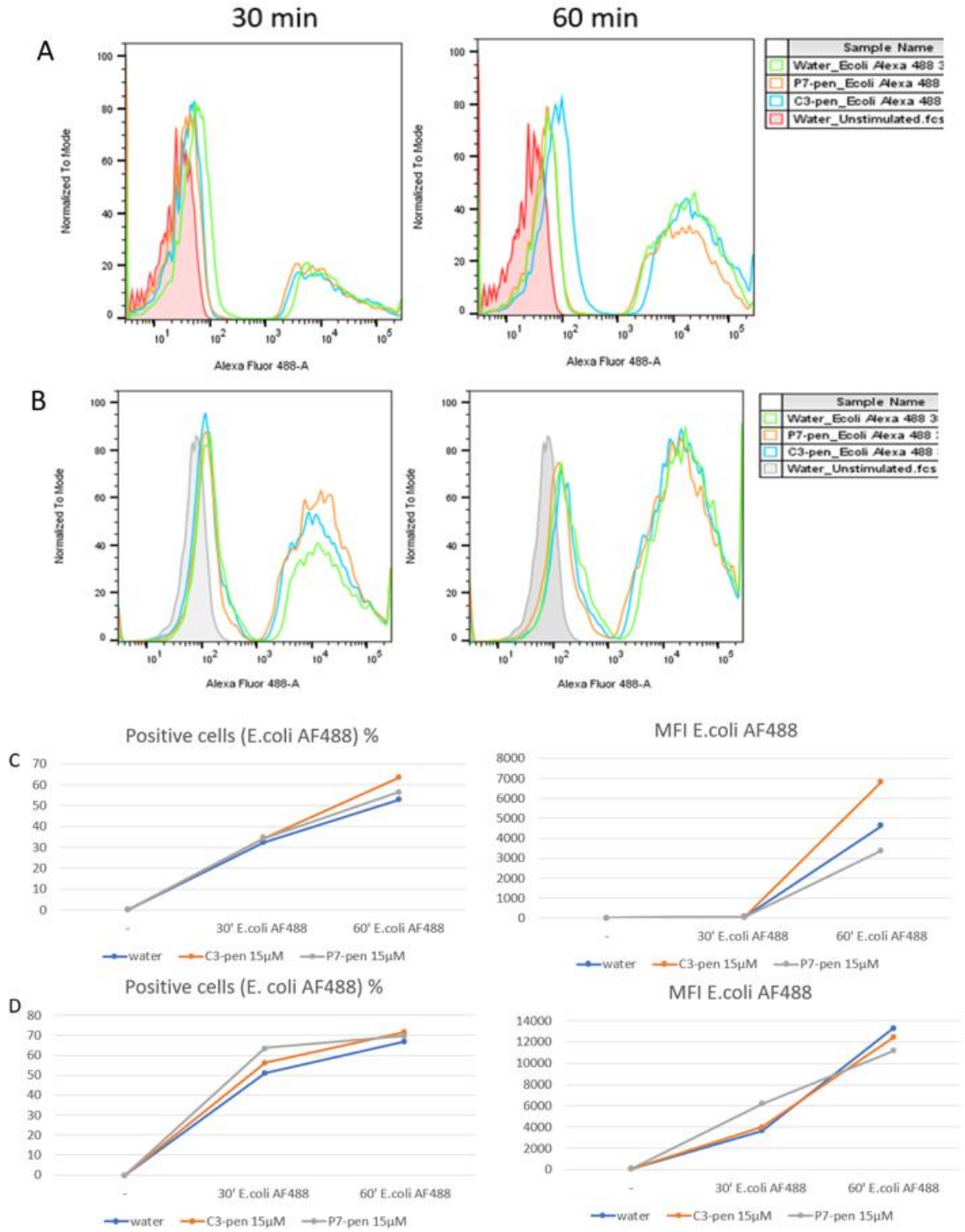

Figure 3.6: **Opsonisation of *E. coli* particles by 30% human serum significantly decreased the inhibitory effect of P7-pen peptide on phagocytosis.** Human monocytes were pre-treated with 15µM P7-pen or C3-pen, or water (solvent control) followed by incubation of AF488 conjugated *E. coli* particles with monocytes (A) and macrophages (B) for 30- and 60- min. MDMs were differentiated with 25 ng/ml M-CSF for four days from the monocytes of the same donor prior to the experiment. (A, B) Data presented as normalised to mode graphs from FlowJo software. (C, D) Graphs for percentage of positive cells and (MFI) for *E. coli* particle uptake by monocytes (C) and macrophages (D). Results for one donor.

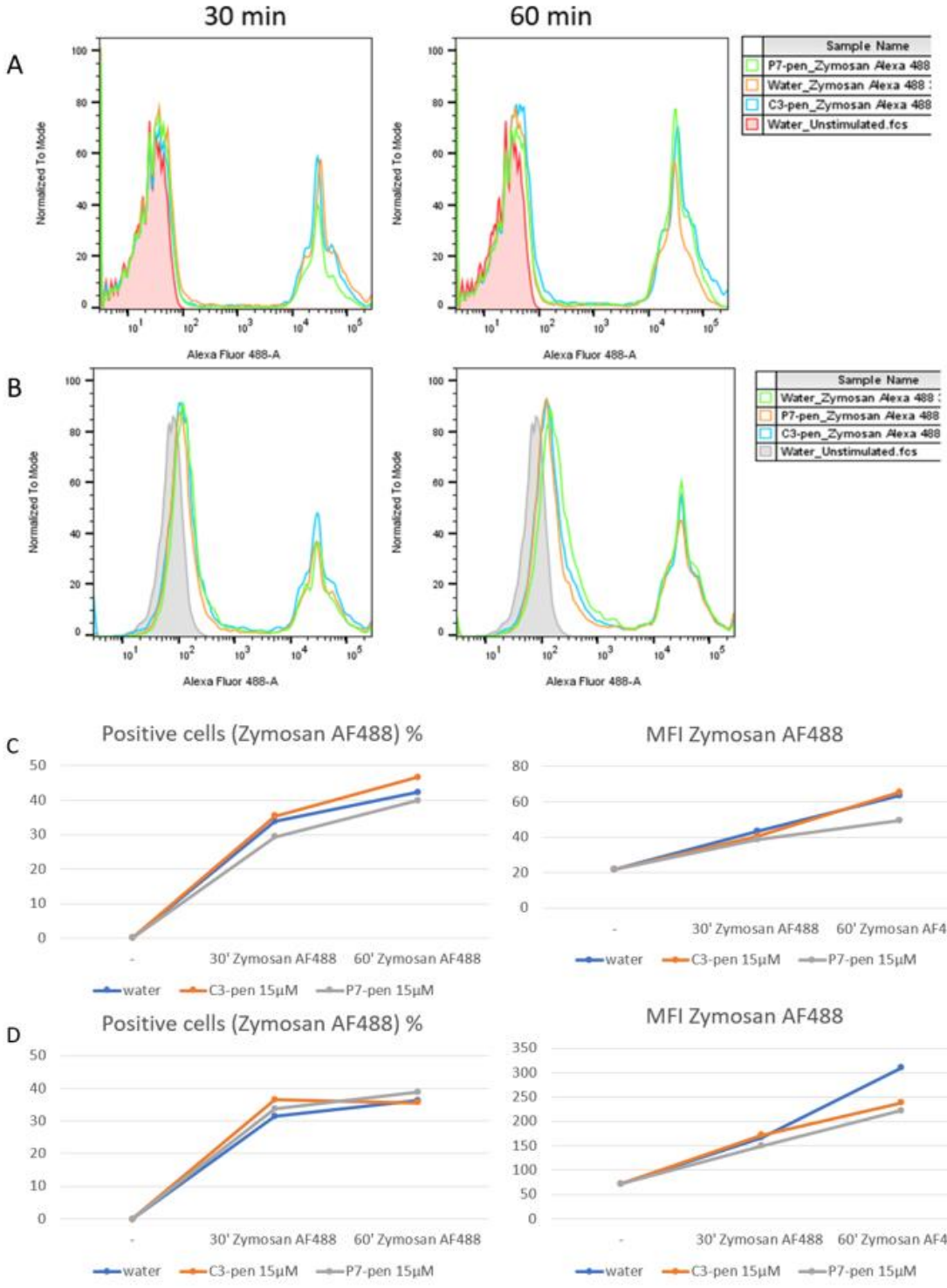

Figure 3.7: **Opsonisation of Zymosan particles by 30% human serum increases the uptake efficacy, with no effect of P7-pen pre-treatment.** Human monocytes were pre-treated with 15µM P7-pen or C3-pen, or water (solvent control) followed by incubation with AF488 conjugated Zymosan particles with monocytes (A) and macrophages (B) for 30- and 60- min. MDMs were differentiated with 25 ng/ml M-CSF for four days. (A, B) Data presented as normalised to mode graphs from FlowJo software. (C, D) Graphs for percentage of positive cells and (MFI) for Zymosan particle uptake in monocytes (C) and macrophages (D). Results for one donor.

Contrary to previous results with non-opsonised *E. coli* particles (**supplementary figure 7.1, S4D**), there was no considerable difference between percentage of positive cells for P7-pen treated monocytes or macrophages and control treatments (C3-pen and water) (**figure 3.6 C, D**). However, MFI for *E. coli* particles in monocytes was slightly decreased

when compared to the control peptide (**figure 3.6C**). As we have seen for non-opsonised Zymosan particles (**figure 3.5**), P7-pen was not inhibiting phagocytosis of opsonised particles by monocytes or macrophages (**figure 3.7**). Overall, serum opsonisation affected the uptake mechanism for *E. coli* particles, making it much less sensitive to the inhibitory effect of P7-pen.

Testing how different opsonisation protocols affect the inhibitory efficacy of P7-pen towards phagocytosis

Given that the inhibitory ability of P7-pen is decreased by opsonisation of *E. coli* bioparticles, we wanted to further expand the serum treatment and opsonisation conditions, which could help to elucidate P7-dependent and independent uptake mechanisms. Thus, bioparticles were opsonised in a different way to investigate how it could affect the phagocytosis regulation by P7-pen peptide (**table 3.1**).

After pre-treatment by C3-pen or P7-pen peptide (15 μM), we have added *E. coli* AF488 particles prepared as listed in **table 3.1**. Heat inactivated serum (h.i) was used, as heating of serum inactivates complement and phagocytosis of cells can be diminished as a consequence of loss of opsonic activity [70]. The monocytes were later stimulated with *E. coli* AF488 bioparticles for 60 min.

Table 3.1: **Opsonisation and serum treatment of monocytes with AF488 conjugated *E. coli* bioparticle.**

Conditions
No water bath incubation, dissolved in media with 1% heat inactivated FCS before adding to the cells
No water bath incubation, dissolved in media with 10% heat inactivated FCS
Opsonisation 30 min, 37 ºC, in 10% heat inactivated human A+ serum
Opsonisation 30 min, 37 ºC, in 10% human A+ serum

As could be seen from **figure 3.8**, opsonisation by human serum strongly increased the overall MFI for AF488 signal. Uptake of non-opsonised particles (in media with 1% or 10% FCS) was strongly inhibited in P7-pen pre-treated cells. On the other hand, the percentage of positive cells for opsonisation conditions with human serum resulted in considerably higher uptake by P7-pen pre-treated cells. As illustrated on **figure 3.8E**, opsonisation by 10% human A+ serum decreases the phagocytic ability of P7-pen, as we observed with even higher extent when 30% serum was used (**figure 3.6**). However, AF488 MFI for the cells that got particles opsonised with heat-inactivated serum was strongly decreased by P7-pen pre-treatment. Heat inactivation of serum is known to inactivate complement system [71], and preliminary results indicate that phagocytosis in the presence of active complement system is not much affected by P7-pen.

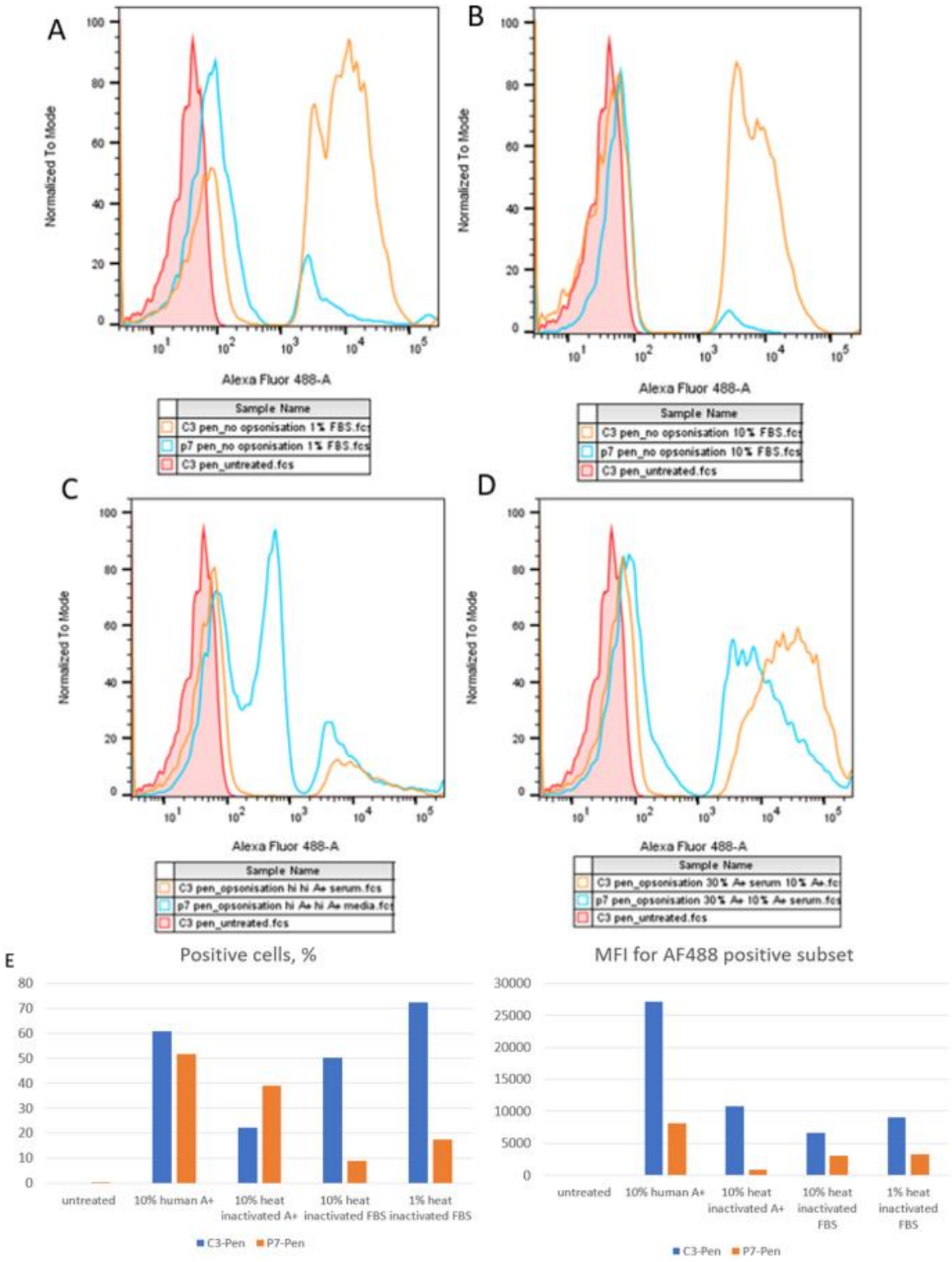

Figure 3.8: **Opsonisation by 10% human A+ serum decreases the efficacy of P7-pen peptide to inhibit *E. coli* particles phagocytosis.** Human monocytes were pre-treated with 15 µM P7-pen or C3-pen, followed by incubation with AF488 conjugated *E. coli* particles in media with 1% FCS, no opsonisation condition (A), with 10% FCS, no opsonisation condition (B), with 10% heat- inactivated human A+ serum with opsonisation step (C) and 10% human A+ serum with opsonisation step (D). (A-D) Data presented as normalised to mode graphs from FlowJo software. (E) Graphs for percentage of positive cells and (MFI) for *E. coli* particles. Results of one experiment.

3.1.6 Complement inhibition restores the ability of P7-pen to inhibit phagocytosis of *E. coli* particles

Heat inactivation of serum does not only "kill" complement activity, but it also decreases the activity of other opsonins in serum like immunoglobulins. Thus, in our next experiments we have examined the effect of more specific complement inhibition on phagocytosis regulation by P7-pen using compstatin inhibitor (**figure 3.9**). Compstatin is a C3 inhibitor that binds directly to C3 [72, 73]. The inhibitor controls the C3-activity by prohibiting the binding of C3 to its convertase [72].

Monocytes from buffycoats were pre-treated with water (solvent control) or 15µM P7-pen and stimulated with AF488 conjugated *E. coli* bioparticle for 60 min. Since there were limited amount of compstatin reagent, it was only tested for one time point. The experiment was performed twice with cells from overall three donors. Flow cytometry data for one of the donors is shown on **figure 3.9,** with graphs and quantification for other two donors shown in supplementary (**supplementary figure 7.1**). Details for opsonisation conditions for these assays are presented in **table 3.2**.

Table 3.2: **Opsonisation and serum treatment of monocytes with AF488 conjugated *E. coli* bioparticle**

Conditions
No water bath incubation, dissolved in media with 10% FCS before adding to cells
Opsonisation 30 min, 37 ºC, in human serum A+ serum
Opsonisation 30 min, 37 ºC, in human A+ serum with compstatin
Opsonisation 30 min, 37 ºC, in 2% heat inactivated serum

As in previous assay (**figure 3.8**), **figure 3.9** (and **supplementary 7.1**, **S5** and **S6)** show that opsonisation by intact human serum (10%) strongly decreases the ability of P7-pen to inhibit phagocytosis, while inhibition was strong towards uptake of particles dissolved in media with FCS (**figure 3.9E**). Uptake of particles opsonised in the presence of compstatin or in heat inactivated human serum was comparable, and P7-pen strongly inhibited particles uptake for these opsonisation conditions. Thus, the negative effect of opsonisation on ability of P7-pen to inhibit phagocytosis is most likely mediated by active complement system that initiate particles uptake by mechanism that is independent from P7-pen target proteins.

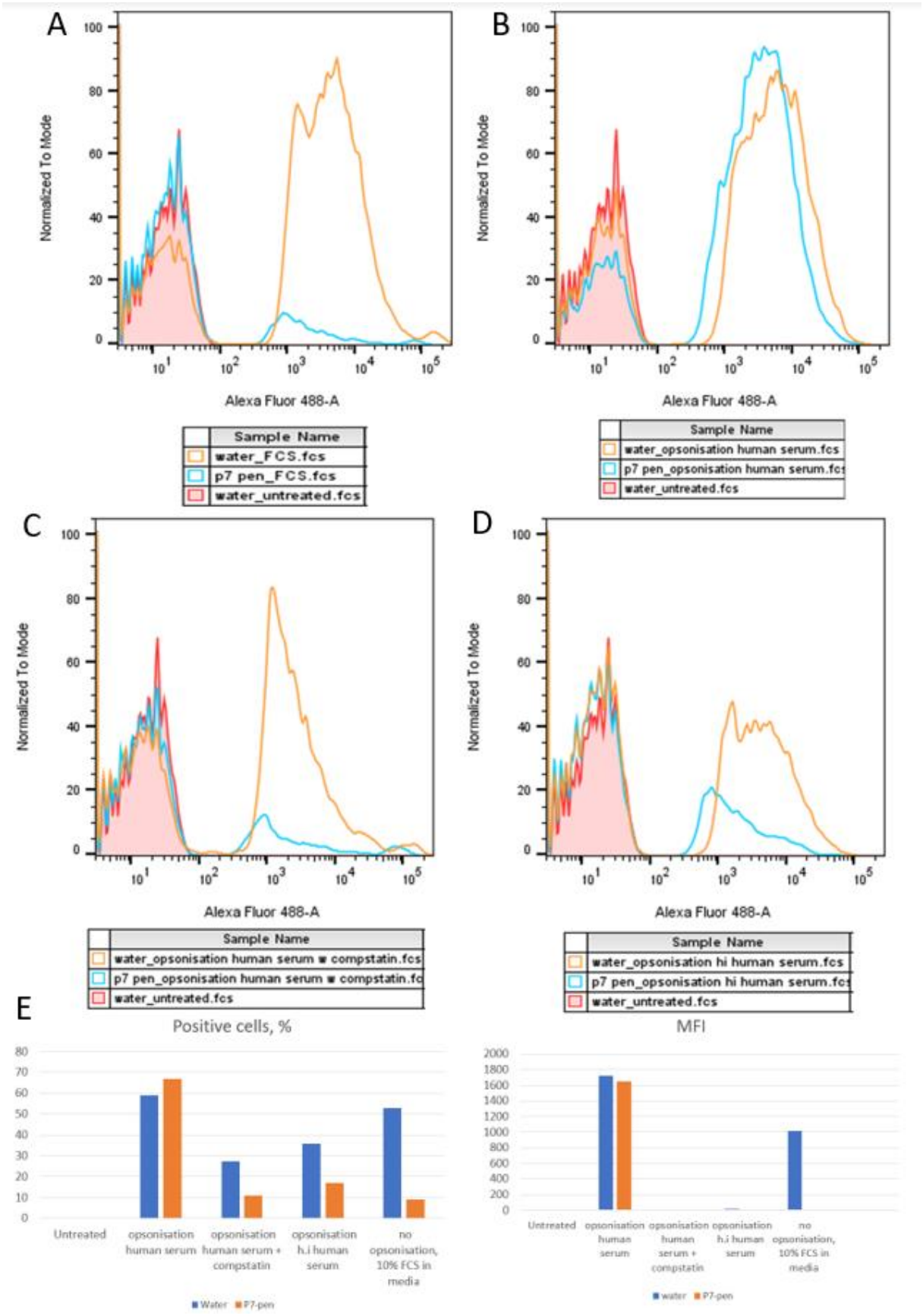

Figure 3.9: **Application of compstatin inhibits C3 component and restores P7-pen ability to inhibit phagocytosis of opsonised *E. coli* particles**. Human monocytes were pre-treated with 15µM P7-pen or water (solvent control) followed by incubation with AF488 conjugated *E. coli* particles in 10% FCS, no opsonisation (A), with human A+ serum, with opsonisation

step (B), with human A+ serum and compstatin, with opsonisation step (C), with heat-inactivated human A+ serum, with opsonisation step (D). (A-D) Data presented as normalised to mode graphs from FlowJo software. (E) Graphs for percentage positive cells and (MFI) for *E. coli* particle uptake in monocytes.

Regulation of E. coli particles-mediated cytokines expression by different opsonisation conditions and P7-pen peptide

E. coli uptake is a pre-requisite for TRAM-TRIF dependent signalling and *IFN-β* expression and secretion, while not affecting much signalling leading to pro-inflammatory cytokines expression initiated from cell surface [16]. As we were manipulating with uptake by opsonisation conditions, complement inhibition, and P7-pen peptide, we decided to follow up the effect of these treatments on *TNF-α* and *IL-1β* pro-inflammatory genes expression and *IFN-β* expression for the same donors. In addition to the flow cytometry analysis of *E. coli* bioparticles uptake (**figure 3.9**), we have stimulated parallel plates by *E. coli* particles and prepared lysates for RNA isolation and gene expression analysis (**figure 3.10**).

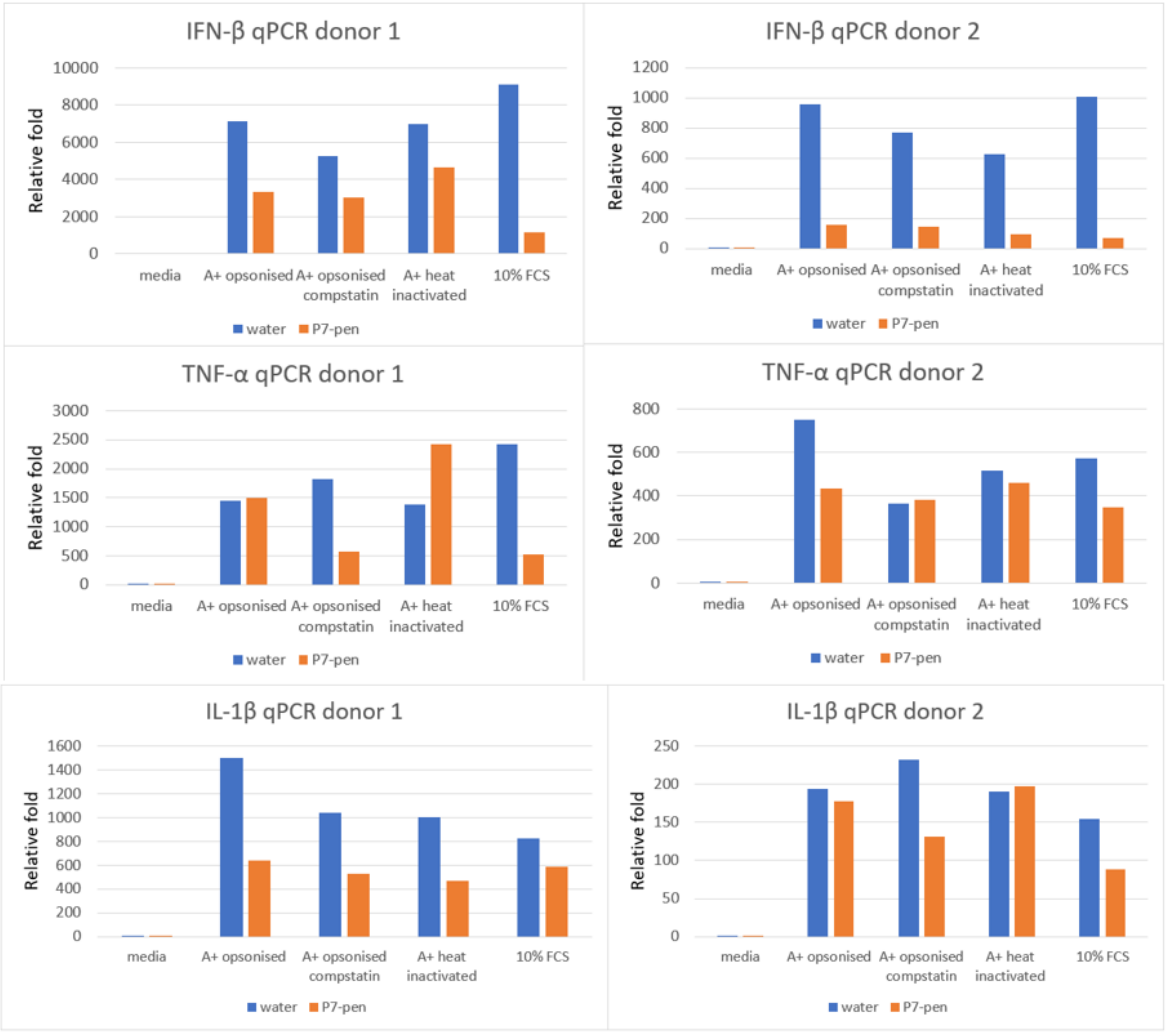

Figure 3.10: ***IFN-β, TNF-α* and *IL-1β* gene expression in monocytes pre-treated by P7-pen peptide and stimulated by *E. coli* particles with different opsonisation conditions.** Quantification of *IFN-β*, *TNF-α* and *IL-1β* mRNA expression by human monocytes was performed by RT-qPCR. Results from one experiment with cells from two donors.

There was an overall decrease in the expression of *IFN-β* and *TNF-α* by P7-pen in monocytes with different opsonisation conditions (**figure 3.10**). The results suggest that

P7-pen inhibits the MyD88 and TRIF-dependent pathway, with the most effect on the latest. At the same time, the effect of opsonisation conditions on *IFN-β* expression was not as prominent as the effect on the uptake of *E. coli* particles (**figure 3.9E** *vs* **figure 3.10**, top row).

3.1.7 Different levels of immunoglobulins in FCS have not altered phagocytosis regulation by P7-pen peptide

We had no possibility to deplete the human serum for immunoglobulins to exclude these opsonins from the assay but decided to check if FCS with normal or low immunoglobulins levels could alter P7-pen inhibitory activity towards *E. coli* phagocytosis.

Monocytes were pre-treated with 15μM P7-pen or C3-pen and stimulated with AF488 conjugated *E. coli* bioparticles. Bioparticles were pre-treated with media containing 10% FCS with either normal or low IgG levels, and incubated with monocytes for 30- and 60-min. The experiment was performed with two donors. Flow cytometry data for one of the donors is shown on **figure 3.11,** with graphs and quantification for the other donor shown in supplementary (**supplementary figure 7.1**).

Overall, **figure 3.11** and (**supplementary 7.1, S7**) show similar trend in percentage of positive cells and MFI for the uptake of particles between normal and low IgG serum, with comparable inhibitory activity of P7-pen. Overall, these results suggests that the IgG level in FCS serum does not affect the ability of P7-pen peptide to regulate *E. coli* phagocytosis by human monocytes.

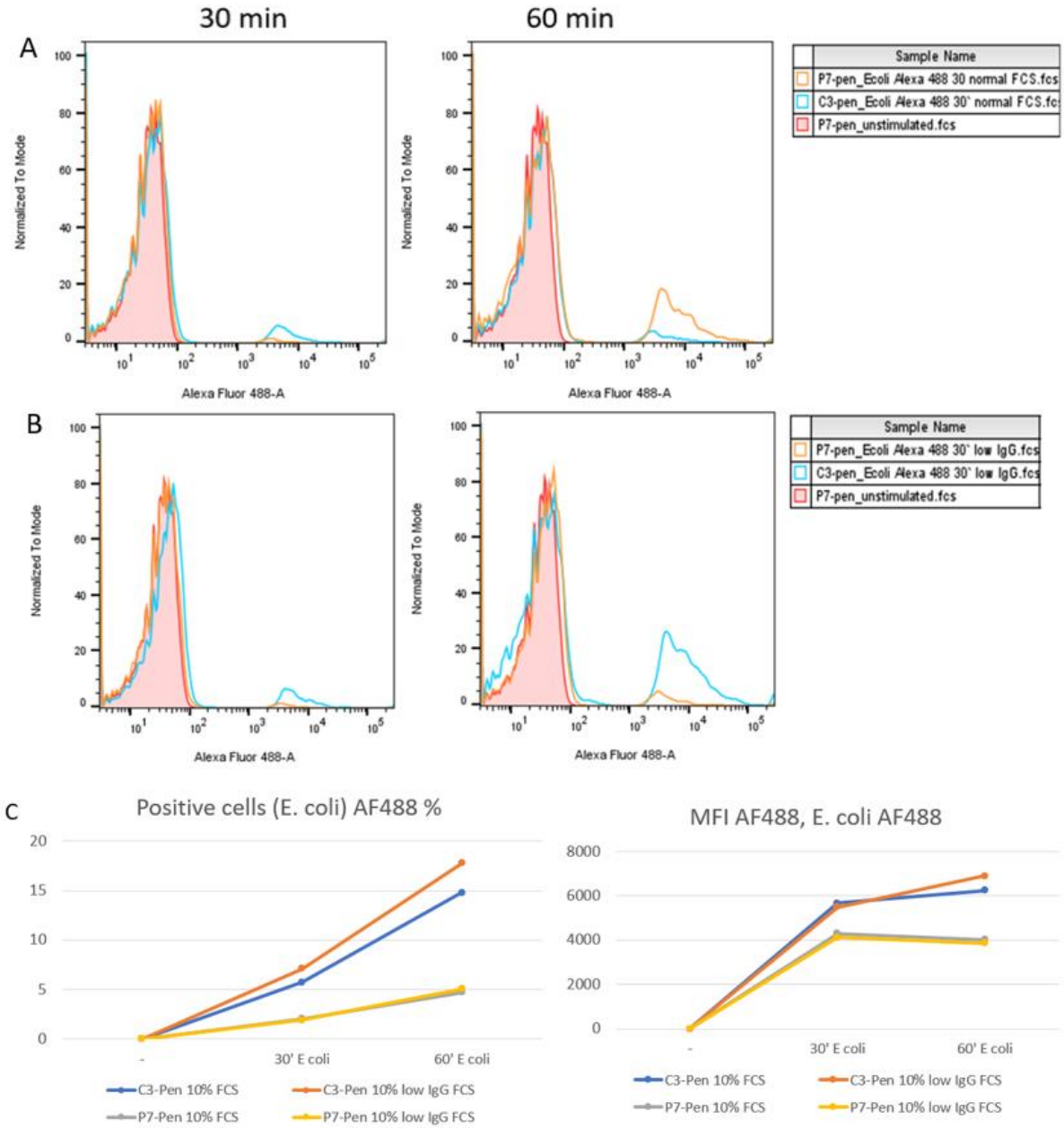

Figure 3.11: **Opsonisation by low IgG FCS serum does not alter phagocytosis regulation of P7-pen peptide.** Human monocytes were pre-treated with 15µM P7-pen or C3-pen followed by incubation with AF488 conjugated E. coli particles opsonised by 10% FCS (A) or 10% low IgG FCS(B) for 30- and 60- min. (A, B) Data presented as normalised to mode graphs from FlowJo software. (C) Graphs for percentage of positive cells and (MFI) for *E. coli* particle uptake in monocytes. Results of one experiment.

3.2 Analysis of live bacteria uptake by THP-1 cells

A number of phagocytosis studies have utilised THP-1 cells as a model for human macrophages [72]. After stimulating THP-1 cells, these cells gain macrophage functions and contrary to MDMs they have less variability from assay to assay (good reproducibility) and are easily available [73]. THP-1 cells were seeded and differentiated with PMA as described in methods. The cells were infected with either *E. coli* (DH5α) or *S. aureus* (wood strain) in all assays and were extensively washed with PBS and detached by water). Subsequently, protein quantification by BCA assay in additional experimental wells (cells lysed by lysis buffer) was utilised to adjust for the loss of cells from the wells due to the poor adherence of cells or cell death. This additional step improved the reproducibility and reliability of the assay results.

3.2.1 SLAMF1 overexpression increases live bacteria phagocytosis with no obvious impact on cytokine expression

The results from flow cytometry-based phagocytic assay demonstrated that overexpression of SLAMF1 or mutant SLAMF1 ΔIgV (IgV-like domain) was not affecting the *E. coli* bioparticle uptake (**figure 3.1A**). Phagocytic assays for live bacteria uptake were used to evaluate the effect of SLAMF1 overexpression or the effect of SLAMF1-derived peptides on uptake of live bacteria (Gram-negative and Gram-positive bacteria) by THP-1 cells.

THP-1 SLAMF1 KO with re-introduced full size SLAMF1, mutant SLAMF1 ΔIgV (IgV-like domain), or empty vector (pLVX control) were infected with *E. coli* laboratory strain (DH5α MOI 20-50). In addition to CFU count for three biological replicates, protein quantification by BCA method was performed for the lysate of 1-2 additional replicates to adjust the bacteria count to the number of cells that were not washed away in the course of washing steps in the assay.

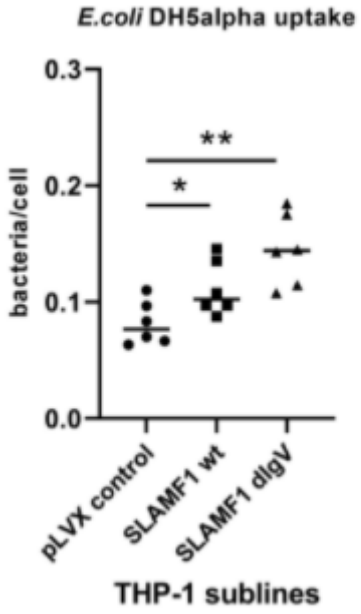

Figure 3.12: **SLAMF1 wt or SLAMF1 ΔIgV drives phagocytosis of *E. coli (DH5α)*.** Phagocytosis assay by live bacteria uptake of *E. coli* (*DH5α*) in differentiated THP-1 cells. Live bacteria uptake for each subline is normalised against empty vector (pLVX control). T-test is used with statistical significance (p-value <0.01). Data for three independent experiments.

Figure 3.12 shows an overall increase in live bacteria uptake by SLAMF1 wt or SLAMF1 ΔIgV compared to the cells that expressed empty vector (pLVX control) (T-test for statistical analysis). Thus, the results suggest that phagocytosis is driven by SLAMF1 wt or SLAMF1 ΔIgV, which is inconsistent with the results obtained for the same sublines in uptake of bacterial particles using flow cytometry approach.

3.2.2 The kinetics of cytokine expression induced in THP-1 sublines

SLAMF1 regulates TLR4 mediated signalling pathway by binding to the signalling adapter TRAM [43]. SLAMF1 overexpression in primary human macrophages increased TLR4-mediated *IFN-β* and *TNF-α* expression and secretion [43]. Here we wanted to address how SLAMF1 overexpression (full size and mutant with IgV domain deletion) in THP-1 cells would affect bacteria mediated cytokines' expression. Upon stimulation of cells by live DH5α *E. coli* bacteria (MOI 20-50), cells were lysed and followed by RNA isolation and gene expression analysis performed by RT-qPCR.

The standard deviation for the biological replicates was very high and was not included. The results are shown in supplementary (**supplementary figure 7.2, S1**). The cytokine expression mediated by *E. coli* (DH5α) shows similar induction of *IFN-β, TNF-α* and *IL-1β* for SLAMF1 wt or SLAMF1 ΔIgV compared to empty vector (pLVX control). Thus, the results revealed that SLAMF1 overexpression or SLAMF1 ΔIgV does not have impact on the *E. coli* mediated *IFN-β* or *TNF-α* expression.

3.2.3 P7-pen peptide inhibits live bacteria uptake

Flow cytometry for monocytes and macrophages pre-treated by SLAMF1-derived peptides revealed different effect on phagocytosis inhibition by P7-pen peptide and its variants. P7-pen was strongly inhibiting phagocytosis of both *E. coli* and *S. aureus*, while P7N4-pen had weak inhibitory activity on bacterial phagocytosis, and P7G10-pen showed no inhibition of *E. coli* phagocytosis. We wanted to explore how these peptides will affect live bacteria uptake by THP-1 cells. THP-1 cells were pre-treated with water (solvent control) and 15 µM of C3-pen (negative control), P7-pen, P7G10-pen, or P7N4-pen for 30 min and infected with *E. coli* (DH5α). Protein quantification by BCA assay was performed to adjust the bacteria count from live bacteria uptake. All experiments were performed in three biological replicates.

In compliance with the flow cytometry results, live bacteria uptake was strongly decreased in P7-pen peptide treated cells (**figure 3.13**). The overall number of bacteria per cell is low due to less efficient phagocytosis of bacteria by THP-1 cells when compared to monocytes or macrophages. However, the results clearly demonstrate significant inhibition of bacteria uptake by P7-pen pre-treatment when compared to solvent (water) or control C3-pen treated cells (T-test).

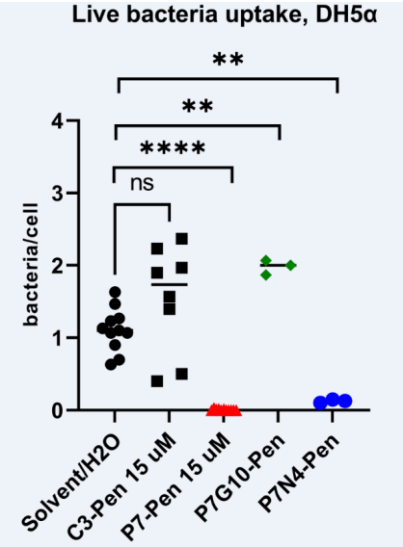

Figure 3.13: **P7-pen peptide inhibits live bacteria uptake of DH5α *E. coli* strain**. THP-1 cells were pre-treated by 15 µM peptides or solvent for 30 min, followed by addition of *E. coli* (DH5α) in serum free media (MOI 20-50), followed by 15 min phagocytosis at 37 ^{o}C, and antibiotic treatment for 30 min to kill bacteria that were not taken up by cells. T-test was used for statistical analysis (** p < 0.01, ****p <0.0001, ns- nonsignificant). Data of three independent experiments, except P7G10-pen and P7N4-pen, with three biological replicates for each assay.

Uptake of bacteria for P7G10-pen pre-treated cells was comparable to the cells pre-treated with control peptide, C3-pen. The result correlates with flow cytometry data for the uptake of bacterial particles (**supplementary 7.1, S4 C, D**). Thus, the amino acid substitution from threonine to glycine in P7 results in the loss of effect on phagocytosis.

P7N4-pen pre-treated THP-1 cells on the other hand showed attenuated bacteria uptake, but with slightly higher values than P7-pen peptide treated cells. This P7-pen variant attains decreased inhibitory effect on live bacteria uptake (60 min). It could be that

P7N4-pen will be less efficient inhibitor if the uptake will be compared with P7-pen for longer time points (15 min for live uptake, **figure 3.13**). Results obtained from P7G10-pen and P7N4-pen is not a concluding remark, but preliminary data set as they were performed once.

P7-pen peptide treated THP-1 cells showed decreased uptake of live bacteria *S. aureus* (wood strain) (data not shown). Experiment was performed only once, thus should be repeated before making final conclusions. However, preliminary data from this assay have shown decreased uptake of *S. aureus* particles by P7-pen pre-treated cells, which correlated with flow cytometry data (**figure 3.2**), where P7-pen strongly inhibited phagocytosis of *S. aureus* particles by human primary monocytes.

3.2.4 Regulation of *IFN-β* and *TNF-α* mRNA expression by P7-pen in THP-1 cells in response to live bacterial infection

IFN-β and *TNF-α* are essential cytokines induced as inflammatory response to Gram-negative bacterial infections via TLR2- and TLR4-signalling cascades [74]. P7-pen peptide inhibited bacterial uptake of *E. coli* (DH5α), and in parallel with uptake assays we wanted to address if P7-pen treatment could inhibit *TNF-α* and *IFN-β* expression in response to live bacterial infection. Lysates were prepared with QIAzol for RNA isolation and gene expression analysis performed by RT-qPCR (**figure 3.14**).

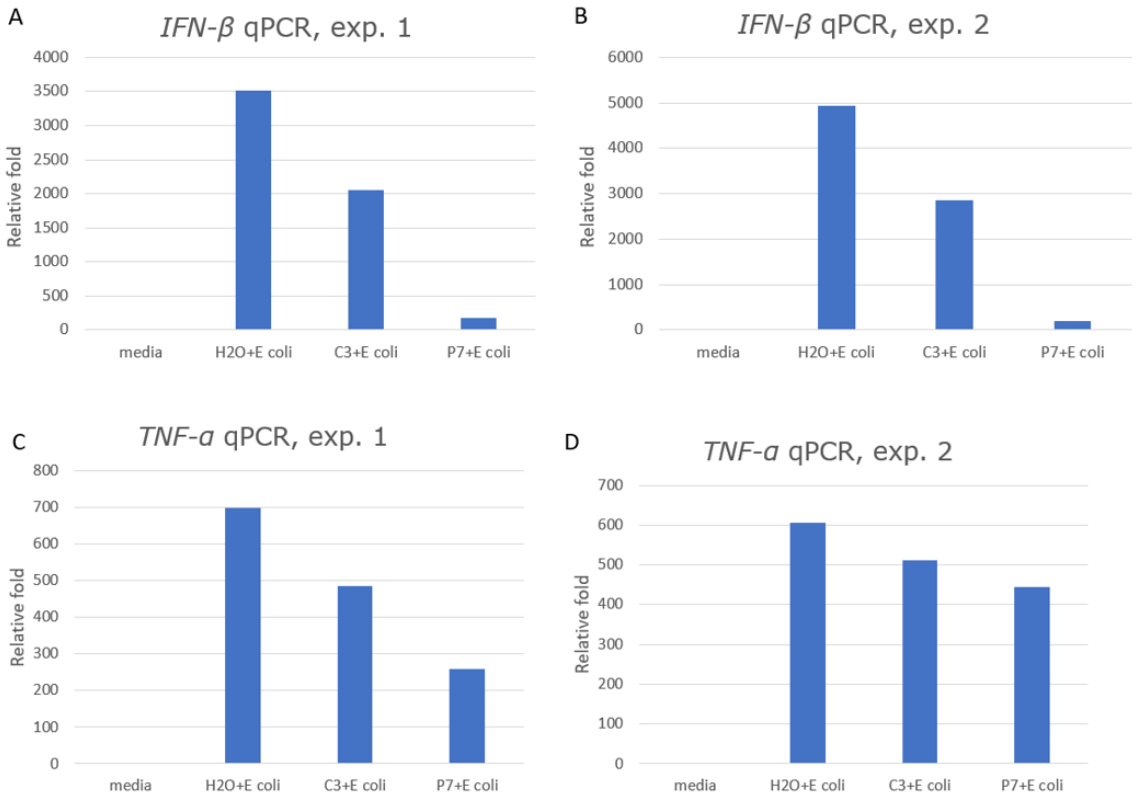

Figure 3.14: ***IFN-β* and *TNF-α* gene expression mediated by live *E. coli* (DH5α) infection of THP-1 cells.** Differentiated THP-1 cells were pre-treated with 15 µM peptides or solvent control (water) for 30 min, followed by live DH5α *E. coli* bacteria (MOI 20-50) in THP-1 media for 60 min. Cell lysates (QIAzol) were used for RNA isolation and qPCR analysis. Results from two independent experiments (exp. 1 and exp. 2).

Unfortunately, there was a technical error in the first experiment, and it had to be excluded. *IFN-β* mRNA expression in response to *E. coli* live infection was overall strongly inhibited by P7-pen peptide pre-treatment of THP-1 cells. *TNF-α* mRNA expression was also slightly decreased by P7-pen pre-treatment. The results suggest that P7-pen inhibits

TLR4-mediated signalling pathway after live bacterial infection with most prominent effect on the TRAM-TRIF dependent signalling pathway.

Flow cytometry results showed that P7-pen peptide inhibited phagocytosis of *S. aureus* bioparticles by human primary monocytes (**figure 3.2**). The effect of P7-pen peptide treatment on live *S. aureus* uptake in THP-1 cells followed the same trend (not shown). The effect of P7-pen peptide on *S. aureus* induced *TNF-α* and *IFN-β* expression was addressed by RT-qPCR. The results are shown in supplementary (**supplementary 7.2**). *IFN-β* and *TNF-α* mRNA expression levels were not so high when compared to those induced by *E. coli* infection, but the cytokines mRNA expression of *IFN-β* and *TNF-α* were overall attenuated by P7-pen peptide treatment. Additional biological replicates are required for analysis of statistical significance since the experiment was performed once and is not a concluding remark.

3.3 Co-precipitation of SLAMF1 or SLAMF1-derived peptides with target proteins

Co-immunoprecipitation (IP), pulldown by tagged proteins or by affinity-based precipitations are common methods used to identify protein interaction in cells. In this study precipitation by peptides and anti-flag immunoprecipitation were performed. We wanted to address the interaction between SLAMF1 or SLAMF1-derived peptides (P7-pen or P7G10-pen) with target proteins from MS hits (**table 1.2**) in primary monocytes and HEK293T cells.

Cell lysates were used to gain access to the protein of interest, which are pulled out by the bait peptide on neutravidin beads or flag-tagged protein on anti-flag beads during co-incubation with the lysate. Unbound substances were removed and the target proteins from the beads were eluated, isolated and subjected to SDS-PAGE and consequently identified by using western blot analysis with antibodies of interest [75].

3.3.1 P7-pen co-precipitates with RhoG in primary human monocytes

The results obtained from phagocytic assay (flow cytometry and live bacteria uptake approach) revealed different efficacy of P7-pen peptide and P7-pen variants (P7N4-pen and P7G10-pen) on regulation of phagocytosis. We wanted to address the interaction between SLAMF1 derived peptides (P7-pen or P7G10-pen), and important regulators in TLR signalling (IRAK1, IRAK4, TIRAP and TRAM), as positive control as they were shown to co-precipitate with P7-pen by Trafficking group) and the target proteins from MS hits (**table 1.2**) in primary human monocytes.

The target proteins were pulled out by immobilised biotinylated peptides, such as penetratin (negative control), P7-pen or P7G10-pen upon co-incubation with monocytes' lysates. The target proteins were subsequently eluated from the neutravidin agarose resin beads and the co-precipitated proteins analysed by western blot analysis.

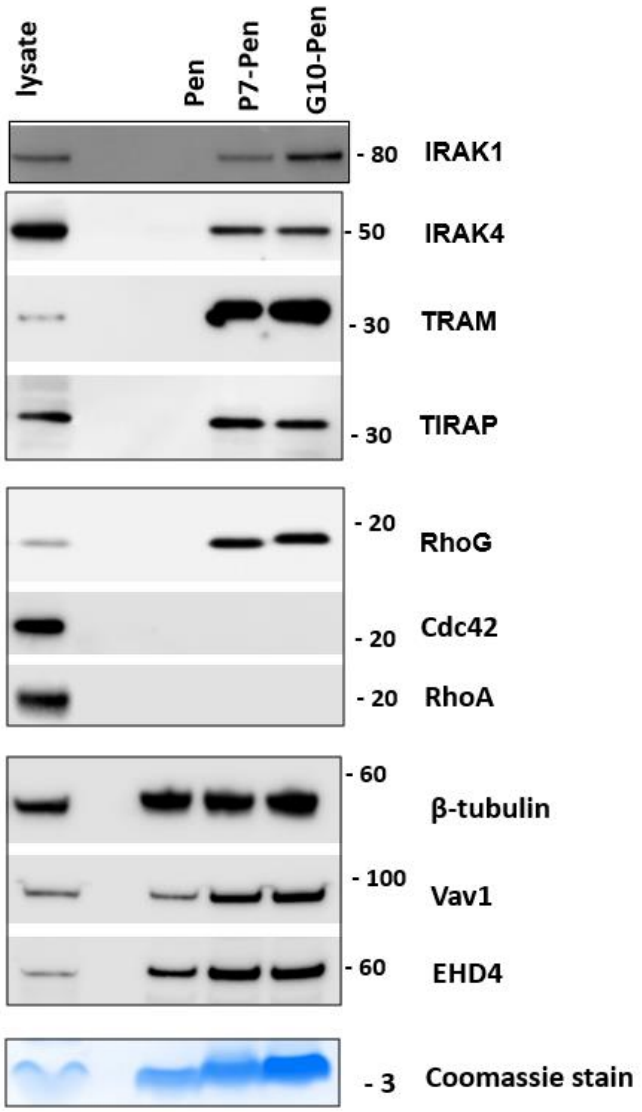

Figure 3.15: **Precipitation of SLAMF1-derived peptides with target proteins.** Biotinylated and peptides: pen (negative control), P7-pen or P7G10-pen were immobilised on neutravidin beads, lysate was pre-cleared with pen peptide on beads for 30 min, followed by co-precipitation with all three peptides for 45 min. Subsequently, the unbound substances were removed, and beads washed by lysis buffer, proteins were eluted and resolved in SDS-PAGE. Co-precipitation of proteins were addressed using western blot analysis, using antibodies indicated in the figure. Molecular weight is presented in kilodaltons (kDa). Lower part of the gel was used for protein staining and visualise the number of peptides used for precipitation.

P7-pen or P7G10-pen, but not pen (negative control) co-precipitated with IRAK1, IRAK4, TRAM and TIRAP proteins (**figure 3.15, top panel**). The result shows that P7-pen interact with important proteins involved in the TLR signalling, which was previously demonstrated by Trafficking group.

Figure 3.15, bottom panel showed that all three peptides co-precipitated β-tubulin, Vav1 and EHD4 proteins. These proteins appeared on MS hits as binding partners for P7-pen (**table 1.2**). Thus, the results suggest that the protein interaction is caused by penetratin (CPP) and not by SLAMF1 sequence. The proteins are not likely to be responsible for the inhibitory effect of P7-pen on bacterial phagocytosis.

RhoG co-precipitated with P7-pen or P7G10-pen, but not with pen, and none of the peptides co-precipitated RhoA or cdc42 (**figure 3.15, middle panel**). Interestingly, we have observed a band shift for RhoG with P7G10-pen, which may indicate that it is either

an unspecific band, or that it is a protein form with posttranslational modifications- despite being a MS hit (**table 1.2**), Cdc42 did not co-precipitate with P7-pen.

3.3.2 P7-pen co-precipitates with Rab14 and RhoG

MS data for P7-pen or P7N4-pen showed that RhoG and Rab14 are amongst proteins (**table 1.2**) with highest MS score for P7-pen. The LC-MS machine identifies proteins by comparing features of the constituents with theoretical or previously identified peptides in the data base [76]. In our current study, P7G10-pen did not inhibit phagocytosis of *E. coli* particles or live bacteria. We did not have antibodies to Rab14, and RhoG band shift in endogenous co-precipitations indicated on possible unspecific band for P7G10-pen. Thuss, we proceeded with an overexpression system that allows to study co-precipitation using antibodies to the tag attached to the protein of interest- flag tag with RhoG and Rab14.

In preliminary experiments, we established that we have to use quite high amount of plasmid for the transfection of flag tagged Rab14 or RhoG to HEK293T cells.

For this, HEK293T cells were transiently transfected with plasmids encoding $Rab14^{Flag}$ or $RhoG^{Flag}$ in a concentration gradient ranging from 200-800 ng, while using 100 ng $Rab11^{Flag}$ as positive control for 48 hours. Cell lysates were prepared by 1X RIPA buffer with inhibitors and subjected to SDS-PAGE and identified using western blot analysis. The result is shown in **supplementary 7.3**. **Supplementary 7.3, S1** showed that $RhoG^{Flag}$ was expressed in all concentrations (200-800 ng), compared to $Rab14^{Flag}$ which was only expressed in 400 and 800 ng, where the observed band for 800 ng was weak. Thus, the results showed that Rab14 was expressed at a concentration from 400 ng, while RhoG expressed at all concentrations.

Next, we transfected cells with 1600ng Rab14 or 800 ng RhoG. The cells were transiently transfected with 1600 ng Rab14 or 800 ng RhoG and repeated the precipitations. Concomitantly, the peptides were quantified by Simple Blue staining of the lower part of the gel used for detection of co-precipitated proteins. The staining was used to quantify the ratio between signal for precipitated protein and individual peptides. Blots from western blot analysis and protein quantification from one experiment is shown on **figure 3.16**, with blot and quantification of the other experiment in supplementary (**supplementary figure 7.3**).

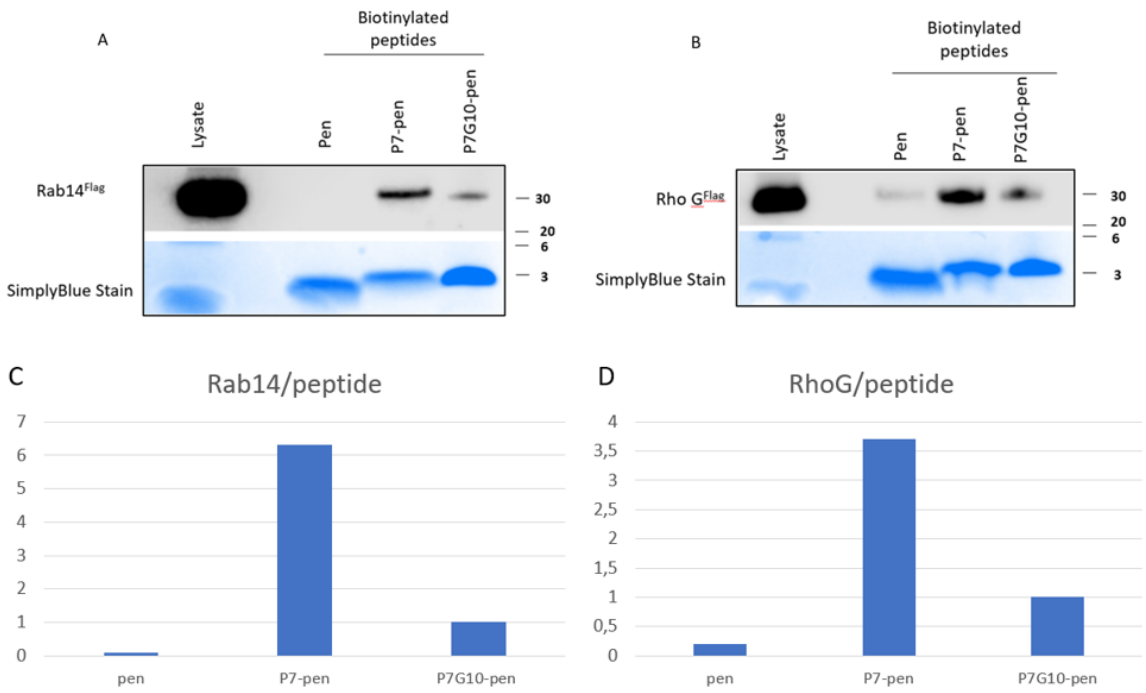

Figure 3.16: **P7-pen peptide co-precipitated with RhoG^{Flag} and Rab14^{Flag} proteins.** HEK293T cells were transiently transfected with plasmids encoding 1600 ng Rab14^{Flag} (A) or 800 ng RhoG^{Flag} (B) for 48 hours. Cell lysates were prepared in 1X RIPA buffer with inhibitors. Target proteins from lysates were precipitated under stringent conditions (400 mM NaCl) using biotinylated pen (negative control), P7-pen, or P7G10-pen immobilised on neutravidin beads. Cell lysate and eluate samples were subjected to SDS-PAGE and target proteins accessed by western blot analysis. Antibodies are indicated in the figure and molecular weight is presented in kilodaltons (kDa). Lower part of the gels was stained with Simple Blues proteins stain, and intensity of staining determined in image Lab (Biorad) software. Intensity of western blot staining analysed in Odyssey software, followed by quantification of ration for Rab14 (C) and RhoG (D) in precipitations.

Figure 3.16 and (**supplementary 7.3, S2**) showed co-precipitation of P7-pen with Rab14 or RhoG, with much less efficient co-precipitation of these proteins by P7G10-pen.

3.3.3 SLAMF1 protein co-precipitates with Rab14 and RhoG

Next, we wanted to address if SLAMF1 protein itself could co-precipitate with Rab14 or RhoG. HEK293T cells were transiently transfected with plasmids encoding Rab14, RhoG, or empty flag vector (negative control) and SLAMF1 (SLAMF1 wt) or SLAMF1 Δ c-terminal (ct) for 48 hours. Cell lysates were prepared in 1X RIPA buffer with inhibitors (containing Triton X-100) or 1X-NP40 lysis buffer (containing NP-40 detergent) and incubated with anti-FLAG (M2) affinity agarose beads, where target proteins were pulled down. Triton X-100 is a detergent which is stronger than NP-40 detergent and minimises the large complex formation. Subsequently, the target proteins were eluated from the beads and subjected to SDS-PAGE and western blot analysis.

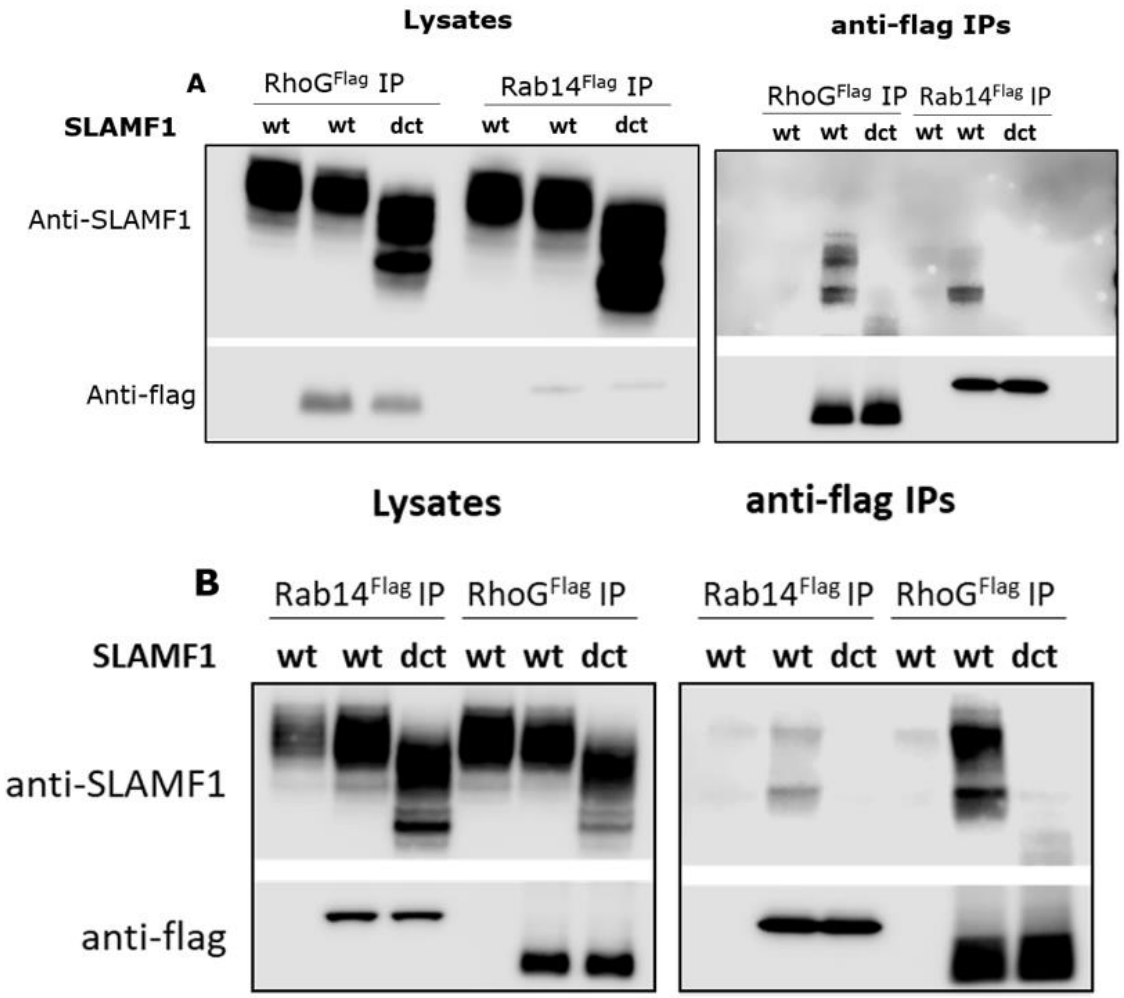

Figure 3.17: **SLAMF1 wt co-precipitates with Rab14^{Flag} and RhoG^{Flag}.** HEK293T cells were transiently transfected with plasmids encoding empty flag (negative control), Rab14^{Flag} or RhoG^{Flag} and SLAMF1 wt or SLAMF1 Δct for 48 hours. Lysates were prepared using 1X RIPA buffer with inhibitors (with 1% Triton X-100) (A) or 1X- NP40 buffer (with 0.5% NP-40) (B). Lysates and eluated samples were subjected to SDS-PAGE and target proteins were accessed by western blot analysis. Antibodies are indicated in the figure.

We observed that SLAMF1 wt, but not the mutant lacking cytoplasmic tail (SLAMF1 dct) co-precipitated with RhoG^{Flag} and Rab14^{Flag} both in mild NP40 buffer and strict conditions (1X RIPA buffer) (**figure 3.17**). We also observed some background precipitation of SLAMF1 with anti-flag beads, but it was still less prominent than SLAMF1 band for Rab14^{Flag} precipitations. Thus, the results suggest that SLAMF1 could form the complex with these proteins.

4. Discussion

The aim of the thesis was to investigate the effect of SLAMF1 and SLAMF1- derived peptides with focus on the mechanism of bacterial uptake inhibition. It was done by addressing the uptake of bacterial bioparticle, live bacteria, co-precipitation of SLAMF1, mutant SLAMF1 or SLAMF1-derived peptides with target proteins, and by addressing regulation of gene expression by SLAMF1 derived peptides or SLAMF1 overexpression.

To gain an overview of the effect of novel potential peptide-based drug originating from SLAMF1 molecule on the uptake of bacteria, we have performed phagocytic assays by flow cytometry and live bacteria uptake. Preliminary data from the Trafficking group demonstrated that P7-pen inhibits the uptake of *E. coli* bioparticles by primary human monocytes. In line with these preliminary data, we demonstrated that P7-pen inhibits the uptake of *E. coli* bioparticles, and *S. aureus* bioparticles by monocytes (fig.3.2). Similarly, live bacteria uptake of *E. coli* and *S. aureus* was inhibited by P7-pen (fig. 3.13). Thus, the results show that P7-pen was able to inhibit the uptake of both Gram-negative and Gram-positive bacteria.

One of the P7 variants, P7N4 showed decreased inhibitory effect on bacterial phagocytosis at 60 min (supplementary 7.2, S3), but showed strong inhibitory effect of *E. coli* live bacteria uptake at 15 min (fig. 3.13). These results indicate that P7N4-pen attains decreased inhibitory activity towards phagocytosis compared to P7-pen at longer time points. The other P7 variant, P7G10 did not have inhibitory effect on phagocytosis of *E. coli* bioparticles (supplementary 7.2, S4) or live bacteria uptake of *E. coli* (DH5α) (fig. 3.13). P7 peptide was previously shown to be sensitive for modification at position 10 in its sequence (**table 1.1**), and amino acid substitution T/G resulted in the loss of the effect on phagocytosis. It could be important to find such peptide variant as P7G10 that do not alter the clearance of bacteria (our data) but can still decrease the pro-inflammatory cytokines and *IFN-β* secretion downstream TLR4 (data from Trafficking group, not shown).

Phagocytosis of pathogens could be mediated by Fc receptors (FcR) and complement receptors. Pathogen phagocytosis mediated by FcR stimulates the recognition and engulfment of pathogens opsonised by serum immunoglobulins when IgG is covering the pathogen and recognised by FcR. The F-actin phagocytic cup extends around the particle with help of the active Cdc42 and Rac1 GTPases (fig. 4.1A). In pathogen phagocytosis mediated by complement, the membrane extends on one side of the particle and the active RhoA engulfs it (fig. 4.1B) [35]. When the pathogen is recognised by TLR it is engulfed through actin polymerisation by RhoGTPases, Rac1 and Cdc42 [77]. The localisation and the specific role of other GTPase- RhoG in FcR, complement- mediated or TLRs- initiated phagocytosis is not clearly demonstrated [35].

Results of our study showed that the inhibitory effect of P7-pen was affected by opsonisation (fig. 3.6). In addition, inhibition of complement by compstatin treatment or heat inactivation of human serum restored the inhibitory capacity of P7-pen (fig. 3.9), which indicates that phagocytosis in the presence of active complement system is not much affected by P7-pen.

P7-pen did not have an effect of uptake of Zymosan particles. The Zymosan particles which are derived from yeast are phagocytosed when recognised by dectin-1 receptor or opsonised by serum proteins (via complement-mediated mechanism) [67, 78]. The results indicate that P7-pen could not alter both complement-driven and the β-1,3-glucan- dependent phagocytic mechanisms during yeast bioparticles uptake.

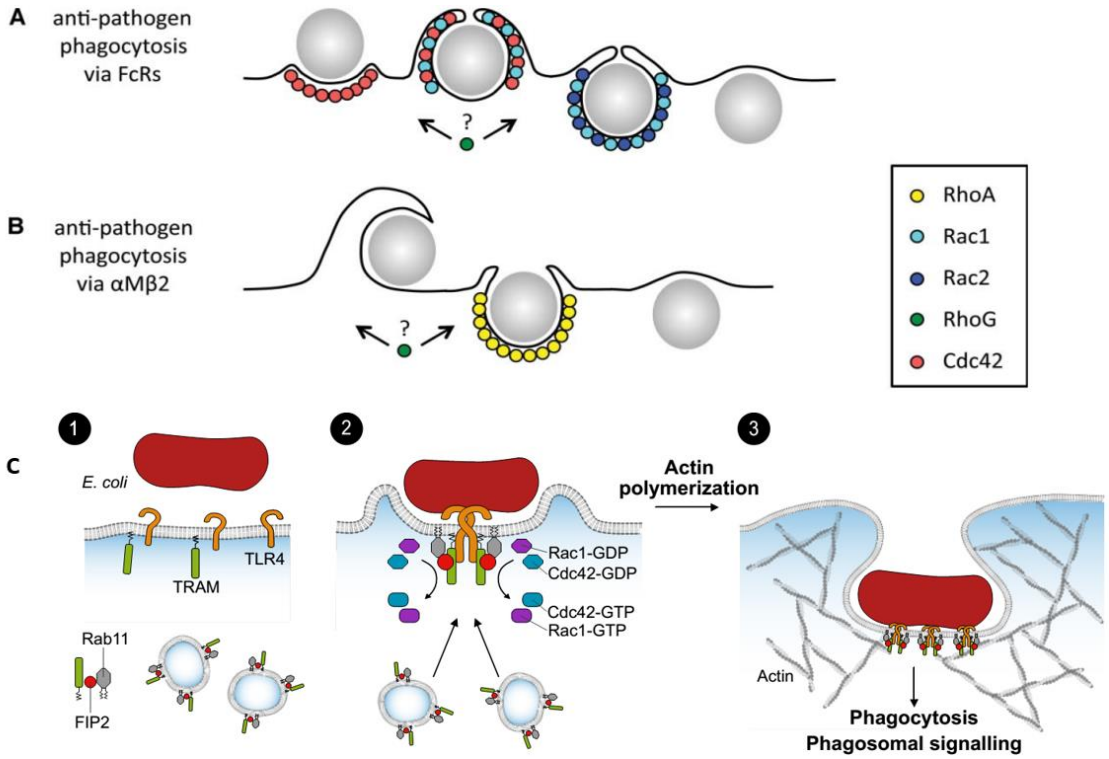

Figure 4.1: Phagocytosis of pathogens mediated by three different receptors. Pathogen phagocytosis mediated by FcR required the active Cdc42, Rac1 and Rac2 (A), while pathogen phagocytosis mediated by complement required the active RhoA (B) and (C) TLR mediated phagocytosis of pathogen requires active Cdc42 and Rac1. (A, B) obtained from [35] and (C) obtained from [77].

In this study we have not addressed Fcγ- mediated phagocytosis regulation by P7 peptide, and only checked if the amount of IgG in FCS or different percentage of FCS in media could alter the inhibitory activity of P7-pen towards phagocytosis (fig. 3.11), which was not the case. We suggest that P7-pen may specifically inhibit TLRs-mediated phagocytosis, which is regulated by similar set of GTPases and has similar mechanism of particles engulfment as FcR mediated phagocytosis (fig. 4.1A, C). It is known that TLR-mediated uptake is clathrin dependent and the phagosome closure is performed with F-actin remodelling and activity of Cdc42 and Rac1 similar to FcR mediated phagocytosis [77] (fig 4.1C). Based on the results obtained in our project, we can hypothesise that P7-pen could not interfere with phagocytosis mediated by complement, which provides a clue to the mechanism of action of P7 peptide.

Previous LC-MS data showed that among proteins involved in the regulation of phagocytosis and endocytosis Cdc42, Vav1, Rab14, RhoG and EHD4 were the most relevant binding partners of P7-pen. Here we explored the interaction between P7-pen or P7G10-pen (as it is not active towards phagocytosis inhibition) and the target proteins (MS hits) by co-precipitation to elucidate which target proteins are responsible for the P7-pen peptide inhibitory effect on phagocytosis. Our results revealed that both P7-pen and P7G10-pen co-precipitate with target proteins IRAK1/4, TRAM and TIRAP which are important key regulators of TLR4 downstream signalling, which coincides with data from Trafficking group on the inhibitory activity of both peptides towards TLR4-mediated gene expression (not shown). Both peptides along with the negative control-penetratin co-precipitated with β-tubulin, Vav1 and EHD4 proteins, which appeared as binding partners of P7-pen in MS (fig. 3.15, bottom panel). Due to the unspecific binding of these proteins to penetratin (pen) cell penetrating peptide (CPP), we can suggest that co-precipitation with these proteins is mediated by penetratin itself and not by SLAMF1-derived

sequence. This indicates that these proteins are not likely to be responsible for the inhibitory effect on P7-pen of bacterial phagocytosis.

We have shown that P7-pen or P7G10-pen co-precipitated RhoG, but not with RhoA or Cdc42 (fig. 3.15, middle panel) from lysates of human monocytes regardless of Cdc42 being an MS hit for P7-pen. An interesting observation was the band shift for RhoG on western blot P7G10-pen precipitation. This shift could indicate that the RhoG band in co-precipitation with P7G10 is unspecific or that P7G10 co-precipitates with RhoG with some posttranslational modifications. These results indicates that RhoG could be the specific target of P7, but not P7G10. Unfortunately, we did not have antibodies to Rab14 to check for potential differential binding to P7 or P7G10 in the endogenous co-precipitations, and we have used different model system to address it.

The co-precipitation between RhoG, Rab14 with P7-pen or P7G10-pen was further investigated in HEK293T cells, where we transiently overexpressed RhoG or Rab14 as flag-tagged proteins. Our results show that P7-pen co-precipitates with both Rab14 and RhoG, while P7G10 has much attenuated interaction with these proteins. We then hypothesise that RhoG could be a specific target for P7-pen which mediates peptide's inhibitory effect on phagocytosis. We suggest that P7-pen, but not P7G10-pen could bind and inhibit some downstream effects of RhoG that will abrogate TLR's mediated phagocytosis for both TLR4 and TLR2, as we see an effect of P7-pen on both Gram-negative and Gram-positive bacteria uptake. It was previously shown that RhoG could act as upstream regulator of Rac1 and Cdc42, which is in line with our hypothesis [79]. However, our hypothesis should be further explored as there are no studies showing that RhoG could be involved in regulation of bacterial phagocytosis. As to Rab14, targeting this protein by P7 peptide may also contribute to phagocytosis inhibition. Rab proteins attains the function of molecular switch from inactive GDP-bound and active GTP-bound forms. Rab14 is involved in phagocytosis in fusion of early endosomes and phagosomes in the trafficking between Golgi and endosomes [80], and it could be interesting to explore in the future if Rab14 could function as a master regulator of bacterial phagocytosis.

Based on our findings that peptide derived SLAMF1 was co-precipitating RhoG and Rab14, we decided to check if these proteins could be interaction partners of SLAMF1 receptor itself. Co-precipitation of SLAMF1 receptor or SLAMF1 deletion mutant (no cytoplasmic tail, negative control) with RhoG or Rab14 was investigated in HEK293T cells. SLAMF1 protein, but not deletion mutant, co-precipitated with RhoG and Rab14 (fig. 3.18). It is an interesting and novel finding, because SLAMF1 acts as a measles virus receptor [62] and could be involved in the regulation of viral entry during infection by measles virus. Elucidation of novel interaction partners for SLAMF1, trafficking regulators Rab14 and RhoG, could contribute to the understanding of measles virus entry and suggest novel treatments for prevention of viral infection of immune cells.

There were several other findings during the work on the project. The results obtained from flow cytometry with uptake of bioparticles showed that overexpression of SLAMF1 or SLAMF1 mutant (deletion of the IgV-like domain) had no effect on the uptake of *E. coli* bioparticles (fig. 3.1A, B). At the same time, SLAMF1 or the mutant protein increased bacterial uptake of live bacteria *(E. coli*) with no impact on downstream *IFN-β* or *TNF* expression (fig. 3.12, supplementary 7.2, S1). These contradictory data for live and heat killed bacteria uptake is currently difficult to explain and requires further investigation.

It was previously shown that P7-pen inhibited *IFN- β* mRNA expression and secretion mediated by heat killed bacteria. Accordingly, our results showed for the first time that P7-pen could efficiently inhibit *IFN-β* mRNA expression and secretion in response to live bacterial infection in THP-1 cells (*E.* coli, DH5α) (fig. 3.14). However, *TNF-α* mRNA

expression and secretion was not strongly depleted by P7-pen. Both TLR2 and TLR4 induce the production of *TNF-α* amongst other cytokines [7], and it is already known from previous studies performed by the Trafficking group that TLR2-mediated *TNF* expression is not inhibited by P7-pen. This could explain why *TNF* mRNA expression was not substantially depleted by P7-pen upon live *E. coli* infection.

The regulation of live *S. aureus* mediated *IFN-β* and *TNF* mRNA expression by P7-pen has not been addressed before. Our preliminary data from this study indicates that P7-pen treatment of THP-1 cells could inhibit *IFN-β* and *TNF* mRNA expression and secretion mediated by live *S. aureus* bacteria (supplementary 7.2, S2). The results build on the existing data from Trafficking group (data not shown) where *IFN-β* and *TNF* expression induced by heat killed *S. aureus* bacteria particles were also inhibited by P7-pen. However, the experiment was performed once and is merely preliminary. To make concluding remarks on the effect of P7-pen expression of *IFN-β* and *TNF* by live *S. aureus* bacteria several experiments should be done.

5. Conclusion

In this thesis, the effect of SLAMF1-derived peptides on bacterial uptake and the mechanism of uptake inhibition was investigated. We showed that P7-pen decreased the uptake of *E. coli* and *S. aureus* bioparticles (fig. 3.2), and the uptake of live *E. coli* (DH5α) and *S. aureus* (wood strain) bacteria (fig. 3.13). Collectively, the results indicates that P7-pen inhibits the uptake of Gram-negative and Gram-positive bacteria. Y/N amino acid substitution at position 4 in P7N4-pen showed decreased inhibitory activity of *E. coli* bioparticle uptake in flow cytometry at 60 min. (supplementary 7.1, S3), but strong inhibitory activity of live *E. coli* uptake at 15 min (fig. 3.13). The results suggest that P7N4-pen has decreased inhibitory activity at longer time periods compared to P7-pen. The T/G amino acid substation at position 10 in P7G10-pen showed uptake of *E. coli* bioparticle in flow cytometry (supplementary 7.1, S4 C, D) and of live *E. coli* bacteria (fig. 3.13) demonstrating that P7G10-pen did not inhibit uptake of bacteria. Flow cytometry data revealed that P7-pen did not inhibit uptake of opsonised *E. coli* bioparticles (fig. 3.6), while compstatin treatment (fig. 3.9) or heat inactivation of serum in complement (fig. 3.8) restored the inhibitory function of P7-pen. Thus, P7-pen does not affect complement mediated phagocytosis.

We showed that P7-pen or P7G10-pen co-precipitated with IRAK1/4, TIRAP and TRAM which are key regulators of the TLR4 signalling pathway (not shown). However, the western blot analysis did not show co-precipitation between the peptides and Cdc42 or RhoA (fig. 3.15, middle panel). Both peptides, including the negative control co-precipitated with β- tubulin, Vav1 and EHD4 (fig. 3.15, bottom panel) suggesting that the interaction is mediated by penetratin and not the SLAMF1 sequence. Collectively, the results demonstrated that the binding partners from MS (table 1.2) are not responsible for the inhibitory effect of P7-pen on bacterial phagocytosis. Co-precipitation of P7-pen or P7G10-pen with RhoG was illustrated (fig. 3.15, middle panel), where a band shift was observed in P7G10. This could be an unspecific band or posttranslational modification. Thus, RhoG could be a specific target protein for P7-pen but not for P7G10-pen. Additional experiment with HEK293T model revealed that P7-pen co-precipitated with RhoG and Rab14, while P7G10-pen had weakened interaction with the target proteins (fig. 3.16), amplifying that RhoG is a specific target for P7-pen and could regulate the inhibitory effect of the peptide. We showed that SLAMF1 protein co-precipitated with RhoG and Rab14, while SLAMF1 mutant (deletion of c-terminal) did not (fig. 3.17). The novel finding suggests that RhoG and Rab14 could regulate viral entry of measles virus.

Flow cytometry results demonstrated that SLAMF1 or SLAMF1 mutant (deletion of IgV-like domain) did not affect the uptake of *E. coli* bioparticles (fig. 3.1 A, B). On the other hand, SLAMF1 and mutant SLAMF1 showed increased uptake of live *E. coli* (fig. 3.12). The results are difficult to explain, and further investigation is required.

Our results showed for the first time that P7-pen efficiently decreased *IFN-β* expression mediated by live *E. coli* (fig.3.14), additionally P7-pen decreased the *IFN-β* and *TNF* expression mediated by live *S. aureus.* Thus, P7-pen can inhibit signalling mediated by live bacteria.

To further understand the effect and mechanism of inhibition of bacterial uptake by P7-pen, several aspects should be investigated. The impact on proinflammatory cytokines and *IFN-β* by P7G10-pen should be investigated. It would be informative to elucidate how P7-pen could possibly affect FcR mediated phagocytosis (using human serum) or TLR-initiated phagocytosis. Studies looking at the RhoG mediation of the inhibitory effect of P7-pen should be investigated since no studies have shown that RhoG could be involved in the regulation of phagocytosis. It would be informative to elucidate the role of RhoG

and Rab14 in measles virus entry. Most of the results are preliminary and further investigations are required to give a conclusion.

6. References

1. Marshall, J.S., et al., *An introduction to immunology and immunopathology.* Allergy, Asthma & Clinical Immunology, 2018. **14**(S2).
2. Parkin, J. and B. Cohen, *An overview of the immune system.* Lancet, 2001. **357**(9270): p. 1777-89.
3. Owen, J.P.S.S.P.J.J., *Kuby Immunology*. Vol. 8th edition. 2019: W.H Freeman and Company. 113.
4. Kubelkova, K. and A. Macela, *Innate Immune Recognition: An Issue More Complex Than Expected.* Front Cell Infect Microbiol, 2019. **9**: p. 241.
5. Pasare, C. and R. Medzhitov, *Toll-like receptors and acquired immunity.* Semin Immunol, 2004. **16**(1): p. 23-6.
6. Giamarellos-Bourboulis, E.J. and M. Raftogiannis, *The immune response to severe bacterial infections: consequences for therapy.* Expert Review of Anti-infective Therapy, 2012. **10**(3): p. 369-380.
7. Elson, G., et al., *Contribution of Toll-like receptors to the innate immune response to Gram-negative and Gram-positive bacteria.* Blood, 2007. **109**(4): p. 1574-1583.
8. Carrillo, J.L.M., et al., *Physiology and Pathology of Innate Immune Response Against Pathogens*. 2017, InTech. p. 111.
9. Owen, J.P.S.S.P.J.J., *Kuby Immunology*. 2019: W.H Freeman and Company. 120.
10. Chaplin, D.D., *Overview of the immune response.* J Allergy Clin Immunol, 2010. **125**(2 Suppl 2): p. S3-23.
11. Carrillo, J.L.M., et al., *Physiology and Pathology of Innate Immune response Against Pathogens*. 2017, inTech. p. 107.
12. Bonilla, F.A. and H.C. Oettgen, *Adaptive immunity.* J Allergy Clin Immunol, 2010. **125**(2 Suppl 2): p. S33-40.
13. Takeuchi, O. and S. Akira, *Pattern Recognition Receptors and Inflammation.* Cell, 2010. **140**(6): p. 805-820.
14. Kawai, T. and S. Akira, *Toll-like receptors and their crosstalk with other innate receptors in infection and immunity.* Immunity, 2011. **34**(5): p. 637-50.
15. Kawasaki, T. and T. Kawai, *Toll-like receptor signaling pathways.* Front Immunol, 2014. **5**: p. 461.
16. Kawai, T. and S. Akira, *The role of pattern-recognition receptors in innate immunity: update on Toll-like receptors.* Nature Immunology, 2010. **11**(5): p. 373-384.
17. Yoneyama, M. and T. Fujita, *RNA recognition and signal transduction by RIG-I-like receptors.* Immunological Reviews, 2009. **227**(1): p. 54-65.
18. Jialal, I., H. Kaur, and S. Devaraj, *Toll-like receptor status in obesity and metabolic syndrome: a translational perspective.* J Clin Endocrinol Metab, 2014. **99**(1): p. 39-48.
19. Akira, S., S. Uematsu, and O. Takeuchi, *Pathogen recognition and innate immunity.* Cell, 2006. **124**(4): p. 783-801.
20. Carpenter, S., et al., *Toll-like Receptor 3 (TLR3) Signaling Requires TLR4 Interactor with Leucine-rich Repeats (TRIL).* Journal of Biological Chemistry, 2011. **286**(44): p. 38795-38804.
21. Kawai, T. and S. Akira, *TLR signaling.* Cell Death Differ, 2006. **13**(5): p. 816-25.
22. Blasius, A.L. and B. Beutler, *Intracellular toll-like receptors.* Immunity, 2010. **32**(3): p. 305-15.
23. El-Zayat, S.R., H. Sibaii, and F.A. Mannaa, *Toll-like receptors activation, signaling, and targeting: an overview.* Bulletin of the National Research Centre, 2019. **43**(1).
24. Tanimura, N., et al., *Roles for LPS-dependent interaction and relocation of TLR4 and TRAM in TRIF-signaling.* Biochem Biophys Res Commun, 2008. **368**(1): p. 94-9.
25. Barton, G.M. and R. Medzhitov, *Toll-like receptor signaling pathways.* Science, 2003. **300**(5625): p. 1524-5.
26. de Oliviera Nascimento, L., P. Massari, and L. Wetzler, *The Role of TLR2 in Infection and Immunity.* Frontiers in Immunology, 2012. **3**.

27. Rosales, C. and E. Uribe-Querol, *Phagocytosis: A Fundamental Process in Immunity.* Biomed Res Int, 2017. **2017**: p. 9042851.
28. Underhill, D.M. and H.S. Goodridge, *Information processing during phagocytosis.* Nature Reviews Immunology, 2012. **12**(7): p. 492-502.
29. Moretti, J. and J.M. Blander, *Insights into phagocytosis-coupled activation of pattern recognition receptors and inflammasomes.* Curr Opin Immunol, 2014. **26**: p. 100-10.
30. Stuart, L.M. and R.A.B. Ezekowitz, *Phagocytosis.* Immunity, 2005. **22**(5): p. 539-550.
31. Aderem, A., *Phagocytosis and the Inflammatory Response.* The Journal of Infectious Diseases, 2003. **187**(s2): p. S340-S345.
32. Underhill, D.M. and B. Gantner, *Integration of Toll-like receptor and phagocytic signaling for tailored immunity.* Microbes Infect, 2004. **6**(15): p. 1368-73.
33. Freeman, S.A. and S. Grinstein, *Phagocytosis: receptors, signal integration, and the cytoskeleton.* Immunol Rev, 2014. **262**(1): p. 193-215.
34. Feng, M., et al., *Phagocytosis checkpoints as new targets for cancer immunotherapy.* Nat Rev Cancer, 2019. **19**(10): p. 568-586.
35. Mao, Y. and S.C. Finnemann, *Regulation of phagocytosis by Rho GTPases.* Small GTPases, 2015. **6**(2): p. 89-99.
36. Goodridge, H.S., D.M. Underhill, and N. Touret, *Mechanisms of Fc receptor and dectin-1 activation for phagocytosis.* Traffic, 2012. **13**(8): p. 1062-71.
37. Uribe-Querol, E. and C. Rosales, *Phagocytosis: Our Current Understanding of a Universal Biological Process.* Front Immunol, 2020. **11**: p. 1066.
38. Groves, E., et al., *Molecular mechanisms of phagocytic uptake in mammalian cells.* Cell Mol Life Sci, 2008. **65**(13): p. 1957-76.
39. Cannons, J.L., S.G. Tangye, and P.L. Schwartzberg, *SLAM Family Receptors and SAP Adaptors in Immunity.* Annual Review of Immunology, 2011. **29**(1): p. 665-705.
40. Veillette, A., *SLAM-Family Receptors: Immune Regulators with or without SAP-Family Adaptors.* Cold Spring Harbor Perspectives in Biology, 2010. **2**(3): p. a002469-a002469.
41. van Driel, B.J., et al., *Responses to Microbial Challenges by SLAMF Receptors.* Front Immunol, 2016. **7**: p. 4.
42. Sidorenko, S.P. and E.A. Clark, *The dual-function CD150 receptor subfamily: the viral attraction.* Nature Immunology, 2003. **4**(1): p. 19-24.
43. Yurchenko, M., et al., *SLAMF1 is required for TLR4-mediated TRAM-TRIF–dependent signaling in human macrophages.* Journal of Cell Biology, 2018. **217**(4): p. 1411-1429.
44. Lundberg, P. and U. Langel, *A brief introduction to cell-penetrating peptides.* J Mol Recognit, 2003. **16**(5): p. 227-33.
45. Jones, S.W., et al., *Characterisation of cell-penetrating peptide-mediated peptide delivery.* Br J Pharmacol, 2005. **145**(8): p. 1093-102.
46. Perkins, D.N., et al., *Probability-based protein identification by searching sequence databases using mass spectrometry data.* Electrophoresis, 1999. **20**(18): p. 3551-67.
47. Eng, J.K., A.L. McCormack, and J.R. Yates, *An approach to correlate tandem mass spectral data of peptides with amino acid sequences in a protein database.* J Am Soc Mass Spectrom, 1994. **5**(11): p. 976-89.
48. Wakatsuki, T., et al., *Effects of cytochalasin D and latrunculin B on mechanical properties of cells.* J Cell Sci, 2001. **114**(Pt 5): p. 1025-36.
49. Shoji, K., et al., *Cytochalasin D acts as an inhibitor of the actin-cofilin interaction.* Biochem Biophys Res Commun, 2012. **424**(1): p. 52-7.
50. Adan, A., et al., *Flow cytometry: basic principles and applications.* Critical Reviews in Biotechnology, 2017. **37**(2): p. 163-176.
51. McKinnon, K.M., *Flow Cytometry: An Overview.* Curr Protoc Immunol, 2018. **120**: p. 5.1.1-5.1.11.
52. Park, Y., et al., *Imaging Flow Cytometry Protocols for Examining Phagocytosis of Microplastics and Bioparticles by Immune Cells of Aquatic Animals.* Front Immunol, 2020. **11**: p. 203.

53. Selvarasu, S., et al., *Characterizing Escherichia coli DH5alpha growth and metabolism in a complex medium using genome-scale flux analysis.* Biotechnol Bioeng, 2009. **102**(3): p. 923-34.
54. Balachandran, M., et al., *Complete Genome Sequence of Staphylococcus aureus Strain Wood 46.* Genome Announc, 2017. **5**(13).
55. Scientific, T.F. *Introduction to Transfection*. Available from: https://www.thermofisher.com/no/en/home/references/gibco-cell-culture-basics/transfection-basics/introduction-to-transfection.html.
56. Scientific, T.F. *Types of Transfection*. Available from: https://www.thermofisher.com/no/en/home/references/gibco-cell-culture-basics/transfection-basics/types-of-transfection.html.
57. Scientific, T.F. *Overview of the Immunoprecipitation (IP) Technique*. Available from: https://www.thermofisher.com/no/en/home/life-science/protein-biology/protein-biology-learning-center/protein-biology-resource-library/pierce-protein-methods/immunoprecipitation-ip.html.
58. Taylor, S.C. and A. Posch, *The Design of a Quantitative Western Blot Experiment.* BioMed Research International, 2014. **2014**: p. 361590.
59. Boero, E., et al., *Use of Flow Cytometry to Evaluate Phagocytosis of Staphylococcus aureus by Human Neutrophils.* Front Immunol, 2021. **12**: p. 635825.
60. Yoon, H., E.K. Kim, and Y.H. Ko, *SLAMF1 contributes to cell survival through the AKT signaling pathway in Farage cells.* PLoS One, 2020. **15**(9): p. e0238791.
61. Berger, S.B., et al., *SLAM is a microbial sensor that regulates bacterial phagosome functions in macrophages.* Nat Immunol, 2010. **11**(10): p. 920-7.
62. Tatsuo, H., et al., *SLAM (CDw150) is a cellular receptor for measles virus.* Nature, 2000. **406**(6798): p. 893-7.
63. Husebye, H., et al., *The Rab11a GTPase controls Toll-like receptor 4-induced activation of interferon regulatory factor-3 on phagosomes.* Immunity, 2010. **33**(4): p. 583-96.
64. Mankovich, A.R., C.Y. Lee, and V. Heinrich, *Differential effects of serum heat treatment on chemotaxis and phagocytosis by human neutrophils.* PLoS One, 2013. **8**(1): p. e54735.
65. Underhill, D.M., *Macrophage recognition of zymosan particles.* J Endotoxin Res, 2003. **9**(3): p. 176-80.
66. Venkatachalam, G., S. Arumugam, and M. Doble, *Synthesis, Characterization, and Biological Activity of Aminated Zymosan.* ACS Omega, 2020. **5**(26): p. 15973-15982.
67. Goodridge, H.S., R.M. Simmons, and D.M. Underhill, *Dectin-1 stimulation by Candida albicans yeast or zymosan triggers NFAT activation in macrophages and dendritic cells.* J Immunol, 2007. **178**(5): p. 3107-15.
68. Cockram, T.O.J., et al., *The Phagocytic Code Regulating Phagocytosis of Mammalian Cells.* Front Immunol, 2021. **12**: p. 629979.
69. Owens, D.E. and N.A. Peppas, *Opsonization, biodistribution, and pharmacokinetics of polymeric nanoparticles.* International Journal of Pharmaceutics, 2006. **307**(1): p. 93-102.
70. Ricklin, D. and J.D. Lambris, *Compstatin: a complement inhibitor on its way to clinical application.* Adv Exp Med Biol, 2008. **632**: p. 273-92.
71. Namekar, M., et al., *Effect of Serum Heat-Inactivation and Dilution on Detection of Anti-WNV Antibodies in Mice by West Nile Virus E-protein Microsphere Immunoassay.* PLoS ONE, 2012. **7**(9): p. e45851.
72. Khubchandani, K.R., R.E. Oberley, and J.M. Snyder, *Effects of surfactant protein A and NaCl concentration on the uptake of Pseudomonas aeruginosa by THP-1 cells.* Am J Respir Cell Mol Biol, 2001. **25**(6): p. 699-706.
73. Theus, S.A., M.D. Cave, and K.D. Eisenach, *Activated THP-1 cells: an attractive model for the assessment of intracellular growth rates of Mycobacterium tuberculosis isolates.* Infect Immun, 2004. **72**(2): p. 1169-73.

74. Swanson, L., et al., *TLR4 signaling and macrophage inflammatory responses are dampened by GIV/Girdin.* Proceedings of the National Academy of Sciences, 2020. **117**(43): p. 26895-26906.
75. Mahmood, T. and P.C. Yang, *Western blot: technique, theory, and trouble shooting.* N Am J Med Sci, 2012. **4**(9): p. 429-34.
76. Karpievitch, Y.V., et al., *Liquid Chromatography Mass Spectrometry-Based Proteomics: Biological and Technological Aspects.* Ann Appl Stat, 2010. **4**(4): p. 1797-1823.
77. Skjesol, A., et al., *The TLR4 adaptor TRAM controls the phagocytosis of Gram-negative bacteria by interacting with the Rab11-family interacting protein 2.* PLoS Pathog, 2019. **15**(3): p. e1007684.
78. Nagaishi, K., et al., *Herbimycin A inhibits both dephosphorylation and translocation of cofilin induced by opsonized zymosan in macrophagelike U937 cells.* Journal of Cellular Physiology, 1999. **180**(3): p. 345-354.
79. Katoh, H., et al., *Small GTPase RhoG is a key regulator for neurite outgrowth in PC12 cells.* Mol Cell Biol, 2000. **20**(19): p. 7378-87.
80. Yamamoto, H., et al., *Functional cross-talk between Rab14 and Rab4 through a dual effector, RUFY1/Rabip4.* Mol Biol Cell, 2010. **21**(15): p. 2746-55.

7. Supplementary

7.1 Supplementary material from flow cytometry

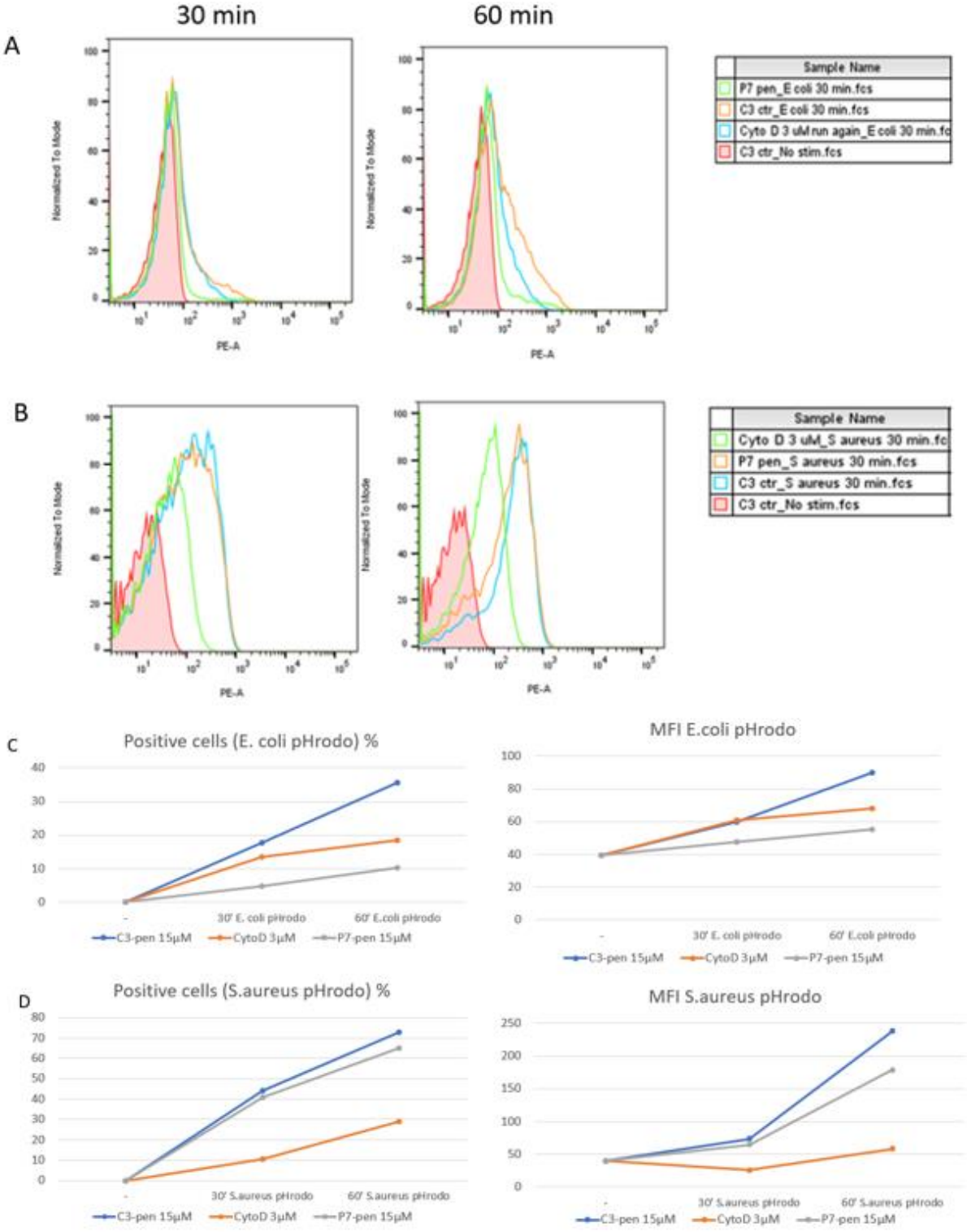

Figure S1: ***P7-pen peptide inhibits phagocytosis of E. coli and S. aureus pHrodo bioparticles.*** Human monocytes were pre-treated with 15 µM P7-pen or C3-pen, or 3µM CytoD followed by incubation with pHrodo *E. coli* (A, C) or *S. aureus* (B, D) bioparticles for 30- or 60-min. (A, B) Data presented as normalised to mode graphs from FlowJo software. (C, D) Graphs showing percentage of positive cells and (MFI) for *E. coli* (C) or *S. aureus* (D) particles uptake. Results for one independent experiment.

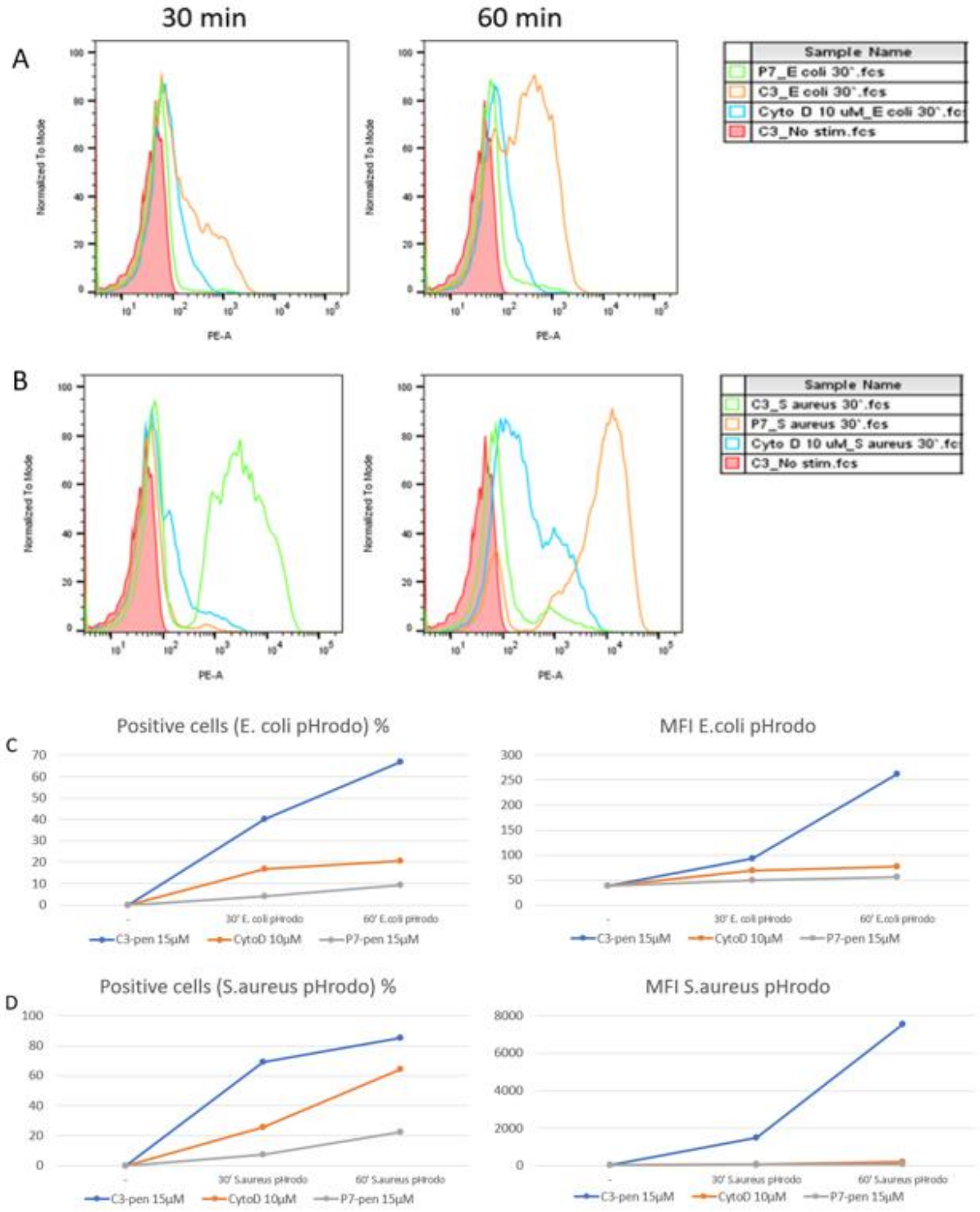

Figure S2: **P7-pen peptide inhibits phagocytosis of *E. coli* and *S. aureus* pHrodo bioparticles**. Human monocytes were pre-treated with 15 µM P7-pen or C3-pen, or 3µM CytoD followed by incubation with pHrodo *E. coli* (A, C) or *S. aureus* (B, D) bioparticles for 30- or 60- min. (A, B) Data presented as normalised to mode graphs from FlowJo software. (C, D) Graphs showing percentage of positive cells and (MFI) for *E. coli* (C) or *S. aureus* (D) particles uptake. Results for one independent experiment.

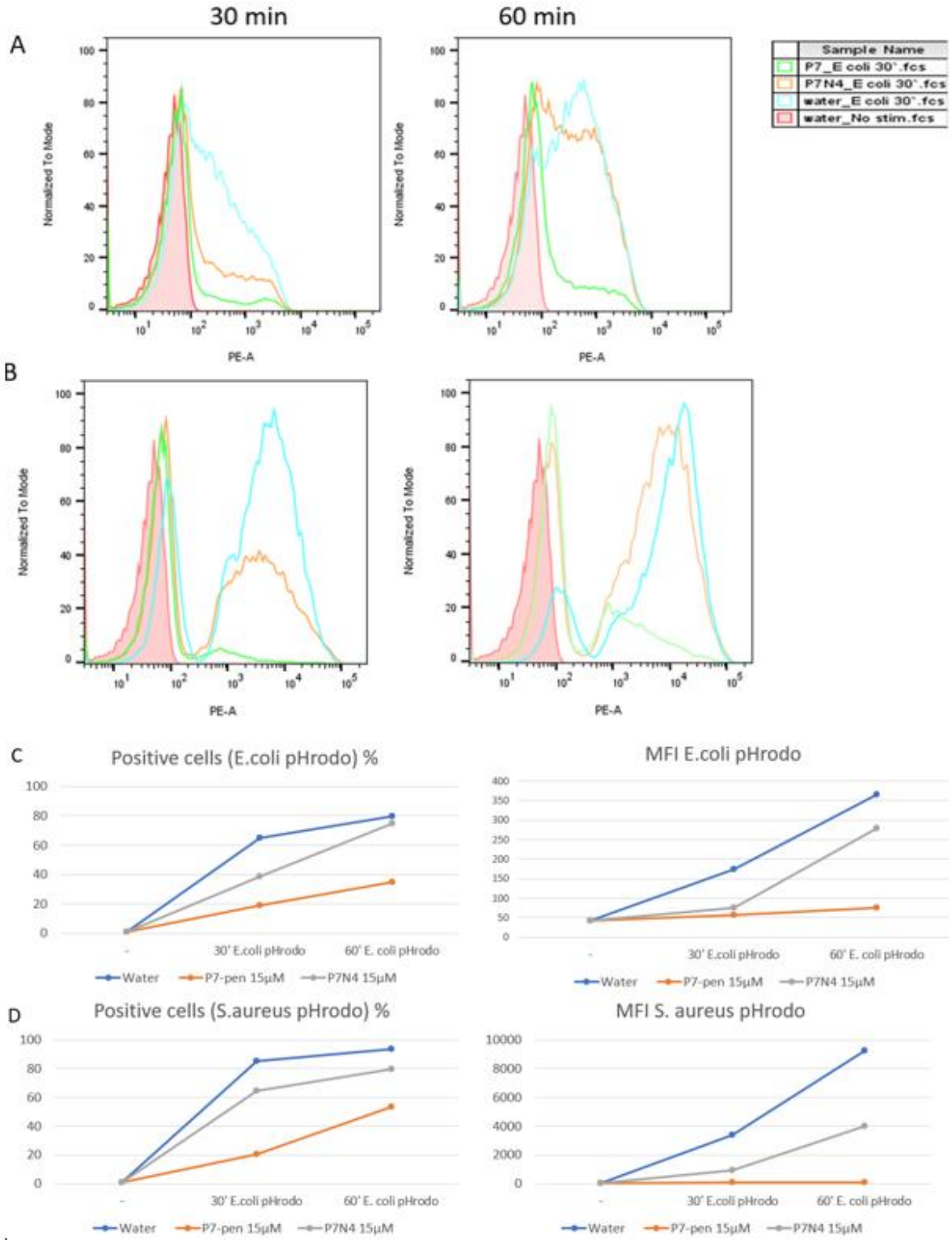

Figure S3: **P7N4-pen does not affect phagocytosis of *E. coli* and *S. aureus* pHrodo bioparticles.** Human monocytes were pre-treated with 15 µM P7-pen or P7N4-pen, or water (solvent control) followed by incubation with pHrodo *E. coli* (A, C) or *S. aureus* (B, D) bioparticles for 30- or 60- min. (A, B) Data presented as normalised to mode graphs from FlowJo software. (C, D) Graphs for percentage of positive cells and (MFI) for E. coli (C) or S. aureus (D) particles uptake. Results for one independent experiment.

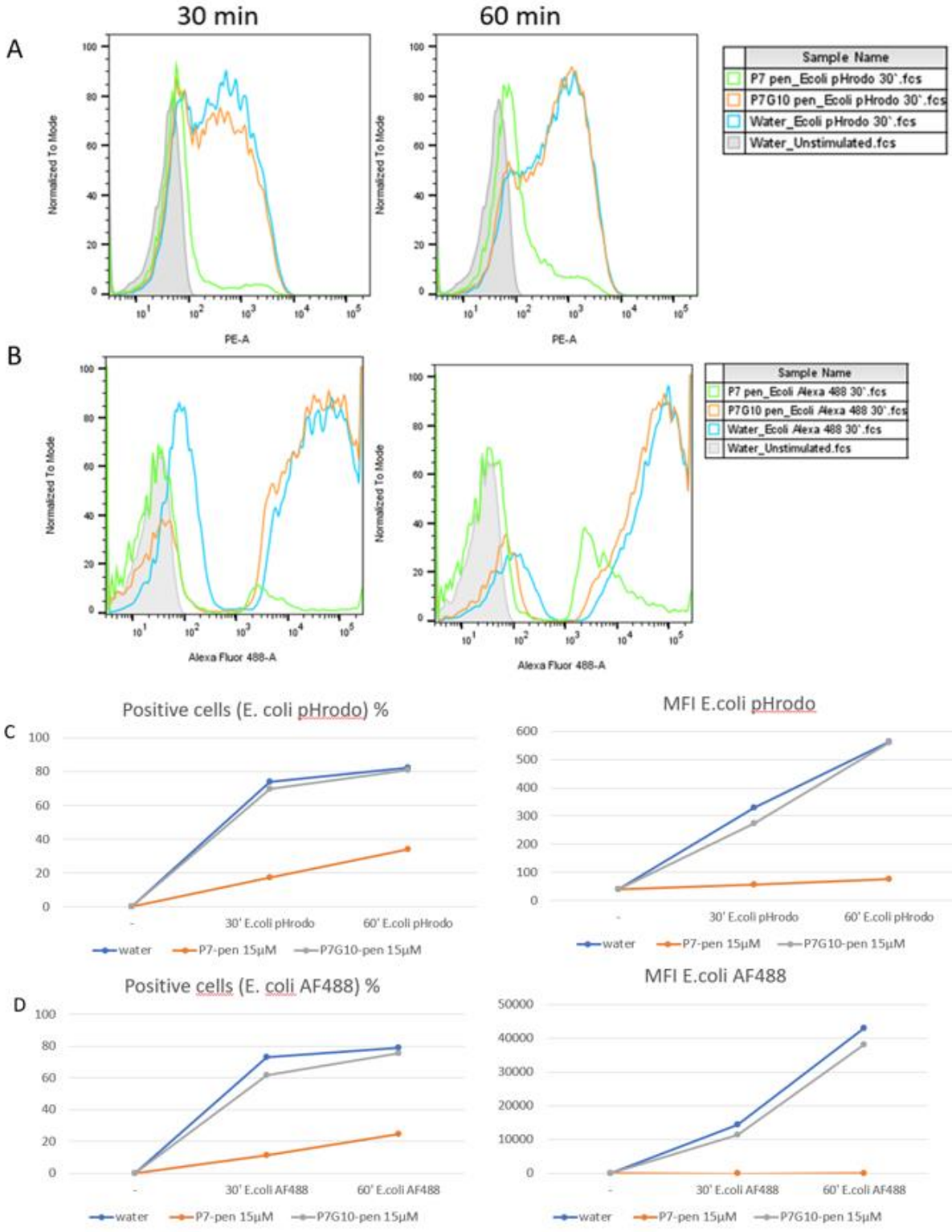

Figure S4: **P7G10-pen does not influence phagocytosis of *E. coli* pHrodo and AF488 bioparticles**. Human monocytes were pre-treated with 15 µM P7-pen or P7G10-pen, or water (solvent control) followed by incubation with *pHrodo E. coli* (A, C) or AF488 (B, D) bioparticles for 30- or 60- min. (A, B) Data presented as normalised to mode graphs from FlowJo software. (C, D) Graphs for percentage of positive cells and (MFI) for *E. coli* pHrodo (C) or *E. coli* AF488 (D) particles uptake. Results for one independent experiment.

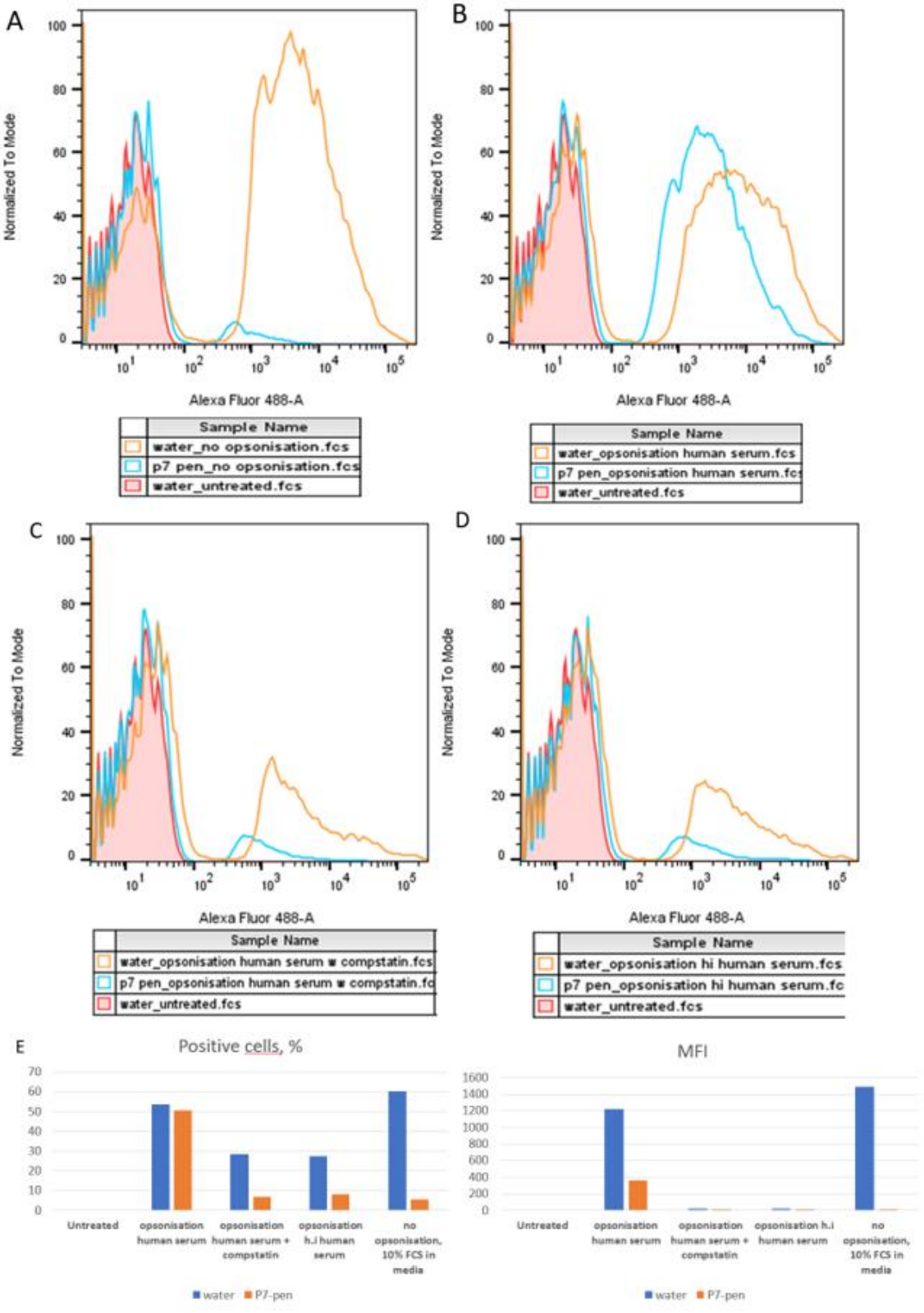

Figure S5: **Application of compstatin inhibits C3 component and restores P7-pen ability to inhibit phagocytosis of opsonised *E. coli* particle.** Human monocytes were pre-treated with 15 µM P7-pen and water (solvent control) followed by incubation with AF488 conjugated *E. coli particles* in 10% FCS without opsonisation condition (A), opsonisation by human A+ serum (B), opsonisation by human A+ serum with Compstatin (C) and opsonisation with heat inactivated (h.i) human A+ serum (D). (A-D) Data presented are normalised to mode graphs from FlowJo software. (E) Graphs show percentage positive cells and (MFI) for *E. coli* particle uptake in monocytes. Results for one independent experiment.

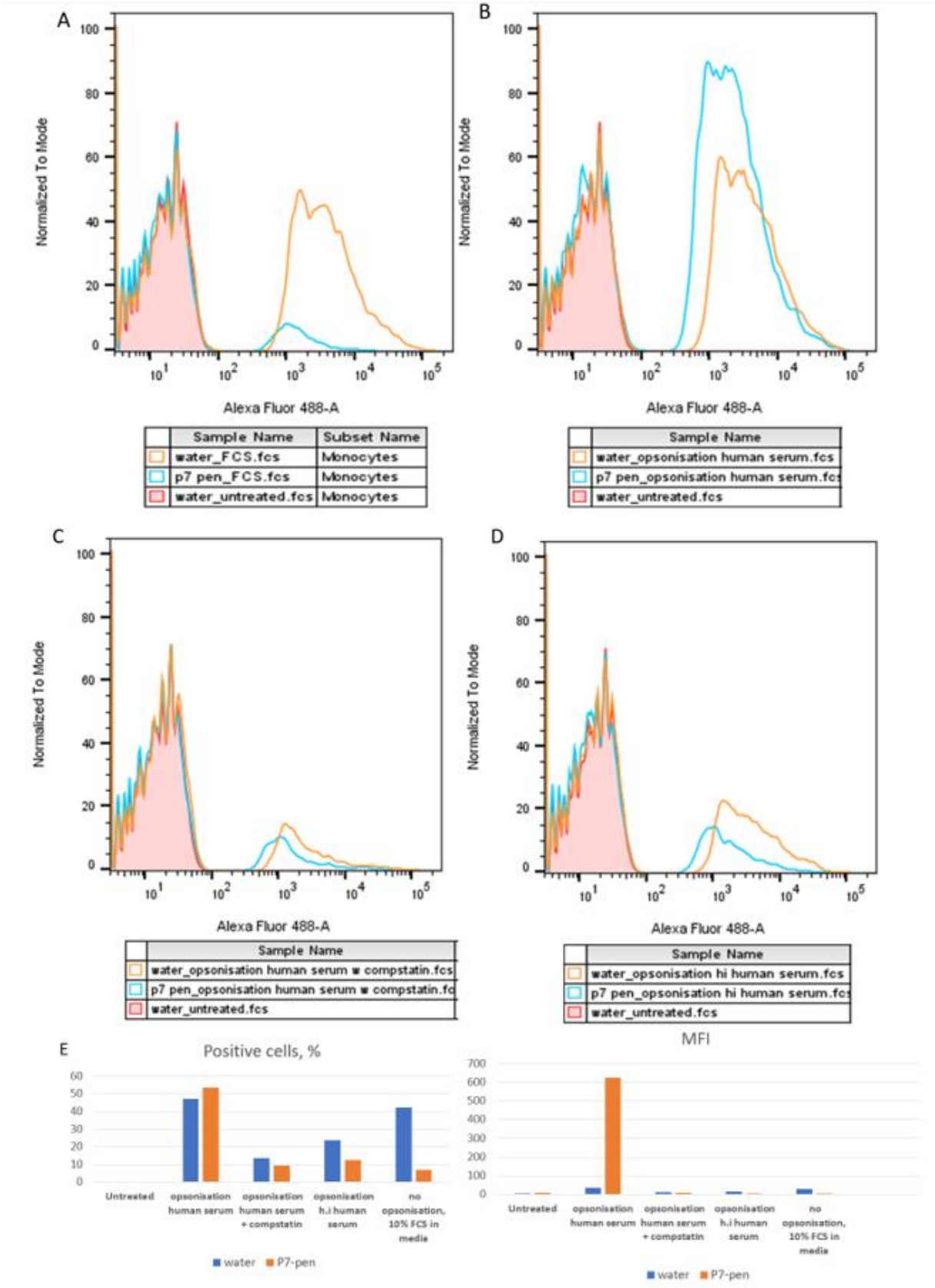

Figure S6: **Application of compstatin inhibits C3 component and restores P7-pen to inhibit phagocytosis of opsonised *E. coli* particle.** Human monocytes were pre-treated with 15 µM P7-pen and water (solvent control) followed by incubation with AF488 conjugated *E. coli* particles in 10% FCS without opsonisation condition (A), opsonisation by human A+ serum (B), opsonisation by human A+ serum with Compstatin (C) and opsonisation with heat inactivated (h.i) human A+ serum (D). (A-

D) Data presented are normalised to mode graphs from FlowJo software. (E) Graphs for percentage positive cells and (MFI) for *E. coli* particle uptake in monocytes. Results for one independent experiment.

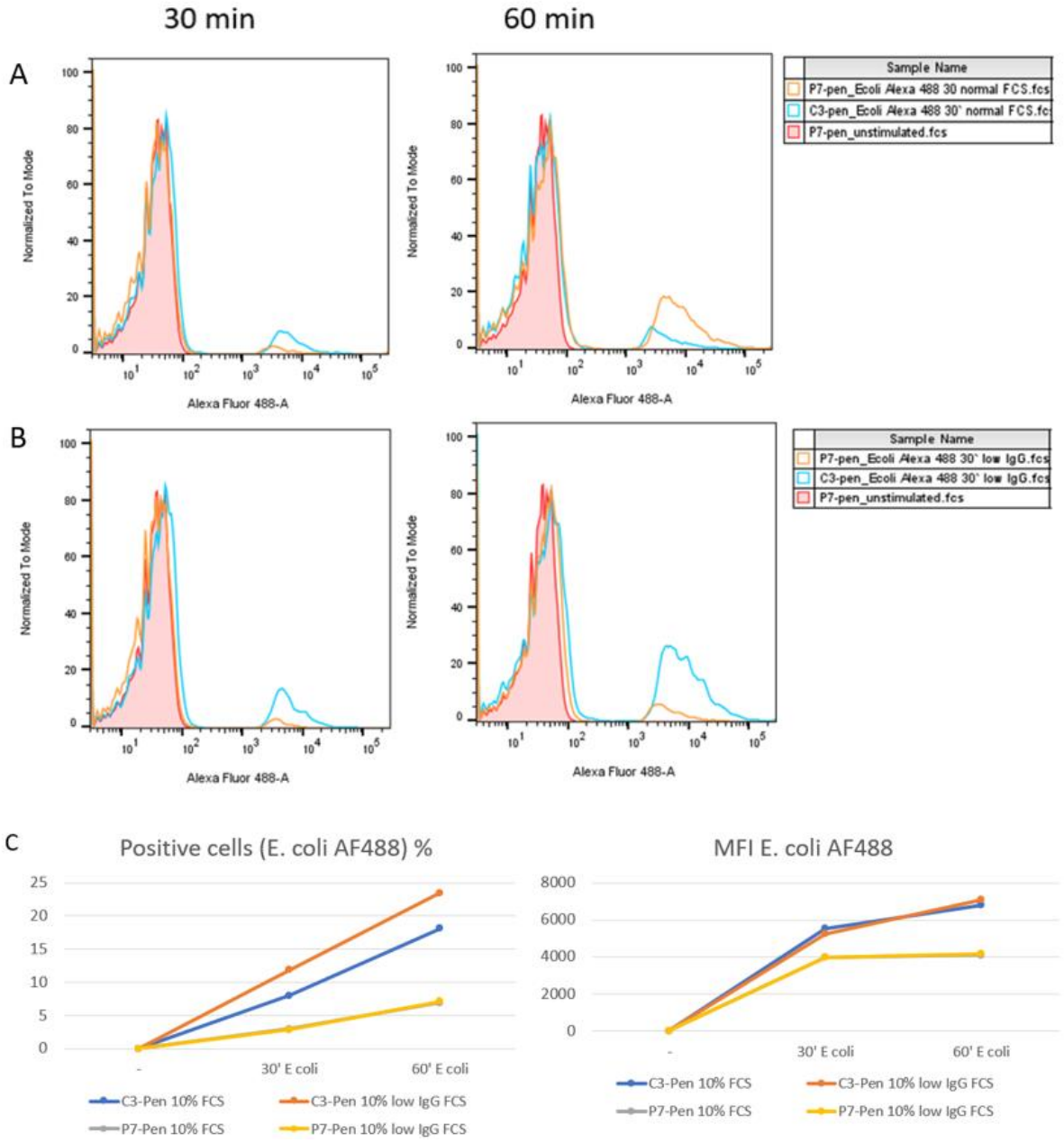

Figure S7: **Opsonisation by low IgG FCS serum does not alter phagocytosis regulation of P7-pen peptide.** Human monocytes were pre-treated with 15 µM P7-pen or C3-pen followed by incubation with AF488 conjugated *E. coli* particles opsonised by 10% FCS (A) or 10% low IgG FCS (B). (A, B) Data presented are normalised to mode graphs from FlowJo software. (C) Graphs show percentage of positive cells and mean fluorescent intensity (MFI) for *E. coli* particle uptake in monocytes. Results of one experiment.

7.2 Supplementary material of live bacteria uptake in THP-1 cells

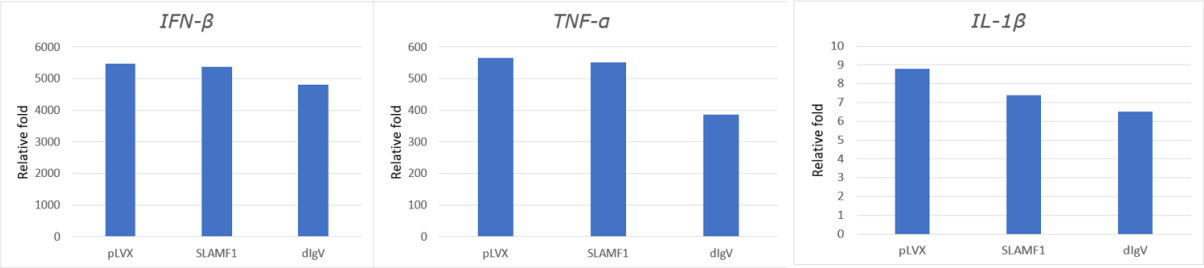

Figure S1: ***IFN-β, TNF-α*** **and** ***IL-1β*** **gene expression of** ***E. coli*** **(DH5a) infected THP-1 sublines.** Quantification of *IFN-β, TNF-α,* and *IL-1β* of THP-1 sublines were performed by RT-qPCR. Data from three independent experiments. CT values are normalised against the reference gene, TBP.

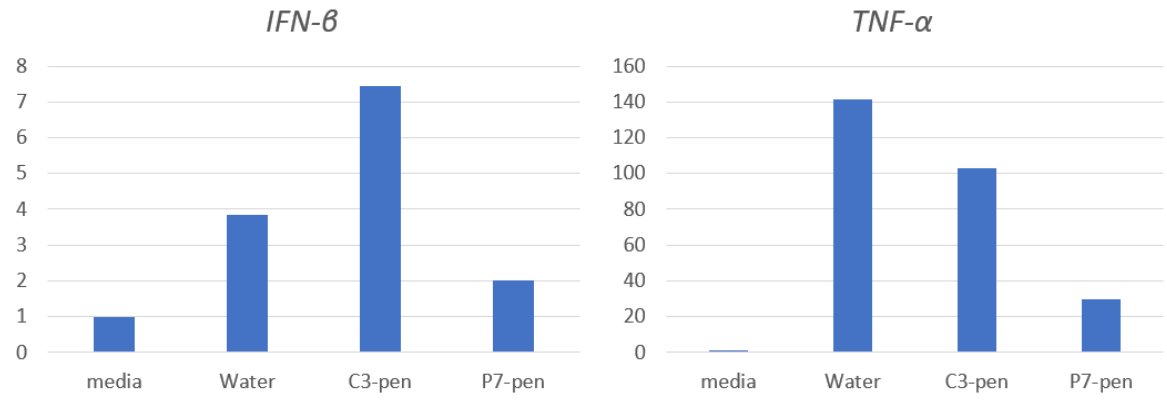

Figure S2: ***IFN-β*** **and** ***TNF-α*** **gene expression mediated by** ***S. aureus*** **(wood strain) infected THP-1 cells pre-treated with P7-*** ***pen peptide.*** *Quantification of IFN-β* and *TNF-α* of THP-1 cells were performed by RT-qPCR. Results from one independent experiment. CT values are normalised against the reference gene, TBP.

7.3 Supplementary material from western blot analysis

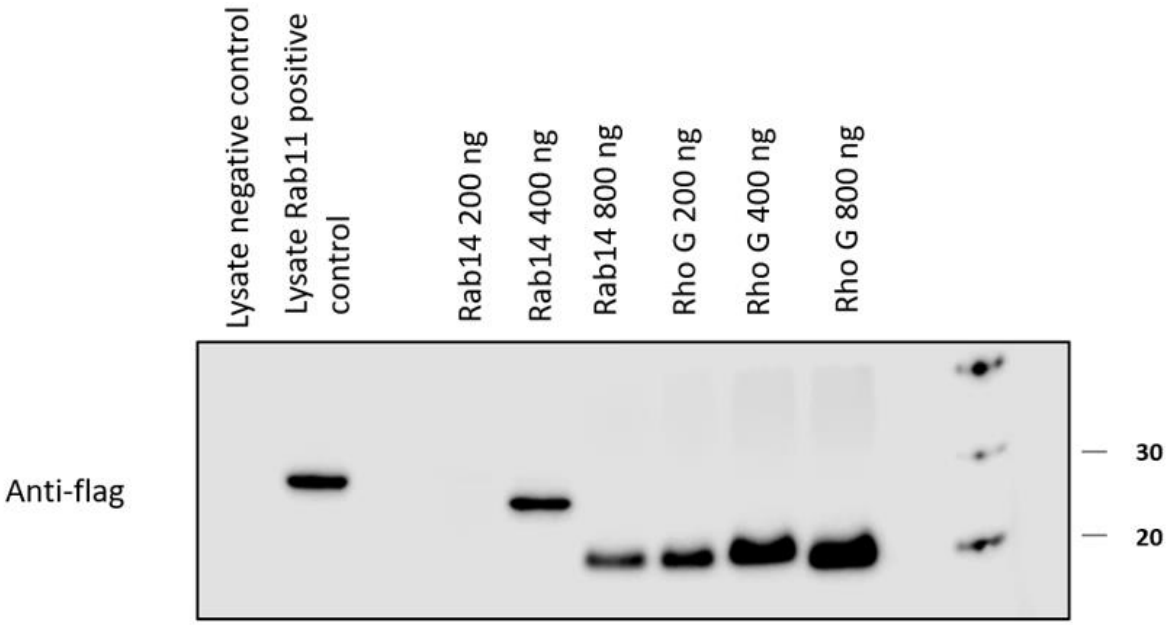

Figure S1: **RhoG is expressed in all concentration, while Rab14 is expressed in 400 and 800 ng.** HEK293T cells were transiently transfected with plasmids encoding 200-800 ng Rab14^{Flag} or RhoG^{Flag} and 100 ng Rab11^{Flag} (positive control) for 48 hours. Cell lysates were prepared in 1X RIPA buffer with inhibitors and subjected to SDS-PAGE and the target proteins

were evaluated by western blot analysis. Antibody is indicated in the figure and molecular weight is presented in kilodaltons (kDa).

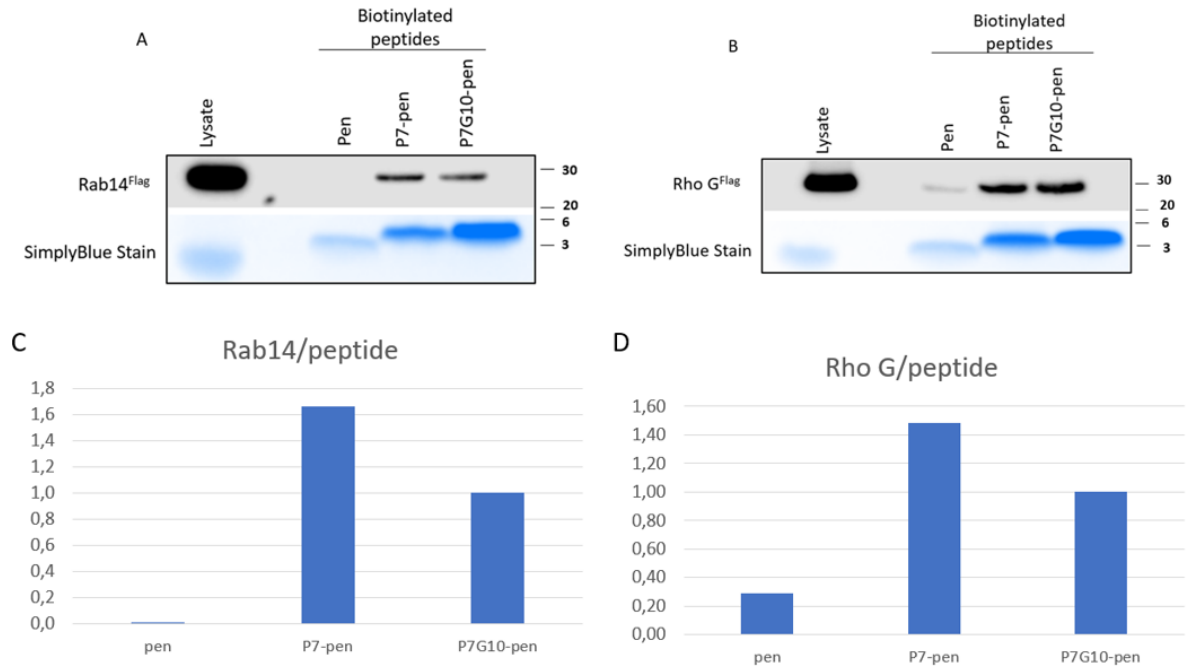

Figure S2: **P7-pen peptide efficiently co-precipitated with RhoGFlag and Rab14^{Flag} proteins.** HEK293T cells were transiently transfected with plasmids encoding 1600 ng Rab14^{Flag} (A) or 400 ng RhoG^{Flag} (B) for 48 hours. Cell lysates were prepared in 1X RIPA buffer with inhibitors. Target proteins from lysates were precipitated under stringent conditions (400 mM NaCl) using biotinylated pen (negative control), P7-pen, or P7G10-pen immobilised on neutravidin beads. Cell lysate and eluate samples were subjected to SDS-PAGE and target proteins were accessed by western blot analysis. Antibodies are indicated in the figure and molecular weight is presented in kilodaltons (kDa). Lower parts of the gels were stained with Simple Blues proteins stain, and intensity of staining determined in image Lab (Biorad) software. Intensity of western blot staining analysed in Odyssey software, followed by quantification of ratio for Rab14 (C) and RhoG (D) in precipitations.

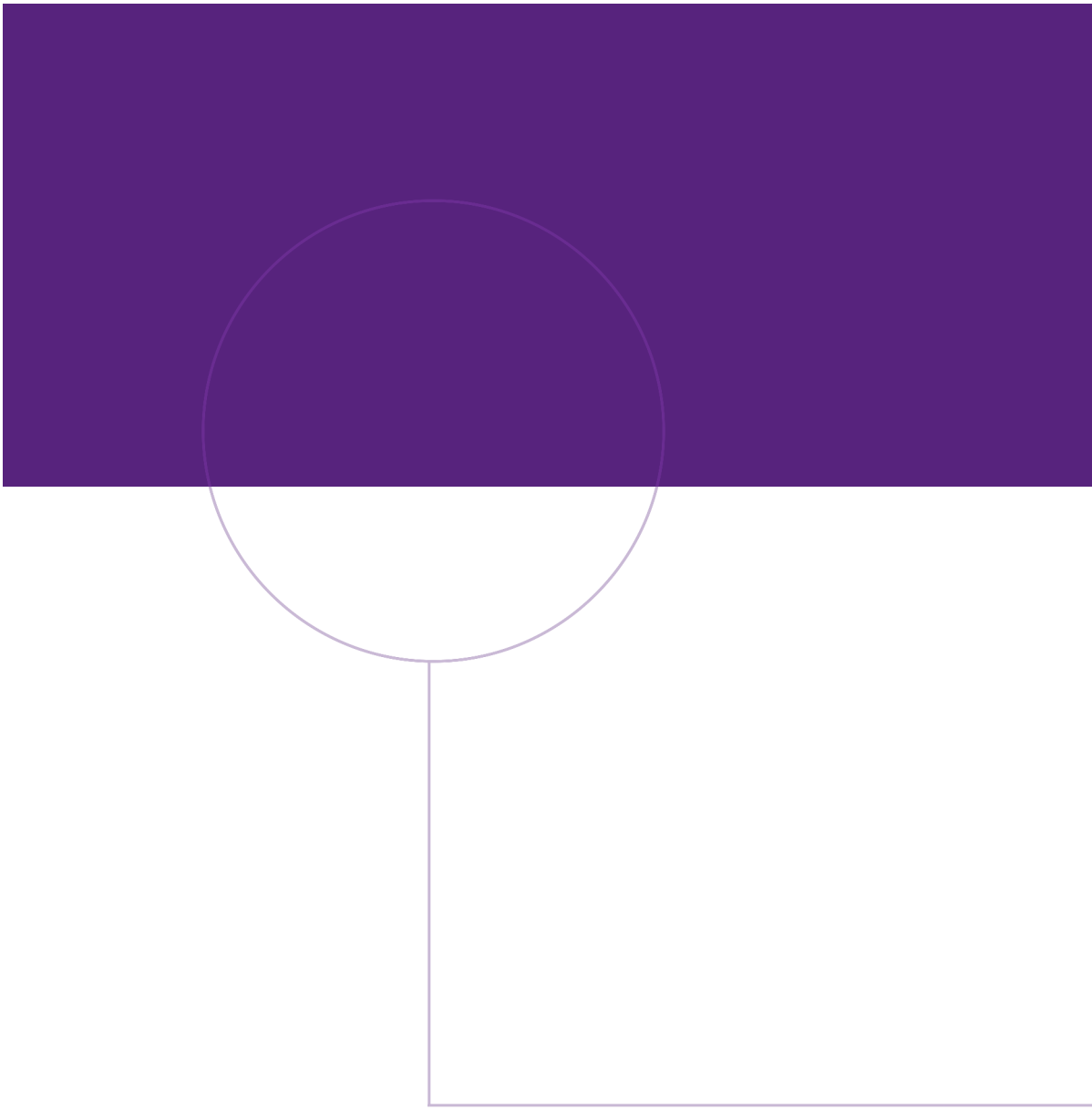

NTNU

Norwegian University of
Science and Technology